ENHANCEMENT OF THE UNITED STATES EXTREME WIND DATABASE AND IMPLICATIONS FOR EXTREME WIND CLIMATOLOGY

BY

ALEXANDER STEVEN ZICKAR

THESIS

Submitted in partial fulfillment of the requirements
for the degree of Master of Science in Civil Engineering
in the Graduate College of the
University of Illinois at Urbana-Champaign, 2019

Urbana, Illinois

Adviser:

Assistant Professor Franklin T. Lombardo

ABSTRACT

Despite the substantial progress made in recent years to improve the characterization of extreme wind climatology in the contiguous United States, uncertainties still remain in its formal quantification. The importance of an accurate assessment of extreme wind climate is paramount, however, due to the outsized weight that the "basic wind speed" value carries in computations of design wind loads specified in ASCE 7 standards. One of many avenues towards improving the accuracy of basic wind speed values is improving the recorded wind observations from which basic wind speeds are derived. The aim of this study is enhance this body of observations—called the extreme wind database—and to provide additional techniques of improving the understanding of extreme wind climatology in the United States.

The existing extreme wind database, formed using the Integrated Surface Dataset (ISD) 3505, was improved most significantly by nearly doubling its spatial resolution by extending the length of time over which observations are reported by approximately 10 years. Two additional techniques were developed that aimed to address temporal and spatial resolution issues related to climatology characterization. One of these employed the use of high temporal resolution wind observations from the Dataset 6405 (DS 6405) and the other made use of high spatial resolution wind observations obtained from the Oklahoma Mesonet (OKM). The improvements and additional techniques were quantified using a standardized extreme value analysis procedure to produce a common metric for comparison: a primordial basic wind speed analog called "V50" that can be compared across datasets of highly disparate character. Full suites of V50 values were generated for a control group of wind observation databases (i.e. existing databases) as well as a set of databases containing the improvements and additional techniques employed.

Using numerous graphical and geospatial analysis methods, the results of database improvements were compared to the control groups in the context of United States extreme wind climatology. It was found that, with regard to improvements of the existing extreme wind database, a doubling of the network spatial density and the extension of time histories led to a slight increase in basic wind speed estimates in most areas of the United States. Regional characteristics of basic wind speed contours were able to be more clearly identified as well. The technique for implementing high temporal resolution data from DS 6405 was found to unviable owing to the widespread existence of unrealistic wind records within the parent dataset that could not be adequately controlled. The spatial resolution improvement technique employing Oklahoma Mesonet observations, however, yielded more promising results. Using a comparison analysis of discrete, co-located wind events, it was found that the less spatially-dense network used to create the existing extreme wind database may not adequately capture small-scale extreme wind events as capably as the more spatially-dense Oklahoma Mesonet. This implies that the existing database, as well as the overarching methodology used to create it, may be systematically insufficient in regards to extreme wind observations. While it is assumed that this insufficiency has significant impacts on United States extreme wind climatology evaluations, further work is needed to quantify these impacts in a more generalized context.

ACKNOWLEDGEMENTS

I would like to first acknowledge the support, wisdom, and altruistic mentorship provided by Dr. Franklin Lombardo at the University of Illinois at Urbana-Champaign. Despite not having any research experience before starting, I was able to quickly develop my skills in research, writing, communicating, and reasoning in large part to his example and support. The opportunity he provided for me to work in a dynamic and unique discipline that spans two of my most profound interests—atmospheric science and civil engineering—was greatly appreciated and will have a guiding impact on my path moving forward.

Furthermore, I would like to thank the members of the Wind Engineering Research Laboratory (WERL) for their undying support and camaraderie they provided throughout this process. To Justin Nevill, Antonio Zaldivar de Alba, Dan Rhee, Guangzhao Chen, Jason Lopez, Rishabh Moorjani and guests of WERL, thank you for the *esprit de corps* that made working each day enjoyable. An additional thanks goes to the staff in the Department of Civil and Environmental Engineering (CEE) who work tirelessly in the best interests of graduate students and their endeavors.

The portion of this work concerning Oklahoma Mesonet data analyses is conceptually based off of similar techniques that were first employed by Matthew Carsello at the University of Illinois at Urbana-Champaign, but were not published. I want to recognize these efforts as the cornerstone and inspiration for the Oklahoma Mesonet analyses described herein.

To Mom, Dad, Avery, and Heather, for their undying support in the pursuit of my dreams.

TABLE OF CONTENTS

CHAPTER 1: INTRODUCTION

Wind loading often plays a significant role in structural design, but is among the more difficult loading sources to accurately quantify. There continue to be uncertainties in how wind interacts with infrastructure, which includes uncertainties in the natural characteristics of wind itself. The wind load design methodology presented in the American Society of Civil Engineers (ASCE) Publication Number 7 (ASCE 7) provides extensive guidance for practicing engineers on how to design for wind and its uncertainties, but is nonetheless the subject of continued improvements and refinements.

One such area where improvements are often sought is in the provisions governing the value of a design or "basic" wind speed, V. The basic wind speed in ASCE 7 is a single-value, location-specific metric that summarily describes the wind speed that can probabilistically be expected at any location in the United States. There are a number of values for basic wind speed that can be selected from ASCE 7 depending on the level of risk that is assumed during design. In this context, risk can be described by a wind speed's "probability of exceedance", which refers to the likelihood that a certain wind speed will be surpassed in a certain timeframe. For instance, a 15% probability of exceedance in 50 years (as is given for Risk Category I in ASCE 7) would correspond to a 15% chance that the a wind speed higher than V occurs within 50 years. It follows, thus, that V is higher or lower for a specific location given the selected probability of exceedance; ASCE 7 in fact provides basic wind speeds for a set of four such probabilities. This information is conveyed in a series of contoured maps that identify basic wind speed as a function of location within the United States. An example of such a map is given in Figure 1.1.

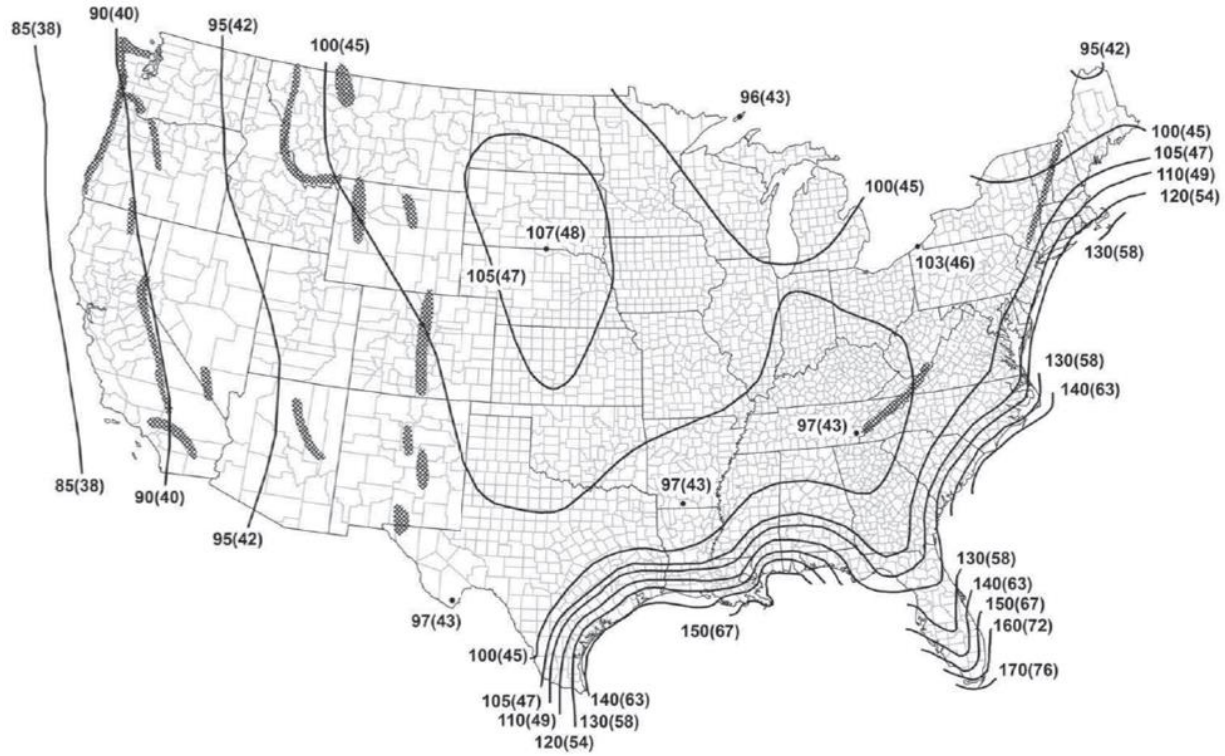

Figure 1.1. Basic wind speed map for Risk Category I taken from ASCE 7-16.

In a general sense, the development of basic wind speeds relies on two key steps: (1) obtaining a quality set of wind observations and (2) using these observations to predict—or extrapolate—the dataset beyond its characteristic range. Step 1 alone presents a significant challenge, as noted by multiple studies (Pintar et al. 2015, Lombardo et al. 2016, DeGaetano 1997). In fact, due to a substantial deficit of verifiable wind speed observations (i.e. at meteorological observation stations) in the United States, the concept of a map displaying location-specific design wind speeds was not formally included in United States structural design standards until 1972 (Lombardo et al. 2016). It was around this time also that detailed wind speed records began to be kept in earnest, and that a standardized regime for observing wind speeds was adopted across the United States (which was nevertheless altered several times before present) (Lombardo 2012). Step 2 is the subject of passionate debate among statisticians and wind engineers, who have developed numerous methods of transforming wind observations into acceptable basic wind speeds (Harris 2005). What is clear overall, however, is that the

inconsistencies and uncertainties brought about by these two steps ultimately result in significant uncertainties with the final product, the basic wind speed. In other words, while basic wind speeds are indeed well-informed estimates of extreme wind climatology in the United States, they are still just estimates.

The fervent debate and competing methodologies for characterizing extreme wind climate (particularly with regard to Step 2) are certainly justifiable. Basic wind speed, as it is implemented in ASCE standards, is a vital component of the wind load design process. This quantity, once selected, forms the basis for calculation of "velocity pressure" which is subsequently factored into the calculation of a more final "design pressure" (ASCE 2017). More significantly, perhaps, is the fact that velocity pressure is computed using the square of basic wind speed, meaning that uncertainties in basic wind speed estimation are amplified in the determination of design wind pressures. This implies that slight changes in basic wind speed can have dramatic cascading effects in the development of structures, from specific design decisions all the way project cost and serviceability.

The overall purpose of this study is to enhance the existing body of knowledge surrounding the creation of these basic wind speeds. More specifically, efforts are aimed at improving the acquisition and preparation of wind observations for estimating basic wind speeds in contiguous United States. A single realization of these wind observations constitute—as referenced throughout this study—an "extreme wind database", of which several varieties are ultimately considered. A suite of statistical extrapolation methods are utilized to evaluate these extreme wind databases, but in themselves are not the subject of this study's findings. A brief overview of what can be found in this study is provided as follows.

Previous work on this topic and information pertinent to this study are discussed in Chapter 2. Chapter 3 details a number of improvements made to existing sets of wind observations and associated procurement methods. In Chapter 4, two novel approaches to procuring wind observations are introduced and described. Chapter 5 provides detailed information on the statistical extrapolation methods implemented—the results of which are ultimately used to compare the improvements described in Chapters 3 and 4. In Chapter 6, results are presented in geographic "ensemble" form, where broad-scale trends and overall conclusions can be derived as discussed in Chapter 7. Future work and recommendations of this study conclude this document in Chapter 8.

CHAPTER 2: DEVELOPMENT OF AN EXTREME WIND DATABASE

In practice, wind observations are acquired using a piece of meteorological equipment known as an anemometer. While there are several types of anemometers that can be used, they all at a bare minimum measure wind speed, wind direction, and the time (known as a "timestamp") at which these two quantities were observed. For the purposes of this study, a series of wind observations recorded at the same location form what is known as a "time history" and a collection of time histories from different locations comprise a "wind database". An "*extreme* wind database", thus, is a more specialized wind database where extreme wind events, or "extrema", have been identified within each time history. Most typically, extrema are determined using some combination of wind speed and timestamp; three such methods are described in greater detail in Chapter 5. This chapter, however, details the process of establishing a generic wind database for the United States using wind observation networks—that is, the process of turning anemometer measurements into useful data.

2.1. Wind Observation Networks and Databases

The primary means of observing wind in the United States is through a collection of weather observation stations administered jointly by the National Weather Service (NWS), the Federal Aviation Administration (FAA) and the Department of Defense (DOD). In general, weather observation stations fall into one of two categories: Automated Surface Observing Systems (ASOS) and Automated Weather Observing Systems (AWOS). According to (NWS), ASOS stations report weather conditions (including wind) every hour and automatically transition to more frequent reporting intervals if the station detects that weather conditions are changing quickly. The various thresholds used to trigger this transition are outlined further in the ASOS User's Guide (Nadolski 1998). AWOS stations, on the other hand, report weather

conditions at consistent intervals (generally every 20 minutes) and do not account for variable conditions in their reporting scheme (NCEI [a]). Records from AWOS stations, however, are among the oldest verifiable weather records maintained by the NWS, outdating ASOS records by as much as 20 years in some instances.

The wind observations produced by both the ASOS and AWOS networks are, as of present, reconciled into a larger surface observation database known as the Integrated Surface Database 3505 (ISD 3505). The ISD 3505 is currently curated by the National Centers for Environmental Information (NCEI) and includes weather observations from more than 35,000 reporting stations around the world (NCEI [b]). Data from ISD 3505 may be accessed using a number of methods, including via an online web protocol as discussed in Chapter 3. Lombardo et al. (2009) provides a detailed assessment of data formatting within this database and discusses methods for extracting the requisite wind information—methods that are employed heavily throughout this study.

Reporting stations contributing to the ISD 3505 are identified and organized using a system of two identifying numbers: a United States Air Force (USAF) number and a Weather Bureau Army Navy (WBAN) number. As it pertains to this study specifically, the following are true regarding these two identification numbers: (1) the USAF number is always six digits long and United States stations typically have a USAF number that begins with "72"; (2) the WBAN number is always five digits long; (3) instances where either the USAF or WBAN numbers are given as all 9's indicate that the particular identification number is unknown or not applicable; (4) a single station can only be identified properly using a combination of *both* USAF and WBAN numbers, since duplicates of each exist within the ISD 3505. These identification schema play a significant role in the extreme wind database improvements detailed in Chapter 3.

Along with the meteorological data itself, NCEI also provides extensive documentation of the observation stations whose readings comprise the ISD 3505. The primary station metadata document is known as the ISD History Document (available at ftp://ftp.ncdc.noaa.gov/pub/data/noaa/isd-history.txt) and contains station identification information (such as USAF-WBAN pairs) as well as descriptions, locations, and dates of operation. This document, as referenced throughout this study, serves as the crucial link between the raw wind data and its application to extreme wind climatology characterization.

Apart from the ISD 3505 is a more specific realization of wind observation data known as the Dataset 6405 (DS 6405), which is also curated by NCEI. DS 6405 contains, among other information, wind observations reported every minute in time and is also accessible using an online web protocol. Wind data from DS 6405 is referred to in this study as "high resolution" wind data, owing to its improved temporal resolution over ISD 3505 wind data. Masters et al. (2010) provides more information on how to obtain this data and extract the useful wind information from it. Unlike the ISD 3505 wind data, DS 6405 data originates only from ASOS stations specifically, making it more limited than the ISD 3505 data in both longevity and in network density (NCEI 2006). Furthermore, DS 6405 data is organized by what is known as a "call sign"—a four-character code (beginning with "K") that is assigned to each airport as its operational identifier. While there is some level of consistency between the USAF-WBAN scheme used in ISD 3505 and the call sign scheme used in DS 6405, reconciling these identifiers can be challenging and prone to errors.

Outside the ASOS and AWOS station networks exist additional observation networks that report useful wind data. Within the United States, these additional networks are largely targeted at specific regions with an interest in monitoring mesoscale climatology. As such, these

networks may be privately funded and tend to be established and maintained by state-level research institutions, rather than by an overarching federal entity like the NWS. This trait leads to a varying level of data accessibility and wind record standardization between the networks. Because these networks, however, tend to be more regional in scope and use reporting stations that are denser geographically, they offer a promising source of validation and enhanced spatial resolution that the other NWS-based networks cannot yet provide. Some examples of these other networks include the West Texas Mesonet (NWI 2019) and the Oklahoma Mesonet (OM 2019a).

2.2. Historical Extreme Wind Databases

Regardless of the observation network used, an extreme wind database is created by extracting wind time histories from a larger meteorological database (such as ISD 3505) and then identifying extrema within these time histories. For the United States, several initial versions of an extreme wind database were devised for use in older design standards. The first well-documented database was developed by (Simiu et al. 1979), which was subsequently used to produce the map of basic wind speeds found in the American National Standards Institute (ANSI) document ANSI A58.1-1982 (Lombardo et al. 2016). This database consisted of wind speed observations from 129 locations across the United States dating from as early as the 1940's to 1979. These observations were comprised of two primary types: fastest mile annual maxima and peak one-minute average annual maxima (Simiu et al. 1979). To create the basic wind speed map in ANSI A58.1-1982, all wind observations in this database were converted to a fastest mile averaging method before extreme value analysis was conducted. This data is available and can be obtained from https://www.itl.nist.gov/div898/winds/nondirectional.htm.

In the mid-1990's, an updated extreme wind database was created, due in part to the discontinuation of fastest mile wind measurements by the NWS (Peterka and Shahid 1998). This newer database, making use of a larger number of stations (nearly 500) and longer time histories

(through 1990) at each station, was comprised of peak 3-second wind speed annual maxima. By use of a station data pooling method—known as the "superstation" approach (Peterka and Shahid 1998)—this database was used to create the basic wind speed maps found in ASCE 7 publications from 1995 through 2010.

2.3. Current Extreme Wind Database

By the mid-2010's, the amount of recorded wind data had increased substantially and improved techniques for collecting and processing this wind data in useful ways (such as that described by Lombardo et al. (2009)) had emerged. It was at this point that the current extreme wind database, used in the creation of the basic wind speed maps found in ASCE 7-16, was developed (available at https://www.itl.nist.gov/div898/winds/NIST_TN/final_qc_data.htm). After the creation of the second extreme wind database in the 1990's, however, many changes in wind reporting schema had occurred. Automated observation stations (ASOS) were introduced, wind gust averaging times were changed to 5-seconds then to 3-seconds, and standard cup anemometers were replaced with sonic anemometers (Lombardo et al. (2016)). Each of these changes imparted different effects onto the wind time histories, but were largely corrected across the network in the database's post-extraction steps. Since the process for developing and standardizing this database is outlined in great detail by Lombardo et al. (2016) and NIST (2012), only the aspects most pertinent to this study are presented.

In summary, the current extreme wind database consists of wind time histories from nearly 1,200 observation locations around the contiguous United States. These observations originate from a larger meteorological repository called the Integrated Surface Hourly (ISH) 3505, which has since been replaced by the more contemporary ISD 3505 database by NCEI (Lott 2017). Time histories for each station are organized solely by USAF number, which are correlated with other station metadata using the ISH History Document—a precursor to the ISD

History Document discussed previously. These time histories span from as far back as the 1940's (for some stations) through 2010, as available. Contained within each time history are peak 3-second average wind speeds only; observations carried over from older databases are converted as necessary from fastest mile and 5-second average observations. Furthermore, these time histories are effectively thresholded such that they only include wind gusts over 25 knots—the reasoning for this is discussed more explicitly by Lombardo et al. (2009).

For the purposes of this study, two different incarnations of this *current* extreme wind database are considered. The first, referred to as the US Lower 48 (US L48) version, consists of 1,180 reporting locations and is the exact version of the database available online from NIST (2012). The second, referred to as the September 12 QC (Sep12 QC) version, is very similar to the first but contains data from 1,195 reporting locations and has been subjected to a more subjective quality control process than the US L48 version. Chapter 3 describes improvement to this current extreme wind database without differentiating between either of these two detailed versions, but Chapter 6 makes use of these two versions separately.

CHAPTER 3: IMPROVEMENTS TO THE CURRENT EXTREME WIND DATABASE

The current extreme wind database provides a thorough and quality-controlled set of observations to use for extreme value analysis, but improving it requires some additional considerations. Aside from any improvements and optimizations of specific extraction parameters or techniques, more raw data is available in 2018 for inclusion in an updated extreme wind database than was available in 2010. This is not only because of the elapsed time between these years, but because additional observation stations in the ASOS network began recording during that time. Since the current extreme wind database only utilizes observations from stations with at least 5 or more years of data (NIST 2012), data from stations added to the network from 2007 onward are effectively excluded. Between 2007 and 2017, approximately 450 additional ASOS stations were added to the network (and hence, their data added to the ISD 3505 dataset) that are geographically distinct from each other and from the stations already comprising the current database. Figure 3.1 describes these changes graphically, with blue bars indicating station additions used for the current extreme wind database and yellow bars indicating station additions that were not previously considered. It is clear from the plot that the set of stations used for the current database can be no longer considered complete. Given this notion and a lack of specific information about which stations were added (and removed) over time, a complete re-extraction of wind data from the ISD 3505 was found to be the most certain path towards database improvement.

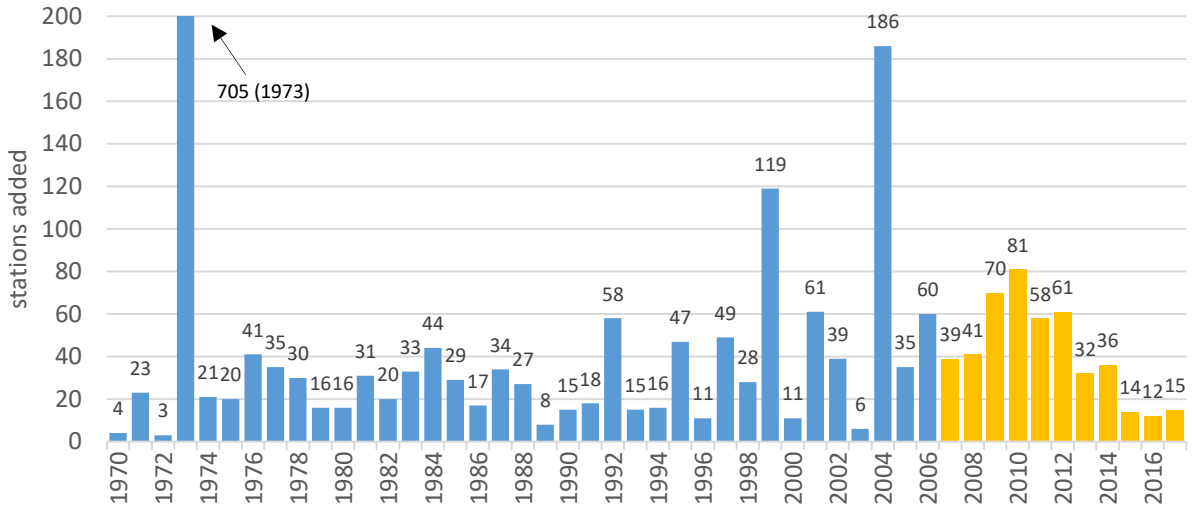

Figure 3.1. Bar graph depicting the number of ISD 3505 observation stations added in the contiguous United States per year. Blue bars indicate station additions before 2007 and yellow bars indicate additions after 2007.

The steps discussed in the following subsections outline the general methodology used to extract wind data from its source and to re-create an updated version of the current extreme wind database. While the steps in this report are presented as being largely linear in organization, the process was actually highly iterative and in many cases required backtracking or multiple attempts of various steps. Most instances of these "non-linearities" are omitted from this report for brevity and clarity such that only steps impacting the resultant extreme wind database are described.

3.1. Initial Station Selection

A complete re-extraction of extreme wind data from the parent dataset, ISD 3505, begins by a thorough investigation of what data is available. NCEI provides extensive metadata documentation for its meteorological observations stations, including the ASOS network. This includes the aforementioned ISD History Document, which details station metadata such as identification information (USAF, WBAN, call sign), location, elevation and timespan of activity, and an additional ISD Inventory Document which enumerates the number of records per

month found in the database for each station (NCEI [c]). Aside from the ISD 3505 itself, these two resources provide the best picture of what information is available.

Before any filtering or analysis, some important definitions were constructed. The ISD History document (as well as the database itself) organizes reporting stations using both USAF numbers and WBAN numbers together (Lott 2017). In other words, it is the combination of one USAF number and one WBAN number that provides a truly unique station identity within this database since some USAF numbers and WBAN numbers may be duplicated across different geographic locations. Therefore, for the purposes of this study, a "station" was defined as a single USAF-WBAN pairing corresponding to a single entry line in the ISD History document.

Initially, it is assumed that each constituent station of the ISD 3505 network reports data that is useful for extreme wind analysis. While this is not true for all stations (see Section 3.4), it allows the full re-extraction process to include as many stations—and as much useful data—as possible. Using the ISD History document, stations were filtered by geographic location using their assigned "country code" and their given latitude and longitude coordinates. Since the contiguous United States is the focus of this study, only stations assigned a country code of "US" *and* whose latitude and longitude lie within the box formed by 24° N -- 51°N -- 66°W -- 126°W were utilized. This winnowed the list of stations in the ISD History from over 35,000 down to just 6,417.

3.2. First Station Groupings

Within this filtered list, however, it was found that many stations were co-located with one another geographically. This can be observed by a number of entry lines having identical or highly similar metadata, as exemplified by the six Abilene/Dyess Air Force Base entries in Table 3.1. Possible explanations for these duplications include prescribed changes in identification numbers over time, physical relocation/updating of observation equipment, repurposing of the

surrounding infrastructure (i.e. converting from an Air Force base to a municipal airport), or even a duplicate set of observation equipment coming online. Regardless of the reason, however, it is evident that selecting just a single station to represent a location's extreme wind history could overlook large portions of available data at that location. This notion is exemplified further by the composite time history for Corbin, KY plotted in Figure 3.2, where different USAF-WBAN pairings comprise mutually exclusive portions of the location's time history. Given these issues with station identification and co-location, it was necessary then to group the 6,417 stations by location such that a comprehensive wind time history for all distinct locations could be created.

Table 3.1. Adapted ISD History document entries pertaining to Dyess Air Force Base in Abilene, TX. Six different USAF-WBAN pairings were found corresponding to this location.

USAF	WBAN	DESCRIPTION	STATE	CALL	LAT	LON	ELEV	BEGIN YR END YR
690190	13910	ABILENE DYESS AFB	TX	KDYS	32.433	-99.85	545.3	1943 2018
720965	13910	DYESS AIR FORCE BASE	TX	KDYS	32.433	-99.85	545	2016 2018
722665	13910	ABILENE DYESS AFB	TX	KDYS	32.433	-99.85	545.3	1973 1988
999999	13910	ABILENE DYESS AAF	TX	KDYS	32.433	-99.85	545.3	1971 1971
690190	99999	DYESS AFB/ABILENE	TX		32.417	-99.85	545	2000 2007
720965	99999	DYESS AFB/ABILENE	TX	KDYS	32.417	-99.85	545	2011 2018

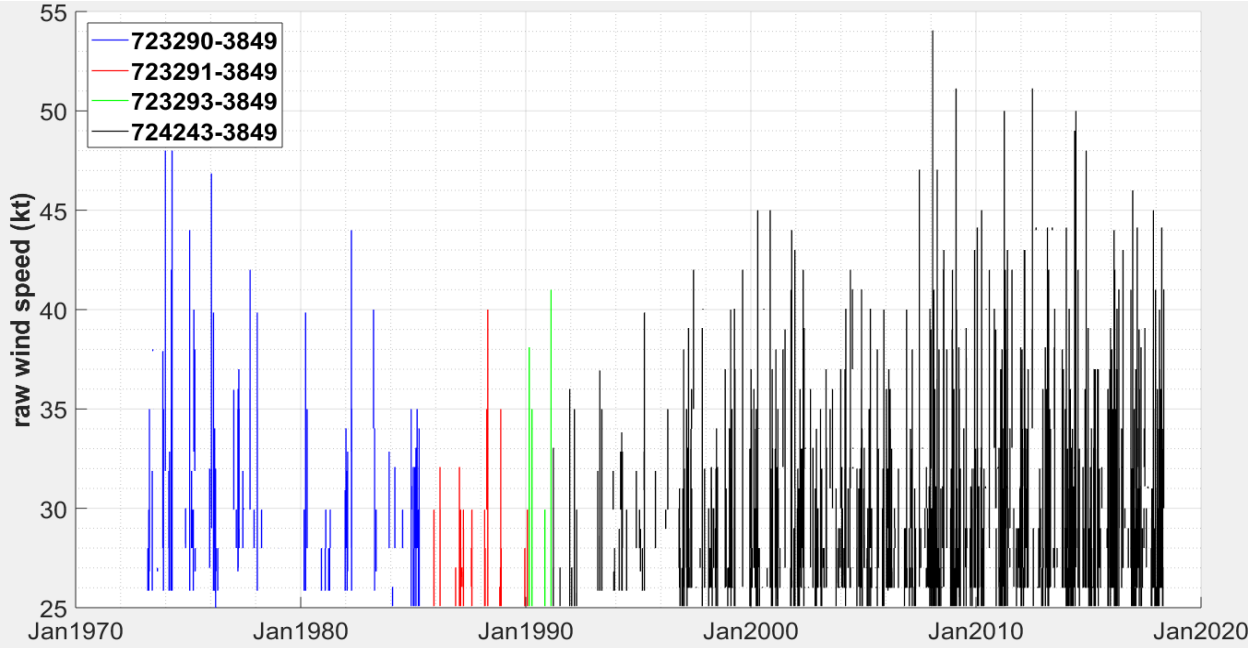

Figure 3.2. Wind speed time history (records over 25 knots only) observed in Corbin, KY comprised of data from four separate stations as defined in the ISD History document.

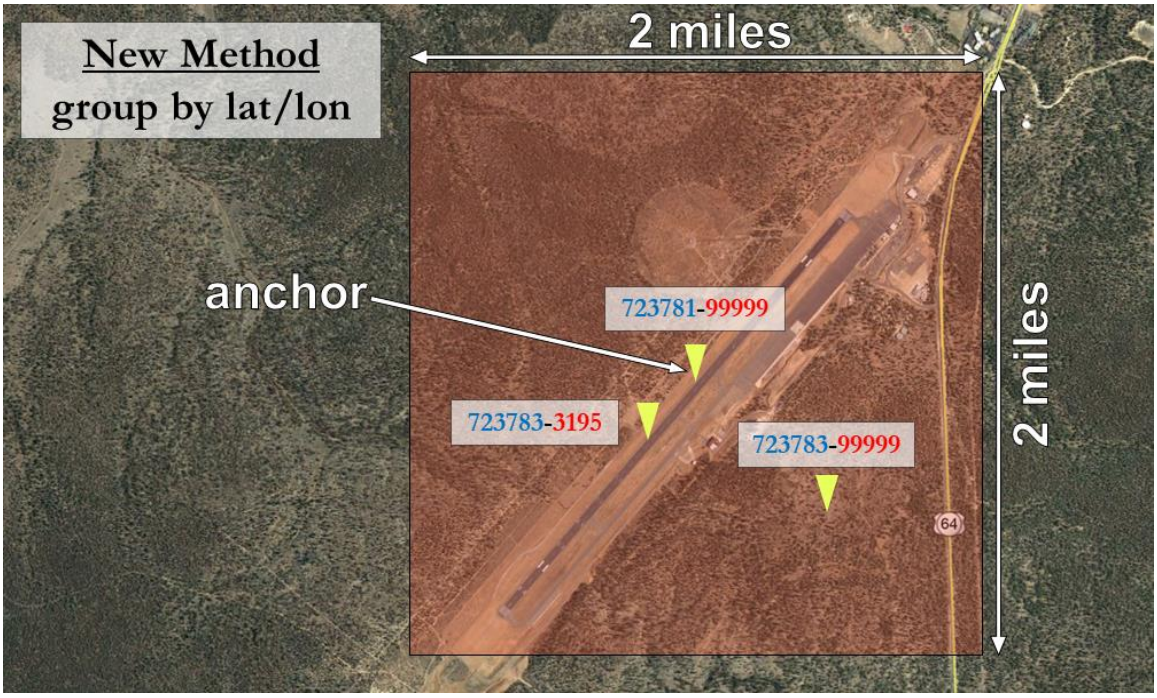

Figure 3.3. Example of the station grouping algorithm implemented at three stations near Grand Canyon, AZ. A 2-mile by 2-mile box constructed around the anchor station identifies two additional stations for grouping.

To group stations together, a grouping algorithm was developed that iteratively assigned stations to location-specific groups. The 6,417 stations' entries in the ISD History document were first sorted by ascending USAF number and were analyzed in that order. The first station

in the list was considered to be an "anchor station" and a square box measuring 2 miles by 2 miles was constructed evenly centered on its latitude and longitude coordinates. Any *other* stations with coordinates inside this box were then grouped with the anchor station. If no other stations were found inside this box, the anchor station was considered to be its own group. Iteration proceeded such that the next ungrouped station became the new anchor station and another box was constructed; further groupings were assigned in this manner until all stations were assigned a group. An example of this process using stations near Grand Canyon, AZ is shown in Figure 3.3, where yellow triangles denote station locations in the same general area.

This process yielded 3,824 geographically-distinct groupings formed from the original 6,417 stations—an average of approximately two stations per group. These groups were "mapped" to a matrix-style architecture shown in Figure 3.4, where groups occupy the "i-dimension" (vertical) and stations within each group occupy the "j dimension" (horizontal). For easier identification, the j-dimension columns are assigned "channel names" from Alpha through Theta, though not every channel of each group is occupied.

Group	Alpha	Beta	Gamma	Delta	Epsilon	Zeta
1	'423630-99999'	'720352-99999'	[]	[]	[]	[]
2	'690014-99999'	[]	[]	[]	[]	[]
3	'690020-93218'	'690020-99999'	'723884-93218'	'723914-93218'	[]	[]
4	'690070-93217'	'724916-93217'	'999999-93217'	[]	[]	[]
5	'690090-99999'	[]	[]	[]	[]	[]
6	'690110-99999'	'725377-14804'	'725377-99999'	'999999-14804'	[]	[]
7	'690138-99999'	'722148-63824'	'722148-99999'	[]	[]	[]
8	'690140-93101'	'722908-99999'	'999999-93101'	[]	[]	[]
9	'690150-93121'	'690150-99999'	'698114-99999'	'723814-93121'	'999999-93121'	[]
10	'690170-99999'	'690174-99999'	'720675-99999'	[]	[]	[]
11	'690190-13910'	'720965-13910'	'722665-13910'	'999999-13910'	[]	[]
12	'690190-99999'	'720965-99999'	[]	[]	[]	[]
13	'690200-99999'	[]	[]	[]	[]	[]
14	'690210-99999'	[]	[]	[]	[]	[]
15	'690220-99999'	[]	[]	[]	[]	[]

Figure 3.4. Example of the matrix-style group mapping architecture.

The grouping algorithm was executed multiple times to investigate the sensitivity of group count on the dimensions of the constructed box around each anchor station. The results, plotted in Figure 3.5, show very gradual decay in group count with increasing box size (length of a single leg on a square box) for box sizes larger than about 2 miles. From 0.1 to 2 miles, however, group count decreases much more rapidly, indicating that 2 miles marks a possible shift in the overall grouping mechanism itself. To ensure that data from grouped stations truly represent the extreme wind climate at a specific point in space and that no obviously disjoint records are combined (i.e. data from two airports that are near each other but are distinct facilities), the box size was kept at 2 miles by 2 miles for the initial set of groupings (further analysis on this is discussed in Section 3.5).

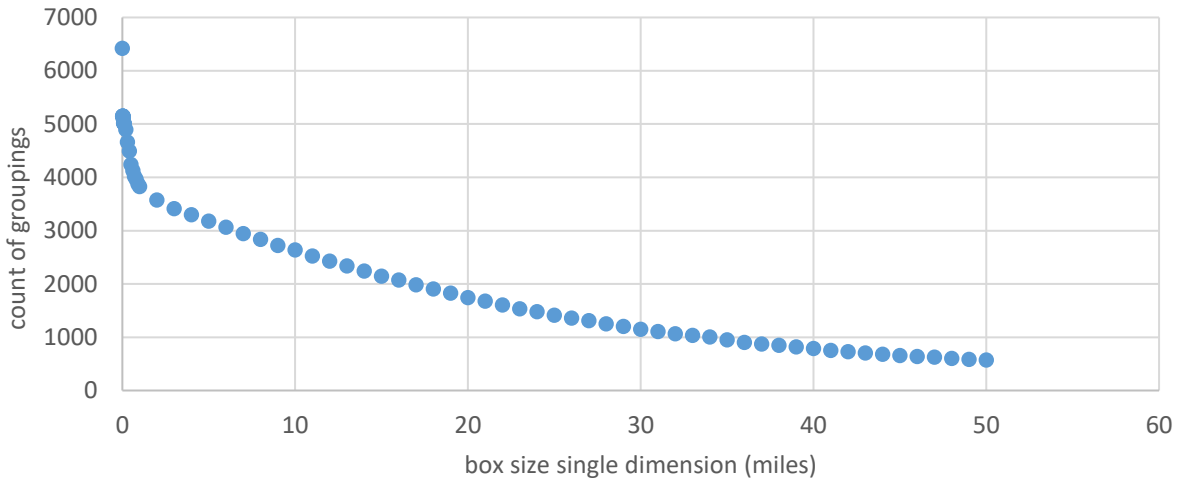

Figure 3.5. Sensitivity analysis results for box size versus number of groupings. Group count decreases quickly from 6,417, where every station is ungrouped.

3.3. Preliminary Raw Data Download

With the initial set of 3,824 station groupings established, an initial download of raw data corresponding to each of the 6,417 stations was conducted. Within the ISD 3505 online access protocol (accessible at ftp://ftp.ncdc.noaa.gov/pub/data/noaa), raw data files are organized in folders by year (from 1901 through present), then sorted by their reporting station's USAF,

WBAN, and corresponding year. For example, a file corresponding to year 2010 for Champaign, Illinois (USAF: 723515 and WBAN: 94870) would appear as "725315-94870-2010.gz" in the folder named "2010". To ensure a complete download for each station, folders were scanned for matching files for each year contained within the beginning/end dates given in the ISD History document (see Table 3.1). Since the ISD History document was acquired in March 2018, no data was acquired for observations after this time (i.e. each "2018" file contained only a partial year of data at the time of download). So for the Champaign, Illinois example, if the 723515-94870 station was shown to begin in 2006 and end in 2018, then all year-folders from 2006 to 2018, inclusive, would be scanned for files containing 723515-94870. In total, 95,322 files were downloaded using this framework and each was sorted by state then by its assigned grouping. This process yielded two important findings.

First, it became clear that there were a number of inconsistencies between latitude/longitude, description, and state code metadata within the ISD History document, as raw data files for some groupings were inadvertently sorted into two different states. To fix this, a manual quality control process was enacted that found which stations had these inconsistencies, edited the ISD History document accordingly, and re-sorted the raw data files into their proper location as needed. For each manual change, it was assumed that USAF, WBAN, and latitude/longitude were correct and thus adjustments were made only to the description and/or state code. Of the 3,824 groups identified, 67 groups were found to have at least one of these inconsistencies in their metadata (see Appendix A for details). For all 67 groups, state codes were manually updated. Descriptions were further manually edited in 8 of these 67 groups. 3 stations were deleted outright from 2 other groups because of their short timespan (less than 2 years) and relative non-recency (all before 1970). This reduced the number of stations in

consideration to 6,414; the number of groupings, however, remained at 3,824 as none were created or deleted in this particular step.

Secondly, this process revealed which years (files) of data are available for each station, including which years are missing from the database altogether. The years with available data were logged and used to inform a second full data download described in Section 3.7. After cross-referencing the downloaded files with the time ranges given in the ISD Inventory document, it was determined that 30 files—from 30 different stations and 25 different station groupings—were missing altogether from the ISD 3505 database. A manual check of these 30 files (see Appendix A) confirmed this result. Despite this finding, it is not likely that the absence of these files impacts the larger body of work, as the 30 stations with missing data represent 0.47% of all 6,414 stations in the study and the 30 missing files represent 0.03% of all 95,522 raw files in total.

3.4. Preliminary Extraction of Basic Wind Gust Data

Since the data of interest for this study is extreme wind data, is thus useful to know which stations of the 6,414 stations (and 3,824 groupings) have raw wind data useful for analysis. To make this determination, wind gust speeds (over 25 knots), directions, and timestamps were extracted from the downloaded raw data files using the automated text-parcing methodology explained by Lombardo et al. (2009); no standardization, storm type separation or independence calculations were done in this round of extraction. Results and process metadata were stored in a MATLAB-styled data structure (rather than in individual spreadsheets as done with former databases) in order to make post-analysis steps more efficient. The layout of this data structure follows the same organization of the "group map" shown in Figure 3.4, where any entry (i, j) corresponds to the j-th station within the i-th identified grouping. The results of the wind data extraction process showed that, of the 6,414 stations and 3,824 groupings processed, 4,324 and

2,600 were found to have least one 25+ knot wind gust record in their reported wind time history, respectively. These results are visualized in an updated version of the group map matrix, shown in Figure 3.6, where stations containing useful wind gust data are shaded green.

Group	Alpha	Beta	Gamma	Delta	Epsilon	Zeta
1	423630-99999	720352-99999				
2	690014-99999					
3	690020-93218	690020-99999	723884-93218	723914-93218		
4	690070-93217	724916-93217	999999-93217			
5	690090-99999					
6	690110-99999	725377-14804	725377-99999	999999-14804		
7	690138-99999	722148-63824	722148-99999			
8	690140-93101	722908-99999	999999-93101			
9	690150-93121	690150-99999	698114-99999	723814-93121	999999-93121	
10	690170-99999	690174-99999	720675-99999			
11	690190-13910	720965-13910	722665-13910	999999-13910		
12	690190-99999	720965-99999				
13	690200-99999					
14	690210-99999					
15	690220-99999					

Figure 3.6. Updated group map matrix with useful stations identified with green shading. Groupings with no useful wind data in any station, such as groups 13 and 15, were hence eliminated from further analysis.

Also generated in this extraction step was a list of all raw data file names that were found to contain wind gust data. This information forms a wind gust "datastream" for each station and is useful for visualizing the overall breadth and duration of the extreme wind data available. In Figure 3.7, the number of files containing useful wind data is plotted against the number of groups with at least that many files in their datastream. So for example, 2,600 groups have at least one useful raw data file among their constituent stations (as stated previously). Approximately 2,050 groups have at least 10 useful files and around 1,000 groups have at least 30 useful files. Since files correspond to individual years of available data, Figure 3.7 also offers a preliminary insight as to how many station groupings have a sufficiently-long time history for extreme value analysis, the accuracy of which increases with increasing length of time history.

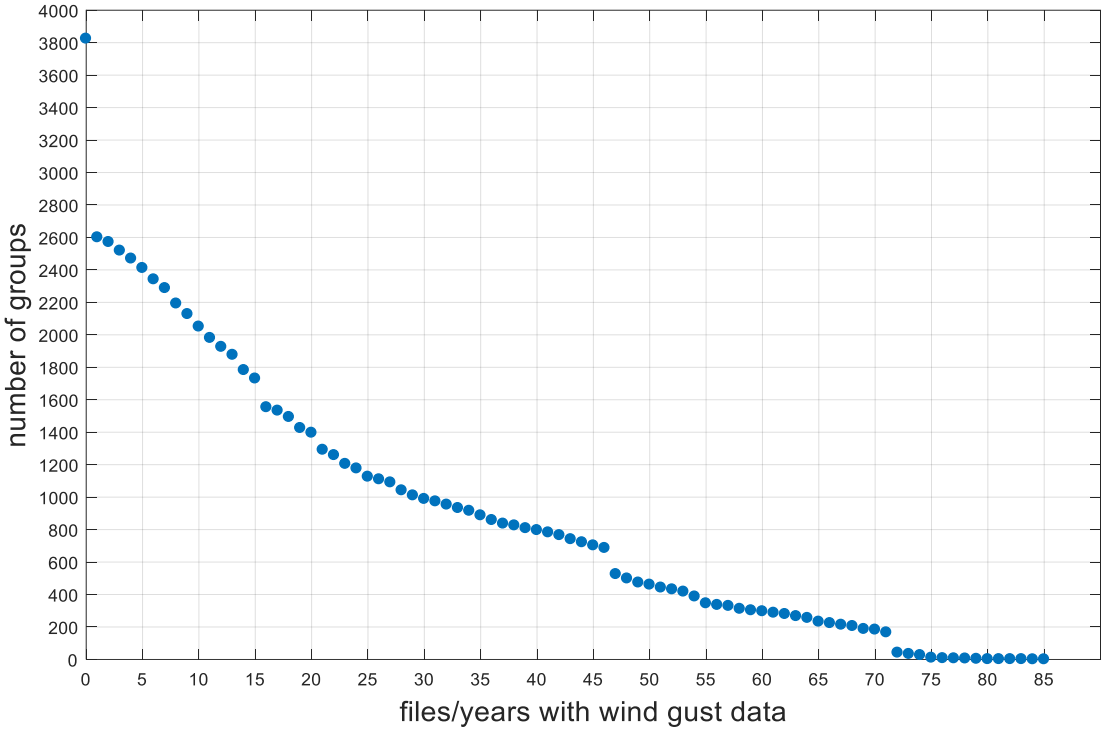

Figure 3.7. Number of groups containing at least the corresponding number of files (or years) of useful wind gust data.

3.5. Quality Control of Station Groupings

While the initial station groupings generated by the analysis in Section 3.2 provided a reasonable first estimate for organizing the stations by location, it became evident upon further inspection of the 2,600 groups identified in Section 3.4 that additional quality control of the groupings was necessary. This determination was made primarily due to the observation that stations with the same or similar descriptions were still grouped separately. Closer inspection revealed that, in some cases, a 2 mile by 2 mile box constructed around an anchor station was not always large enough to include all stations intending to represent the same facility. Air Force bases, which can be many square miles in size, are an example of this particular dilemma. Compounding this issue further is the fact that many stations' coordinates given in the ISD History document lack the decimal precision required to make an accurate assessment of their locations. While most coordinate pairs are reported to the nearest one thousandth of a degree

(approximately 0.069 miles north-south and 0.049 miles east-west at 45° N), some are reported only to the nearest tenth (6.9 miles north-south and 4.9 miles east-west at 45° N). A spot-check of some stations with low-precision coordinates using satellite imagery revealed some largely non-sensical situations, including stations being located the middle of open desert (St. George, UT), in a lake (Litchfield, MN), on a city street (Ontario, CA), or on a residential building (Brookings, OR).

To remedy the issues of optimal box size and imprecise coordinates, a manual quality control process for groupings was developed. First, the 2,600 established groups shown to contain useful wind gust data were examined systematically to see which were close together geographically. Similar to the initial grouping algorithm, a box was constructed around the anchor station of each group and any other groups with constituent stations inside this box were paired with the anchoring group, essentially forming "groups of groups" or "sets". The box size chosen for this analysis was one corresponding to +/- 0.1° latitude and longitude on all sides of the anchor station (a box roughly 14 miles tall by 10 miles wide, depending on the overall latitude). This process yielded 283 sets of nearby station groupings (consisting of 582 groups and 869 stations total) for further manual consideration.

An additional search consisted of finding stations with the same call sign that were not grouped together. Upon closer inspection, it was determined that a number of stations were incorrectly left unpaired in the initial grouping process simply because their coordinates were highly mismatched (Figure 3.10). This second search yielded an additional 22 sets of groupings (44 groups and 45 stations total), bringing the total number of sets for quality control to 295.

For each of the identified 295 sets, the constituent stations were evaluated individually based on their location, description, call sign, begin/end dates, and supporting satellite imagery. The underlying principle supporting this evaluation was that all stations observing data at the same facility—no matter how large the particular facility is—should be grouped together. This notion obviously has limitations since there are some facilities so vast (such as Cape Canaveral Air Force Station in Florida) that multiple stations located within them might accurately report different wind conditions, especially in the presence of small-scale wind events like thunderstorms. In most cases, however, this logic was found to be suitable for individual grouping evaluations. Figure 3.8, for example, shows satellite imagery of two stations (each comprising a separate group) located at Sarasota-Bradenton International Airport in Florida. The two stations were not grouped together in the initial grouping process due to their distance apart, but it is evident from the image and supporting metadata that they both intend to serve the same airport.

Figure 3.8. Satellite imagery confirming that two station groups should be combined into a single group since they are located at the same airport.

Based on all available information, including additional research on facility configuration and history, each set was carefully scrutinized to determine if its constituent groups should be merged. If it was obvious that two or more groups in a set serve the same facility, then the stations within both groups were combined into a single grouping. Conversely, if it was obvious that two groups do not serve the same facility *or* if there was not enough information available to make a decision, then groupings were left in their original configurations. Figure 3.9 shows a scenario in Harrisburg, PA where two groups were rightfully left uncombined as each group was found to clearly represent a separate (albeit nearby) airport. For some situations, as exemplified in Figure 3.10, where various pieces of the metadata were determined to actually be incorrect (thereby affecting the grouping organizations), manual edits were made to the ISD History document to ensure consistency (see Appendix A). In all, this extensive quality control process resulted in the elimination of 153 station groupings and a final group tally of 2,447 geographically-distinct groups. Since no stations were removed in this step, the number of total stations remained at 4,324.

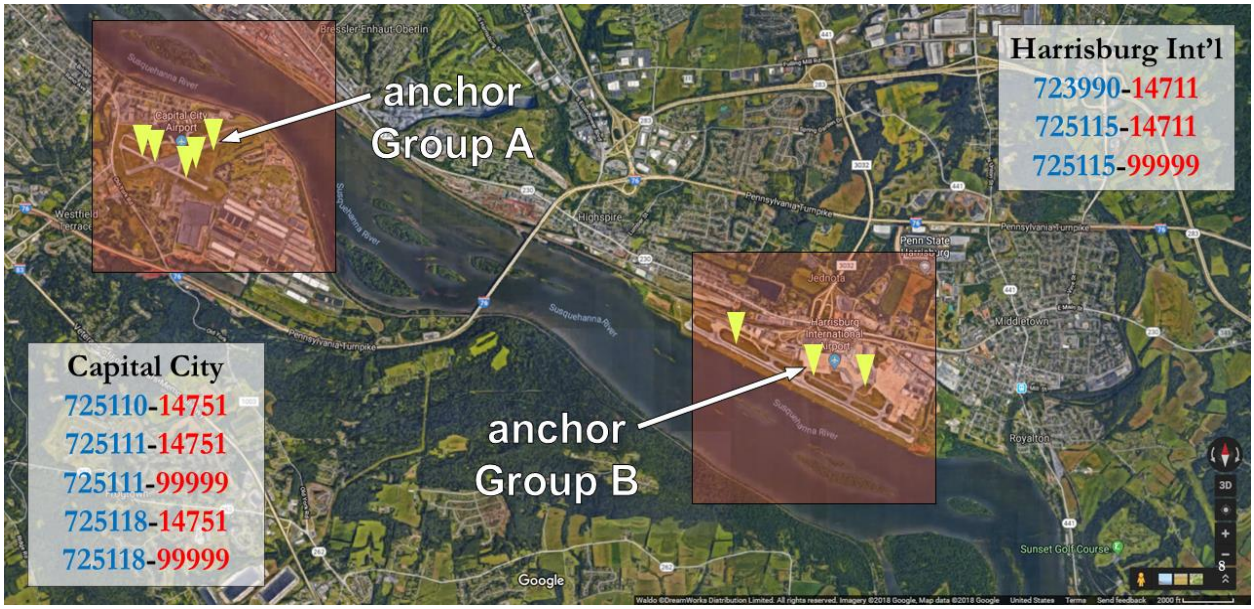

Figure 3.9. Satellite imagery with original grouping scheme (2 mile by 2 mile boxes) overlaid. The two groupings are close together geographically but are clearly associated with different facilities.

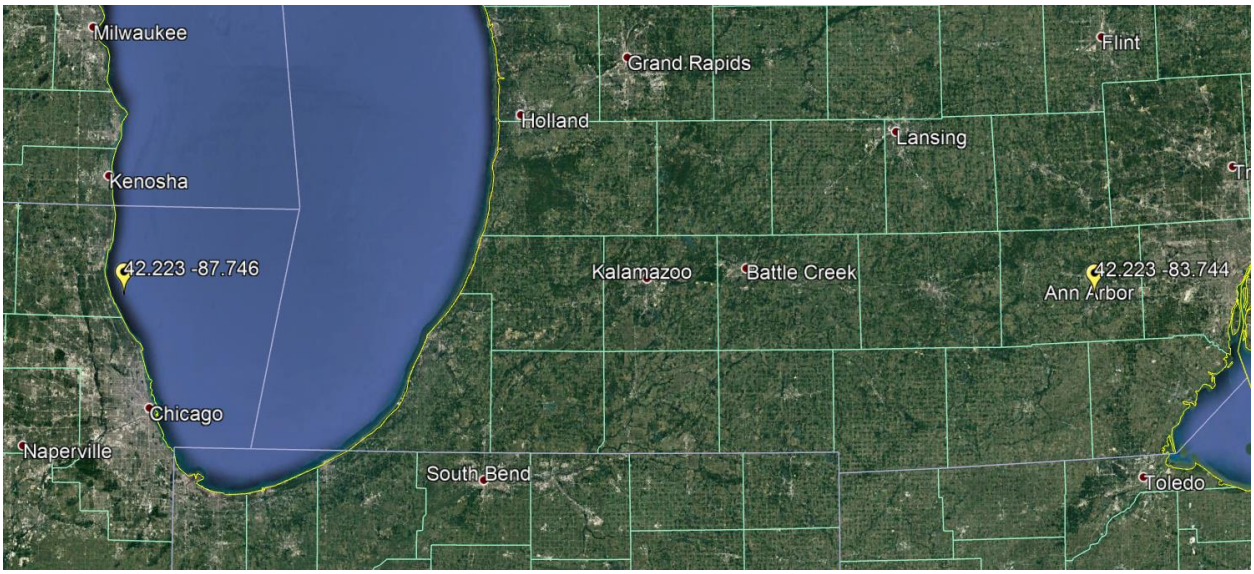

Figure 3.10. Satellite imagery depicting two stations with the same call sign (KARB) and similar descriptions (Ann Arbor Municipal Airport), one of which has clearly erroneous coordinates. The two groupings were combined and the erroneous metadata was corrected.

3.6. Updating the Tropical Event Sub-Database

Before the extreme wind database could be fully updated, however, it was necessary to also update the tropical event "sub-database" such that wind events from 2010 to 2018 could be properly categorized by event type. Since the ISD 3505 dataset does not provide information regarding tropical events (such as hurricanes), use of an additional resource—HURDAT2—was required. The HURDAT2 dataset, maintained by the Hurricane Research Division of NOAA, is a large catalog of all North American tropical events occurring from 1851 to 2017 (Landsea et al. 2014). Nine types of events are documented, including hurricanes, tropical storms, and tropical depressions. For each tropical event, best estimates are provided for its track (location and time, every 6 hours), intensity (maximum wind speed and minimum barometric pressure), and wind field (radii corresponding to different wind speeds at four quadrants).

To utilize this information in the extreme wind database, tropical events and wind reporting stations were algorithmically matched in space and time. First, a uniform radius was chosen to represent the geographic extent of tropical event influence as measured from the center

of any event. Since 200 kilometers was used for creating the existing extreme wind database (NIST 2012), 200 kilometers was selected for this analysis as well. From there, the tropical event tracks were refined to obtain a center location for every 3 hours in time; this was done by linearly interpolating the midpoint between each location reported at 6-hour intervals. Doing this ensured that fast-moving tropical events were adequately captured in space using a static 200 kilometer radius of influence. Figure 3.11 shows the theoretical basis for this midpoint interpolation; the "9am" circles represent interpolated storm locations three hours apart from the "6am" and "12pm" storm locations provided by HURDAT2.

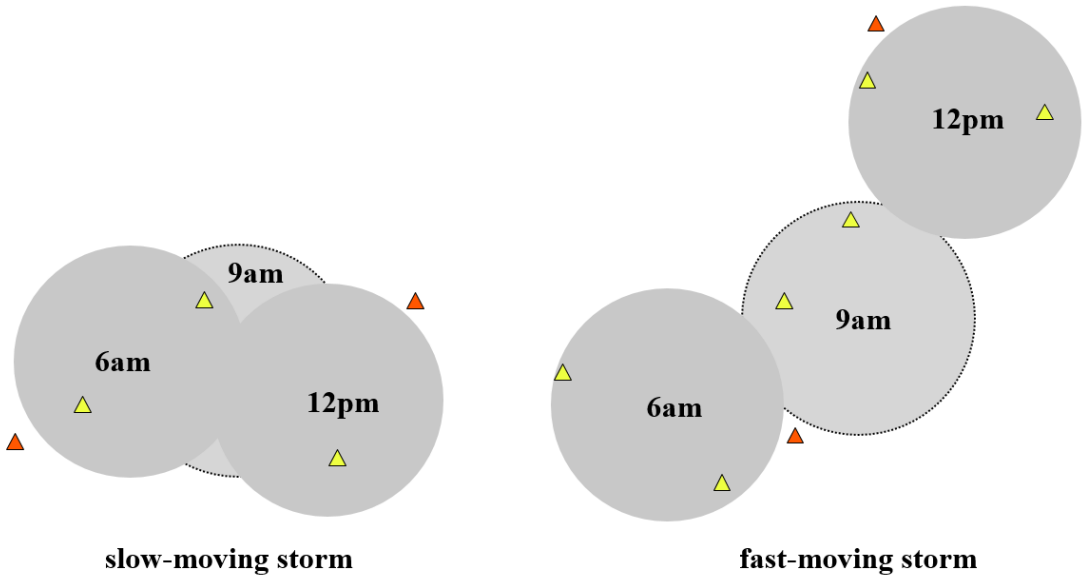

Figure 3.11. Diagram showing the usefulness of a 3-hour midpoint interpolation. Hypothetical reporting stations are shown as triangles—yellow is considered tropically influenced, red is not. Fast moving storms without a 3-hour midpoint might influence some stations but not others along their path.

To make the final evaluations, a rudimentary time-step model was created to plot the movement of tropical events through time (represented by 200 kilometer circles centered on their HURDAT2-specified coordinates) over a static map of contiguous United States weather observation stations. A single frame of the model corresponded to one discrete location and time (every 3 hours) of a single tropical event. For each frame, three 200-kilometer circles were

constructed: one at the tropical event's current location, and one each at the locations +/- one time step from the current frame. Any observation stations located within any of these three constructed circles were classified as tropically-influenced for the entire block of time corresponding to +/- 1 time step (+/- 3 hours, 6 hours total). This process was executed for all tropical events (including sub-tropical and extra-tropical events) from 1851 through 2017 found in the Atlantic basin set of the HURDAT2 records. Pacific basin records were not analyzed as their impact on contiguous United States wind records was expected to be insignificant.

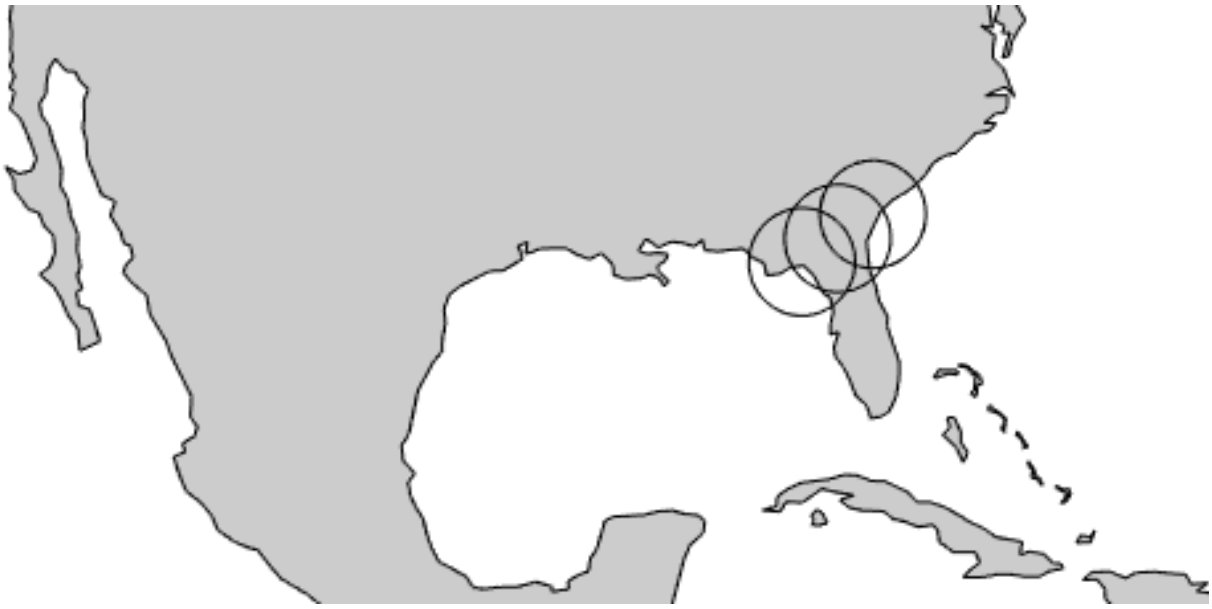

Figure 3.12. Three frames (6 hours) plotted for a tropical event in the southeast United States. Any reporting stations (not shown) within these circles were considered tropically influenced for the six hours depicted.

The result of this analysis was a list of tropical event times and the corresponding weather observation stations affected at those times. Together, these formed the tropical event "sub-database" which spanned the full extents of the updated extreme wind database in both time and space. This updated tropical event information was used to inform post-extraction analyses of extreme wind data discussed in Section 3.7.

3.7. Final Database Creation

With the improvements to post-extraction analysis techniques ready and a rigorous assessment of station organization complete, the final, improved, and updated extreme wind database was created. This was accomplished by a second full raw data download and a more detailed extraction procedure informed by the results of Sections 3.1 through 3.6. Despite having already downloaded a full suite of raw data in Section 3.3, the downloading portion was repeated to ensure proper organization of files by the updated grouping scheme and to prevent accidental deletion of useful download metadata from the first set (used to document the progress of this analysis).

Once the raw data was downloaded and organized into the 2,447 geographically-distinct groups, it was then processed using the overarching methodology described by Lombardo et al. (2009). The text-based raw data files were scanned for character strings indicating wind gusts—including "PK" and "OC1"—and the resultant raw wind time histories were assembled into "station matrix files". To control from including wildly unrealistic wind speeds, a simple automated quality control scheme was implemented for individual wind gusts as described in Table 3.2. Note that gusts within the 75 knot to 110 knot range, while not included in the record, are documented such that they could be included upon further evaluation.

Table 3.2. Quality control routine implemented for ISD 3505 wind gusts.

Wind Gust Speed	**Action Taken**
Less than 75 knots	Considered "acceptable" – included
Between 75 and 110 knots	Considered "suspect" – excluded but documented for future evaluation
Over 110 knots	Considered "erroneous" - excluded

Since anemometer heights, anemometer types, and wind reporting schemes are not consistent across all stations and all periods of time (Lombardo 2012), the raw wind speeds were adjusted to a standardized 10-meter height and 3-second averaging time using a power law profile approximation (Holmes 2015). To standardize from varying heights to a consistent 10-meter height, sectorial terrain roughness values (z_0) were used as developed by Masters et al. (2010). The area surrounding each station was partitioned into eight even directional sectors—each assigned their own surface roughness. The surface roughness values were then used to approximate a power law exponent (α) for each sector, as shown in Equation 3.1 (adapted from ASCE 7-16).

$$\alpha = 5.65 * (z_0^{-0.133}) \quad \text{(Eq. 3.1)}$$

To standardize averaging time to 3 seconds, Durst curve approximations (corresponding to the sectorial surface roughness) were used as applicable (Simiu and Scanlan 1996). Finally, the standardized wind speed was calculated in accordance with Equation 3.2 (from ASCE 7-16).

$$U_{std} = \left(\left(\frac{z}{10}\right)^{\frac{1}{\alpha}}\right)^{-1} * U_{raw} * V_{rat} \quad \text{(Eq. 3.2)}$$

Where

U_{std} = standardized wind speed

U_{raw} = raw wind speed

z = height of raw wind speed observation

α = power law exponent

V_{rat} = wind speed multiplier from Durst curve

This standardization process was used for wind speeds at all stations with existing surface roughness information. For any locations or sectors where roughness data was not available, surface roughness was assumed to be that of "open terrain" and a lower-bound z0 value of 0.03

meters was used. If instead the height of the anemometer was not known, then the anemometer was assumed to be at the standard 10 meters height. For all stations where any of these assumptions were made during this process, an indicator of these assumptions was cataloged in the extraction metadata for later reference.

Following standardization, some post-extraction analyses were performed to facilitate the extreme value analysis methods described in Chapter 5. First, the standardized wind gust speeds were associated with a wind event type ("storm type") using thunderstorm identification information found within the raw data files (Lombardo et al. 2009) as well as information from the updated tropical event "sub-database". Each wind gust entry in the database was therefore associated with either a thunderstorm event or a non-thunderstorm event and (independently) with a tropical event or a non-tropical event (i.e. a single wind gust could be labeled as tropical and thunderstorm simultaneously). Secondly, the wind gust records were scanned to identify discrete and independent wind events within them. This was done using an interval separation algorithm developed by Lombardo et al. (2009) that identifies "independent" events based on a chosen "separation interval"–an amount of time that must exist between individual wind events of the same storm type. For this study, separation intervals of 4 days, 6 hours and 4 days were used for non-thunderstorm events, thunderstorm events, and all events together (commingled), respectively. Finally, wind speed annual maxima were determined. In other words, the timestamps corresponding to the highest wind speed of each year (and for each storm type) were identified.

The results of all extraction, standardization, quality control procedures (including metadata) were compiled into a structure array organized identically to the group mapping scheme shown in Figure 3.4. Upon reaching this stage, the final consolidation of stations within groupings occurred. For each row (each group) of the structure array, data was combined from all columns (all constituent stations). Wind gust time histories, file identifiers, and results of the post-extraction analyses were combined and re-ordered chronologically, as shown in Figure 3.13. For groups where wind gust records from different stations overlapped in time, records were meshed in an alternating fashion such that no records were deleted, as displayed in Figure 3.14. Station metadata was combined such that representative values of each became the "nominal metadata" for the particular grouping. Table 3.3 describes the nominal metadata procedures in more detail. All other information was combined by simply appending stations' information together to form a final 2,447 by 1 structure array containing the completed extreme wind database.

Filestamp: USAF	Filestamp: WBAN	Filestamp: YEAR	Timestamp	Wind Speed (Raw, kt)	Wind Speed (standardized, mph)	Wind Direction (deg)	Non-Thunderstorm	Independent Non-Thunderstorm	Thunderstorm	Independent Thunderstorm
723448	99999	1992	4/20/1992 19:00	29.9376	34.39446303	240	1	1	0	0
723448	99999	1992	7/5/1992 0:00	25.8552	29.79520344	340	1	1	0	0
723448	99999	1992	10/8/1992 18:00	27.9936	31.69489762	230	1	0	0	0
723448	99999	1992	10/8/1992 20:00	26.8272	30.69505857	240	1	0	0	0
723448	99999	1992	10/8/1992 21:00	29.9376	34.49444693	240	1	1	0	0
723448	99999	1992	10/14/1992 17:00	26.8272	30.59507467	200	1	1	0	0
723448	99999	1992	11/2/1992 1:00	30.9096	35.19433426	230	1	1	0	0
723448	99999	1992	12/10/1992 15:00	25.8552	29.39526782	290	1	0	0	0
723448	99999	1992	12/10/1992 17:00	28.9656	33.7945596	290	1	0	0	0
723448	99999	1992	12/10/1992 18:00	32.8536	37.69393187	320	1	1	0	0
723448	99999	1992	12/15/1992 22:00	25.8552	29.49525172	230	1	1	0	0
723448	99999	1993	1/24/1993 6:00	27.9936	32.49476885	310	1	1	0	0
723448	99999	1993	2/21/1993 15:00	28.9656	33.19465618	230	1	0	0	0
723448	99999	1993	2/21/1993 16:00	28.9656	33.49460789	240	1	0	0	0
723448	99999	1993	2/21/1993 17:00	33.8256	38.4938031	250	1	0	0	0
723448	99999	1993	2/21/1993 18:00	37.908	43.2930305	260	1	1	0	0
723448	99999	1993	3/13/1993 5:00	26.8272	30.39510686	330	1	0	0	0
723448	99999	1993	3/13/1993 14:00	25.8552	29.79520344	320	1	0	0	0
723448	99999	1993	3/13/1993 16:00	26.8272	31.294962	310	1	0	0	0
723448	99999	1993	3/13/1993 18:00	26.8272	31.294962	330	1	0	0	0
723448	99999	1993	3/13/1993 20:00	27.9936	31.79488152	320	1	1	0	0

Figure 3.13. Sample combined wind gust time history in the "station matrix" format.

Filestamp: USAF	Filestamp: WBAN	Filestamp: YEAR	Timestamp	Wind Speed (Raw, kt)	Wind Speed (standardized, mph)	Wind Direction (deg)	Non-Thunderstorm	Independent Non-Thunderstorm	Thunderstorm	Independent Thunderstorm
723448	99999	2007	2/6/2007 22:00	25.0776	28.7953644	240	1	0	0	0
723448	53934	2007	2/13/2007 17:15	25.0776	28.59539659	310	1	0	0	0
723448	99999	2007	2/13/2007 17:15	25.0776	29.09531611	310	1	0	0	0
723448	53934	2007	2/13/2007 19:55	25.0776	28.69538049	310	1	0	0	0
723448	99999	2007	2/13/2007 20:00	25.0776	29.19530001	310	1	0	0	0
723448	53934	2007	2/13/2007 23:35	26.0496	29.89518734	310	1	0	0	0
723448	99999	2007	2/13/2007 23:35	26.0496	29.49525172	310	1	0	0	0
723448	53934	2007	2/14/2007 1:15	25.0776	28.9953322	320	1	0	0	0
723448	99999	2007	2/14/2007 1:15	25.0776	28.8953483	320	1	0	0	0
723448	53934	2007	2/14/2007 1:55	27.0216	30.59507467	330	1	0	0	0
723448	99999	2007	2/14/2007 2:00	27.0216	31.49492981	330	1	0	0	0
723448	53934	2007	2/17/2007 14:15	25.0776	29.19530001	310	1	0	0	0
723448	99999	2007	2/17/2007 14:15	25.0776	28.49541268	310	1	0	0	0
723448	53934	2007	2/17/2007 14:35	27.0216	30.79504248	300	1	0	0	0
723448	99999	2007	2/17/2007 14:35	27.0216	31.09499419	300	1	0	0	0
723448	53934	2007	2/17/2007 15:55	27.0216	30.99501029	300	1	0	0	0
723448	99999	2007	2/17/2007 16:00	27.0216	31.1949781	300	1	0	0	0
723448	53934	2007	2/17/2007 16:15	26.0496	29.79520344	310	1	0	0	0

Figure 3.14. Sample combined wind gust time history where two stations reported over the same time interval. Records from both stations are included, even if they have the same timestamps.

Table 3.3. Methodology for assigning “nominal metadata” for each grouping using metadata from the constituent stations.

Metadata Type	**Action Taken**
USAF number	Use lowest USAF number out of stations in group
WBAN number	Use lowest WBAN number out of stations in group
call sign	Use first station CALL sign as appears in ISD History Document
station description	Use first station description as appears in ISD History Document
state	Use first state as appears in ISD History Document
latitude and longitude	Use average latitude and longitude among stations in group
elevation	Use average elevation among stations in group

CHAPTER 4: ADDITIONAL TECHNIQUES TO IMPROVE DATABASE ROBUSTNESS

In an effort to further improve the extreme wind database, additional techniques far outside the scope of current methodologies were explored. The two methods presented in this chapter focus on improving two specific aspects of an extreme wind database: temporal resolution and spatial resolution. This chapter details the general procedures of how these two methods were explored and provides some representative results of the analyses performed. A more ensemble-wide depiction of these results are presented in Chapter 6 along with network-wide results from the ISD 3505 database improvements discussed in Chapter 3. Additionally, flow charts detailing the methods developed in this chapter can be found in Appendix A.

4.1. Improved Temporal Resolution – DS 6405 Study

The network of weather observation stations that contribute to the ISD 3505 database generally conduct observations hourly (ASOS) or sub-hourly (AWOS). ASOS stations in particular are programmed to automatically begin recording higher frequency observations—as fast as several per minute—when weather conditions become highly variable (NWS). These periodic higher frequency observations, as well as the standard hourly observations, are all included in the ISD 3505 database together. These observations should theoretically comprise the complete body of wind data needed for extreme wind analysis, assuming that extreme wind events are adequately captured by the automatically-triggered high frequency reporting regimes. Given the automated nature of ASOS stations and the data collection issues that are known to exist (Powell 1993), however, it is useful to check the quality and completeness of their observed extreme wind speeds using other means. Fortunately, NCEI provides several other meteorological datasets in addition to the ISD 3505 that can serve this purpose.

4.1.1. Introduction to the Dataset 6405 (DS 6405)

One of the aforementioned additional datasets is NCEI's Data Set 6405 (DS 6405), which is comprised of meteorological data reported every minute at nearly 1000 ASOS stations within the contiguous United States since roughly year 2000 (NCEI 2006). DS 6405 time histories are parallel to those found in ISD 3505—they are reported at the same location using the same anemometer and averaging time. The key difference between the two, however, is how they treat the data. ISD 3505 wind data contains hourly observations and "highlights" during times of variable conditions, both of which are quality controlled. DS 6405 data, on the other hand, contains essentially every minute's worth of data and is not subject to any internal quality control procedures.

Included in DS 6405 are values for a 5-second wind gust speed (and direction), which is defined in the documentation as the maximum 5-second average wind speed observed over each 1-minute interval (NCEI 2006). According to Lombardo (2012), however, averaging time at ASOS stations changed from 5 seconds to 3 seconds with system-wide implementation of sonic anemometers that occurred in the early 2000's. This step change in averaging time, thus, is implicitly built into the DS 6405 raw wind speeds since no modifications were made to the archived dataset after being transmitted from the ASOS station (NCEI 2006). While some of the exact dates for averaging time transitions are available, there are known issues with converting wind speed records from one averaging time to another, especially using conventional methods such as the Durst curve (Lombardo 2012). Since the period of sonic anemometer use—that is, the use of a 3-second moving average—constitutes the majority of the reported time histories in the DS 6405 set, all DS 6405 wind gusts are therefore treated as 3-second averages for the purposes of this study. Despite the disparity in averaging time and lack of quality control, the DS 6405 wind gust data is promising since it provides—at least for the years 2000 to present—

an alternate and higher resolution view of the same extreme wind phenomena recorded in the ISD 3505.

4.1.2. DS 6405 Data Preparation

Wind data from the DS 6405 (high resolution data) was extracted and processed with the intention of direct comparison with data found in the ISD 3505. Therefore, high resolution data was only obtained from locations that were found to also have useful ISD 3505 wind data (see Section 3.4). This condition yielded a starting set of 890 stations with high resolution data for analysis, shown as a map in Figure 4.1. Within the DS 6405 online access portal, these 890 stations are all identified by their call sign, rather than by a USAF-WBAN pair as with ISD 3505 data. In order to facilitate comparisons with the ISD 3505, call sign identifiers for the 890 high resolution stations were correlated with station groupings (see Chapter 3) using information in the manually-edited ISD History Document discussed in Section 3.1. In some cases, call sign identifiers were manually paired with station groupings in situations where an automated matching system was insufficient.

High resolution data was downloaded from NCEI's online access portal and was compiled into an initial set of MATLAB-style data structures. In order to avoid excessively tedious record keeping, lists of files downloaded and not downloaded ("datastreams") were not made during this step (unlike with ISD 3505 in Section 3.4). Instead, all data from 2000 through late 2018 was attempted for download and any resultant gaps in the time histories were accommodated as discussed later in this section. For 582 of the 890 stations, files were found for all years from 2005 to 2018, affording a nearly 14 year-long time history at those locations. 222 stations had associated files from 2000 to 2018 (19 years long) and 86 stations had some other date range of files available.

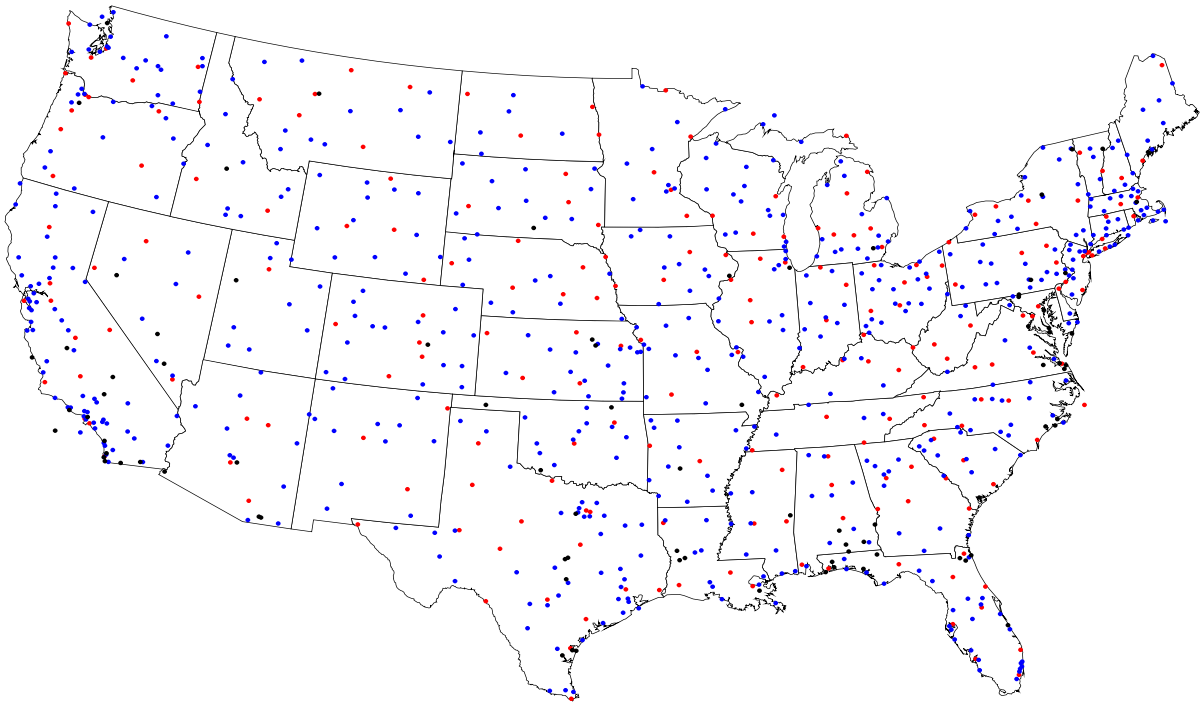

Figure 4.1. Map of all ASOS stations whose observations comprise the DS 6405. Stations coming online in 2000 are colored red; stations coming online in 2005 are colored blue; and stations coming online in a different year are colored black.

At this stage, it was found that the DS 6405 time histories were laden with temporal inconsistencies of two types: gaps and duplicates. Gaps existed either because (1) the corresponding raw data files were unavailable from the online portal, (2) the raw data files were corrupted, or (3) the anemometer output was reported as "M" or "missing". Duplicates (i.e. two or more identical timestamps) were found to exist in at least some quantity across most stations' time histories, though their cause remains unknown. The number of duplicate records found across all 890 stations per month is summarized by the histogram in Figure 4.2.

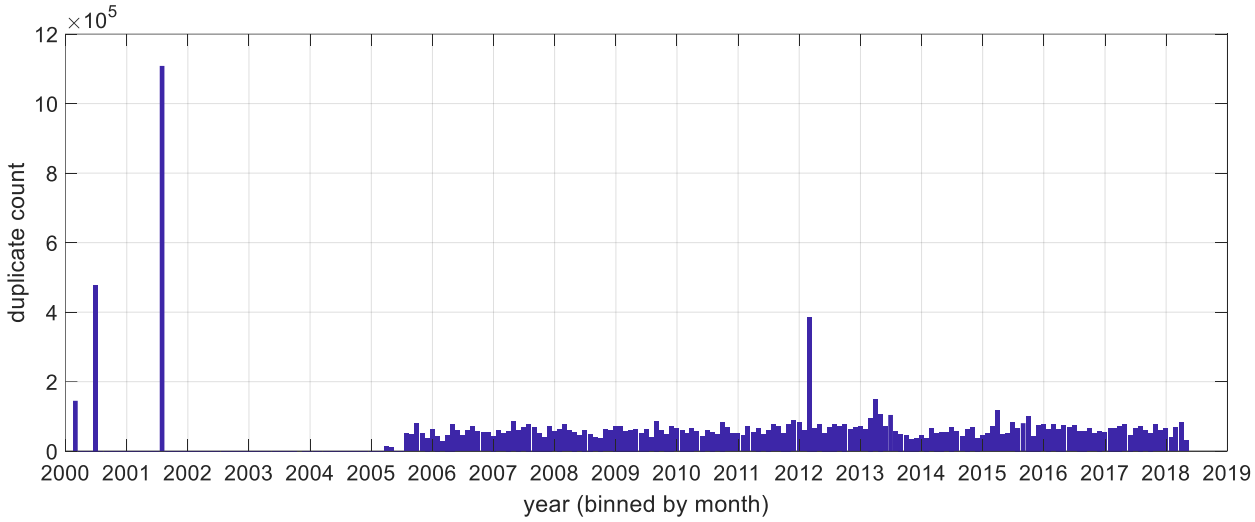

Figure 4.2. Duplicate record counts by month for all stations in the DS 6405 network.

To account for these two temporal issues, a simple correcting algorithm was developed to "clean" the datasets. First, a complete minute-by-minute "blank" timeline was established spanning from the earliest DS 6405 record to the most recent. Raw DS 6405 wind speed and direction data were then placed onto this timeline by matching the time stamps in the record to the corresponding position on the timeline. Doing this ensured that each minute of time was accounted for in the cleaned dataset, regardless if a wind speed and direction was reported at that time. In the case of duplicate timestamps, the record corresponding to the highest wind speed of the duplicates was used and all others were discarded. All other timeline positions with no corresponding wind data were filled in with NaN ("not a number" in MATLAB) as a placeholder. The result from this cleaning process was a 3 x N matrix—a "cleaned time history"—for each of the 890 stations. The three rows correspond to timestamp, wind speed, and wind direction and N equals the number of minutes elapsed from the raw data's first entry to its last (on the order of millions for most stations). To further explain this process and the results, an example cleaning scenario is given in Figure 4.3. The original, uncleaned time history is shown on top, and the cleaned time history is shown on the bottom; red X's show duplicate

records that are deleted and black arrow indicate the assignment of individual wind gusts to the established timeline.

Timestamp	12:01	12:02	12:03	12:03	12:03	12:05	12:06	12:20	12:21	12:22
DS 6405 Wind Speed	15 kt	17 kt	51 kt	55 kt	30 kt	20 kt	25 kt	17 kt	20 kt	13 kt
DS 6405 Wind Direction	210°	200°	200°	190°	220°	210°	200°	230°	220°	230°

Timeline	12:01	12:02	12:03	12:04	12:05	12:06	12:07	12:08	12:09	12:10
DS 6405 Wind Speed	15 kt	17 kt	55 kt	NaN	20 kt	25 kt	NaN	NaN	NaN	NaN
DS 6405 Wind Direction	210°	200°	190°	NaN	210°	200°	NaN	NaN	NaN	NaN

Figure 4.3. Example DS 6405 time history cleaning scenario. The original timeline is on top and the cleaned version is on the bottom.

A quick look at the cleaned high resolution datasets showed, however, that some additional quality controls on the data were still necessary. For example, some stations' time histories contained multiple wind speeds of over 250 knots, a highly unrealistic circumstance. An example of such a time history is given in Figure 4.4. Since extreme value analysis—the intended method for analyzing this data (see Chapter 5)—depends on the veracity of the most extreme events, it was thus critical to remove high wind speeds deemed to be "clearly erroneous". Methods for quality controlling wind time histories (time, speed, and direction) have been well documented by DeGaetano (1997) and Zahumensky (2004) but rely solely on the characteristics of the wind data itself and the consensus understanding of the physical limits of wind variability. Since the objective of exploring high-resolution wind data from DS 6405 is to broaden the understanding of wind extrema (particularly in the temporal sense), quality controlling wind records based on the current understanding of wind extremes likely biases the results towards this current understanding. In an attempt to prevent this bias, a quality control process using non-DS 6405 data was implemented to improve the cleaned DS 6405 timelines. For brevity, the general outline of this process is summarized as follows.

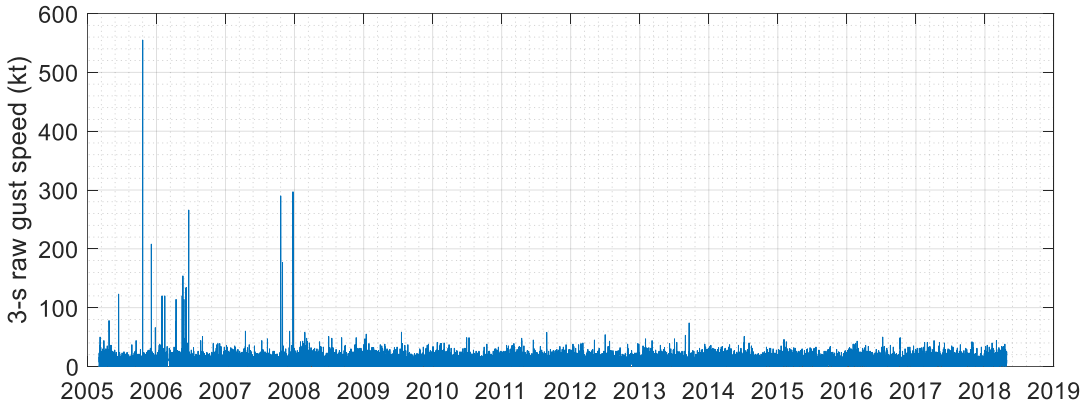

Figure 4.4. Cleaned DS 6405 wind gust time history at New Bern, NC with several anomalous spikes.

Timelines from each station were quality controlled using one data characteristic—wind speed—and three meteorological parameters—temperature, pressure, and relative humidity. The underlying principle of this method was that extreme wind events are generally accompanied by a shift in one or more of these three other weather indicators at or near the same time. First, in order to alleviate the computational effort required to process the millions of records in each timeline, all wind speeds over 175 knots were automatically removed. Then, all remaining records greater than 70 knots were analyzed individually using time histories for temperature, pressure, and relative humidity recorded at the same station. These time histories were obtained from the "mandatory data" section of the ISD 3505 dataset (NCEI 2018) and were matched to the correct timeline using the groupings developed in Chapter 3. Hourly rates of change for each indicator, or "indicator shifts", were then defined: 2.5 °C per hour for temperature, 2.5 millibars per hour for pressure, and 2.5% per hour for relative humidity. A wind gust was determined to be valid if it was accompanied by at least one of these indicator shifts. For example, a wind gust of 75 knots occurring at the same time as a 2.9 °C per hour shift in temperature would be considered valid. Conversely, a wind gust was deemed erroneous if no indicator shifts, as defined, occurred at the same time. Overall, around 41,000 gusts were checked across all 890 stations and nearly 37,000 were eliminated: 30,000 by the indicator shifts and 7,000 by the 175

knot wind speed cap. 72 stations had no wind gusts over 70 knots in their time histories and were thus not affected by this quality control procedure. Figure 4.5 shows the same time history from Figure 4.4 after quality control procedures were applied.

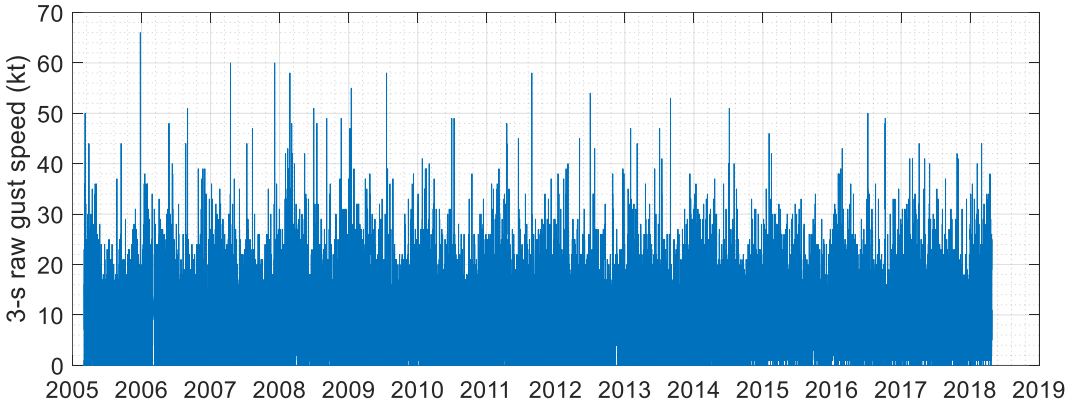

Figure 4.5. Cleaned and quality controlled wind gust time history at New Bern, NC.

4.1.3. Comparison to ISD 3505 Wind Records

To begin comparisons of the cleaned and quality controlled DS 6405 wind records to wind records from the updated ISD 3505 database, a "unified time history" was created for each station. This was made by combining the 3 x N matrix described in Section 4.1.2 (with quality control changes made) with an additional 2 x N matrix containing corresponding ISD 3505 data (wind speed and direction). The result was a 5 x N matrix where the first row consisted of minute-by-minute timestamps and the four other rows contained wind speed and direction from each data source as shown in Figure 4.6. Again, positions on the timeline where no ISD 3505 wind records exist were filled with NaN as a placeholder. Each unified time history spanned only the period of time both datasets had in common, which in most cases, was roughly 2003 to 2017. For stations where no quality control changes were made, the unified time history was created simply using the cleaned DS 6405 time history.

Timestamp	12:03	12:06	12:08	12:09	12:13	12:23
ISD 3505 Wind Speed	54 kt	25 kt	21 kt	23 kt	30 kt	20 kt
ISD 3505 Wind Direction	190°	200°	200°	200°	220°	210°

Timeline	12:01	12:02	12:03	12:04	12:05	12:06	12:07	12:08	12:09	12:10
DS 6405 Wind Speed	15 kt	17 kt	55 kt	NaN	20 kt	25 kt	NaN	NaN	NaN	NaN
DS 6405 Wind Direction	210°	200°	190°	NaN	210°	200°	NaN	NaN	NaN	NaN
ISD 3505 Wind Speed	NaN	NaN	54 kt	NaN	NaN	25 kt	NaN	21 kt	23 kt	NaN
ISD 3505 Wind Direction	NaN	NaN	190°	NaN	NaN	200°	NaN	200°	200°	NaN

Figure 4.6. Example of the Unified Time History created by assigning DS 6405 wind gust time histories and ISD 3505 wind gust time histories to the same minute-by-minute timeline.

Using the unified time history for each station, individual wind gust records between the two datasets were compared. This was done by iterating through all ISD 3505 wind gusts at a given station and performing a number of comparative logical checks with the corresponding DS 6405 wind gusts. The first check was a temporal check, executed as follows. If a DS 6405 wind gust record existed at the exact same time (to the minute) as an ISD 3505 wind gust record, the two gust records were paired and classified as a "timestamp exact match", corresponding to the far right column of the categorization matrix shown in Figure 4.7. If no exact match was found, then an expanded temporal check was conducted to see if any DS 6405 wind gusts existed within two minutes on either side of the particular ISD 3505 gust. If more than one DS 6405 gust was found within this window, the record that was the earliest and closest match in time was selected. These paired records with nearly matching timestamps were classified as "timestamp within 2-min" as labeled in the middle column of Figure 4.7. Finally, if no DS 6405 wind gust records were found meeting any of the above criteria, the ISD 3505 record was classified as having "no corresponding 6405 gust" as shown on the gray, far left box of Figure 4.7. Two stations (K1V4 and KFFZ) were found to have no matching ISD 3505 gusts across their entire time history;

these stations were thus excluded from future analyses bringing the total number of high resolution stations analyzed to 888.

For all temporally-paired wind gust records, a second check was performed regarding wind speed. If the wind speed of both gust records in a particular pairing was the same, the pairing was classified as a "3505 speed EXACT MATCH", corresponding to the green boxes in Figure 4.7. Pairings where the ISD 3505 speed was higher (yellow boxes) and lower (red boxes) were also identified and separated out as shown in Figure 4.7. The seven mutually exclusive categories offer a quantitative description of how the wind gust records between both DS 6405 and ISD 3505 compare at a particular station, where quantities in the dark green box indicate perfect agreement and contents of other boxes indicate varying amounts and types of disagreement.

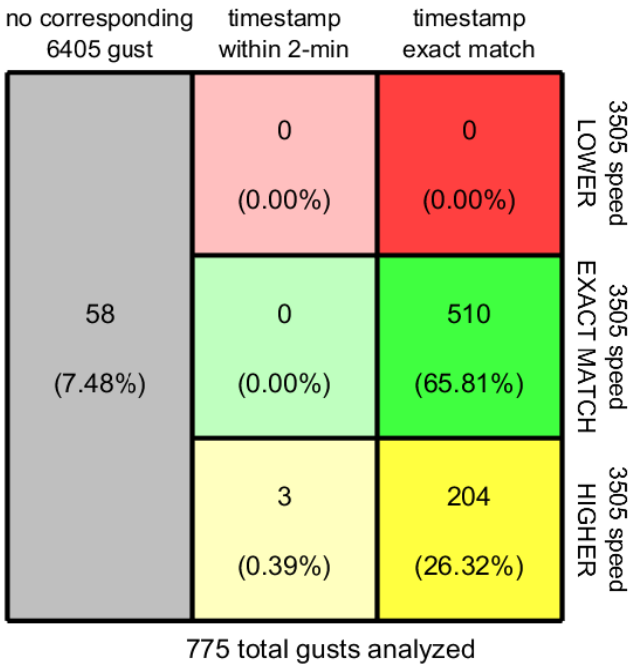

Figure 4.7. Example categorization matrix for wind gust comparisons in Irvine, CA (KSNA) where nearly two thirds of all ISD 3505 wind gusts are matched perfectly to DS 6405 gusts.

What the categorization matrix does not show, however, is what magnitude differences exist among wind speed mismatches between the two sets of records. To gain a better understanding of these differences, the wind gust speeds of each record at a single station were plotted against each other as shown in Figure 4.8. A 1:1 line, indicating a perfect agreement between the records, is shown as a continuous gray line. Each pairing found in the comparison was plotted as a single red marker. From the example in Figure 4.8, it is clear that while many pairings exist on the 1:1 line, there are many pairings with mismatched wind speeds—some of which show disagreement by as much as 50% or more. Overall, many of the mismatched pairings indicate that the DS 6405 wind speed was lower than the ISD 3505 wind speed, despite being recorded at the exact same time. To assess the pairings as an ensemble, a linear regression was performed and the resultant fit was plotted as a dashed line with the slope and intercept given in the plot's legend. Slopes deviating from 1 and intercepts deviating from 0 indicate mismatch between the two data sets over the station's entire unified time history. Network-wide results and implications of these analyses are discussed in Chapter 6 along with other broad scope results presented in this study.

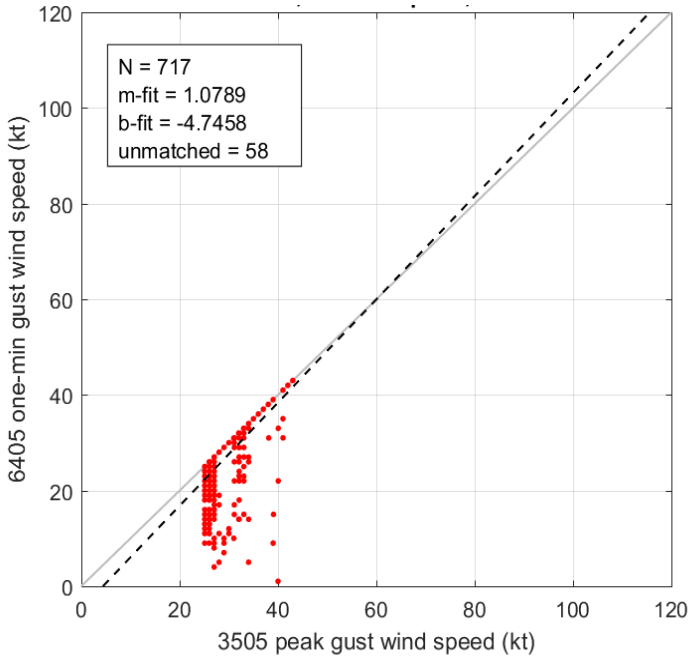

Figure 4.8. Example gust comparison plot for wind gusts in Irvine, CA (KSNA) showing the degree of mismatch between wind gust speeds of the two time histories.

4.2. Improved Spatial Resolution – OKM Study

It is well established that the spatial scales of extreme wind-producing meteorological phenomena vary greatly. Synoptic scale events (frontal passages, extra tropical lows, etc.) can span hundreds of miles whereas isolated thunderstorms may only occupy a single square mile (Holmes 2015). Because of these vast differences in scale, a weather observation network of a single, unchanging density is likely unable to detect extreme wind events of decreasing geographic scale. This notion is confirmed by the frequent observation of small-scale phenomena (supercell thunderstorms, for example) by means of satellite and radar imagery that otherwise go "unnoticed" at the conventional static observation stations. Thus, conventional wind observation networks such as ASOS are limited to detecting events occurring over or very near the stations' physical locations.

In order for an observation network like ASOS to adequately and consistently capture extreme winds from small-scale phenomena, the network must have a characteristic spatial density well-suited to the nature of events it intends to capture. While the airport-based ASOS network has traditionally been the standard-bearer for extreme wind observations within the contiguous United States, its density of stations (especially in areas highly prone to small-scale extreme wind events such as the Great Plains) is arguably deficient. Fortunately, other observation networks exist within the United States that can facilitate the investigation of this dilemma. In the remainder of this section, a weather observation network of a considerably higher spatial density than ASOS—the Oklahoma Mesonet—is described and evaluated. High wind events detected at this denser network are identified and then compared, one by one, to corresponding wind time histories at surrounding ASOS stations. Regression analyses are performed to determine the tendency of ASOS stations to capture or not capture events detected at the higher density network.

4.2.1. Introduction to the Oklahoma Mesonet (OKM)

In 1994, scientists at the University of Oklahoma and Oklahoma State University implemented a meteorological observation network known as the Oklahoma Mesonet (OKM). This network currently consists of over 100 observation stations evenly distributed throughout the state of Oklahoma, most of which have recorded high quality observations from 1994 to present (OM 2019a). In addition to measuring other environmental conditions, these stations record useful wind data, including a peak 3-second average wind gust every 5 minutes. Since the OKM operates independently from (but in the same overall space as) the existing ASOS network in Oklahoma, OKM wind data can provide a useful cross check of extreme wind reports found in the ISD 3505. More importantly, however, given that the OKM stations are laid out in a much denser grid than the ASOS stations, wind observations from the OKM allow for comparisons of

observation networks of different spatial densities. Figure 4.9 shows this relative difference in density using a map of OKM stations plotted with stations observing ISD 3505 data. It is clear that the ISD 3505 stations, from which the ASCE 7 basic wind maps are ultimately derived, are much more limited spatially than the denser OKM stations.

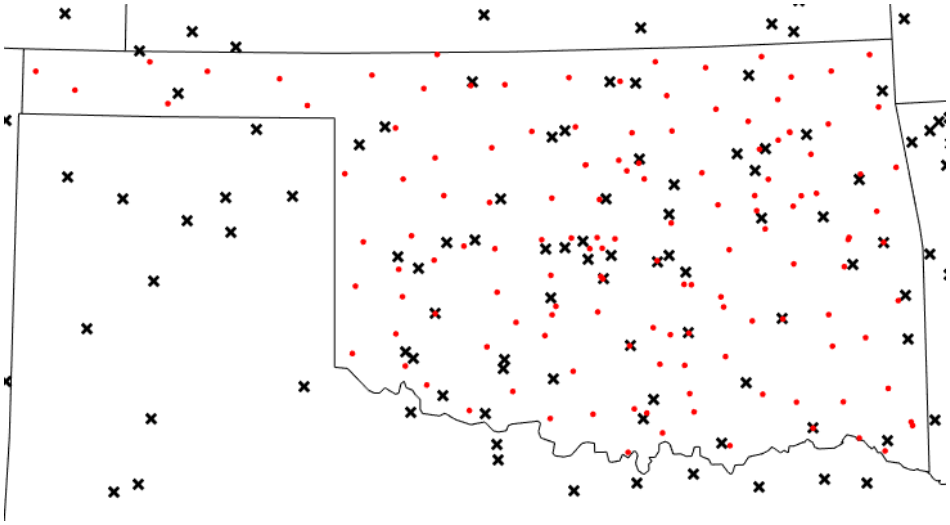

Figure 4.9. Map of Oklahoma and surrounding states showing all station groupings from ISD 3505 plotted as black X's and all OKM stations plotted as red dots.

4.2.2. OKM Data Preparation

To begin, wind data from 1994 (the beginning of the OKM program) through the end of 2018 was acquired from the Oklahoma Mesonet webpage (OM 2019b) and was then compiled into a series of MATLAB-style data structures. This was done for all 143 stations found in the online data repository. While all meteorological data available was collected in this initial download step, the most relevant wind information for this study was the 3-second gust wind speed (WMAX). According to (OM 2019a), WMAX is the maximum 3-second wind speed that is observed during each 5-minute reporting interval. WMAX is measured by a propeller-vane anemometer situated, for all stations, at 10 meters above the ground. A table of all wind data types available from the OKM is presented in Table 4.1. An OKM metadata document was also acquired at this stage, which—like the ISD History document in Chapter 3—detailed the location and identification information for each station in the network.

Table 4.1. Wind-related parameters collected by the Oklahoma Mesonet observation stations.

Code	Description
WSPD	5-minute average wind speed at 10 meters (m/s)
WSSD	standard deviation of 5-minute average wind speed at 10 meters (m/s)
WDIR	5-minuge average vector wind direction at 10 meters (deg)
WDSD	standard deviation of 5-minute average wind direction at 10 meters (deg)
WVEC	vector 5-minute average wind speed at 10 meters (m/s)
WMAX	maximum 3-second average wind speed (m/s)
WS2M	5-minute average wind speed at 2 meters (m/s)

Once the OKM data was acquired, it was found that a number of the 143 stations were located less than 10 miles of one another. Further exploration revealed that over the 25 years of the OKM's existence, several stations were shut down and moved to slightly different locations nearby (within 10 miles in most cases). These happenings can be gleaned from the metadata document as well as from the start/end time of the affected stations' time histories; these changes are also confirmed in a separate OKM documentation of "retired sites" (OKM 2019a).

To account for these discontinuities in location, a simple quality control scheme was implemented that aimed to merge together disjoint time histories describing the same geographic location. First, distances between all 143 stations were computed. Stations within 10 miles of each other were paired into groups of two for further inspection. For each pairing, a subjective evaluation was made to determine if the two stations' records should be merged together. This evaluation was made based off of two factors: the stations' distance apart and start/end times of their time histories. If (1) the end of one station's time history coincided exactly (or extremely close) to the beginning of the other's time history and (2) if the stations' locations were relatively close together, then the records were merged together to form a "pseudo station". In all, 12 sets

of stations were merged together in this manner, reducing the number of OKM stations from 143 to 131. The 12 newly formed pseudo stations were given new station identification numbers and names differing from those in the metadata documentation. The location of each pseudo station was computed as the average latitude and longitude of the two stations that formed it. A complete list of all stations considered and pseudo stations formed during this step is shown in Table 4.2. This process is exemplified visually in Figure 4.10, where stations "WALT" and "WAL2" (it's successor) are combined, forming pseudo station "WAL3" located between them.

Table 4.2. List of all OKM stations found within 10 miles of each other and the result of subjective evaluation for merging them.

Station 1 ID	Station 1 Number	Station 2 ID	Station 2 Number	Distance (miles)	Pseudo Station Number	Pseudo Station ID
ALV2	116	ALVA	3	5.37	1003	ALV3
ANT2	135	ANTL	4	2.54	1004	ANT3
ARD2	126	ARDM	5	0.05	1005	ARD3
BROK	124	BBOW	7	2.1	1007	BRO3
SEMI	143	BOWL	13	3.92	not merged	not merged
HOLD	134	CALV	21	5.56	1021	CAL3
NINN	109	CHIC	27	4.95	not merged	not merged
CLRM	122	CLAR	28	0.37	1028	CLA3
GRA2	117	GRAN	42	0.22	1042	GRA3
KIN2	133	KING	54	3.02	1054	KIN3
MRSH	125	MARS	60	0.33	1060	MAR3
NRMN	121	NORM	69	1.71	1069	NOR3
WAL2	136	WALT	98	2.82	1098	WAL3
WEBR	132	WEBB	103	1.21	1103	WEB3
OKCE	130	OKCN	128	6.33	not merged	not merged
OKCE	130	OKCW	129	6.67	not merged	not merged

Figure 4.10. Example of two stations “WALT” and “WAL2” that were combined to form “WAL3” based on their proximity and relative start/end times.

With the OKM station geographies established and quality controlled, a final filtering was conducted to select only stations at which the complete time history of the OKM (1994 through mid-2018) was recorded. Of the 131 stations available, 108 were found to meet this condition, including 11 out of 12 pseudo stations; these stations are shown in the map in Figure 4.11. These stations and their data formed the basis of all subsequent analyses regarding the OKM. A list of stations eliminated in this final filtering step is provided in Appendix A for reference.

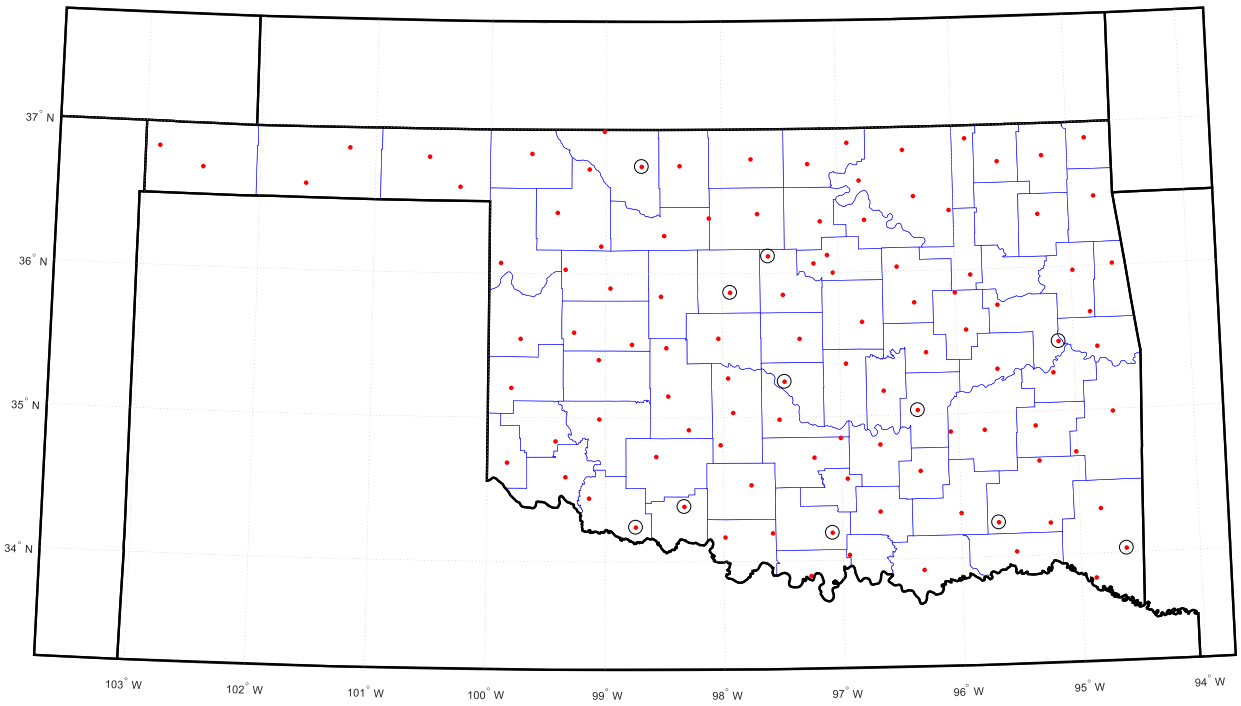

Figure 4.11. Map of the final selection of 108 OKM stations for analysis. Pseudo stations are circled with a black ring.

4.2.3. OKM Wind Event Identification

In order to perform an event-by-event comparison of high wind events between OKM and ASOS, discrete high wind events within the OKM stations' time histories were defined and subsequently identified. First, the 3-second wind gust (at 10-meter height) time histories at each station were scanned for all wind speeds higher than a certain wind speed threshold, V_T. After discarding all records below this threshold, two general types of "high wind blocks" remained. One type was the isolated spike—a relatively short-lived (less than 30 minutes) block of gust records noticeably removed from other high wind events in time. The other type was the extended block—one where wind gusts fluctuated above, and occasionally below, the threshold for a protracted amount of time (more than 30 minutes). An example time history showing both of these types of wind events is given in Figure 4.12.

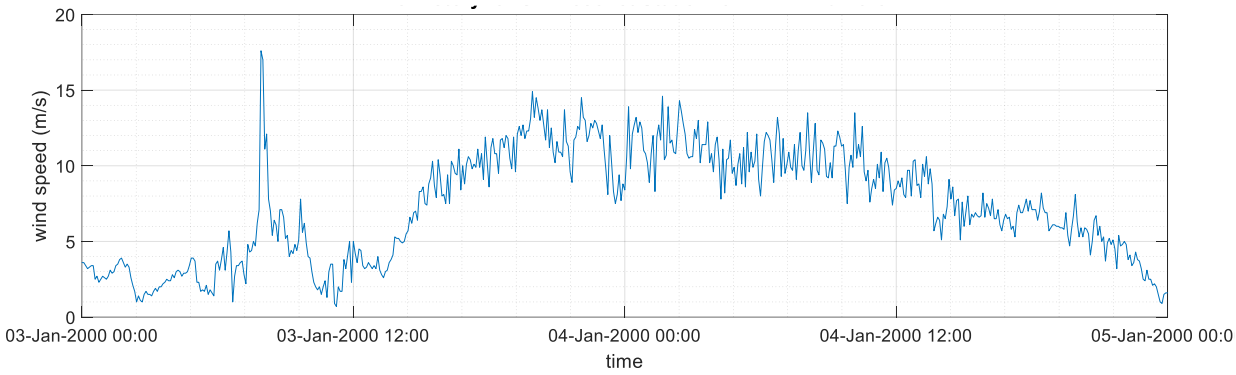

Figure 4.12. Example wind gust time history at Ardmore, OK (ARDM) showing an isolated spike (left side) and an extended block (right side) occurring back to back.

While the specific taxonomy of high wind record blocks was not important, this division had significant implications for the nature of how high wind *events* were defined. If all high wind blocks were characterized by a single wind gust record isolated in time (the isolated spike), then it might be appropriate to define each high wind event as just a single wind gust record over the threshold. If this philosophy were instead applied to an extended block, the result would be a long series of back-to-back high wind events—a description not truly indicative of the physical phenomena. Because high wind events in nature have some amount of duration associated with them, it was necessary to further discretize the blocks of high wind records before officially identifying high wind events.

Blocks of high wind records were initially processed using the separation interval algorithm (Lombardo et al. 2009) designed to identify statistically independent local maxima within a time series. These independent local maxima were considered to be "parent records"—all of which were separated by a minimum time interval of t_{int}. All other wind records exceeding V_T were grouped with the closest parent record in time to form a discrete "event" with a finite duration. This process yielded the final timeline of identified high wind events associated with each OKM station from 1994 to mid-2018. An example of how this discretization process was applied is given in Figure 4.13.

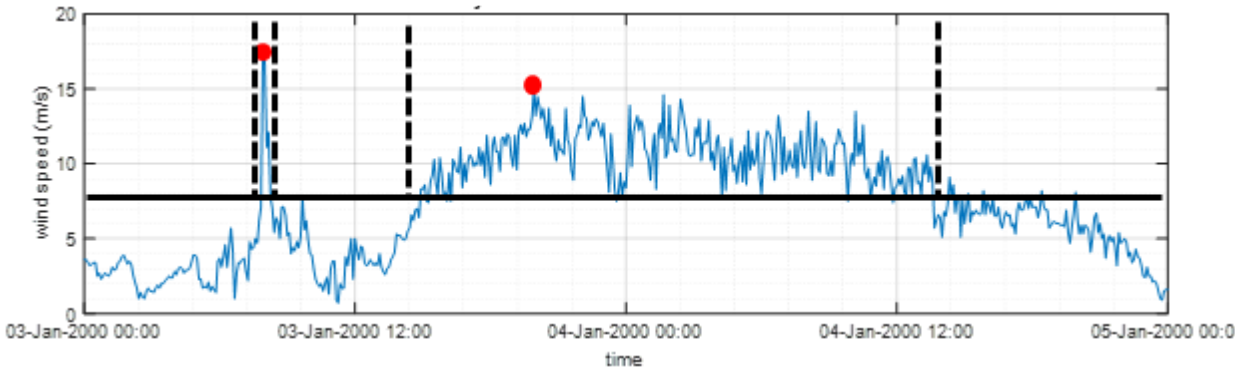

Figure 4.13. Example wind gust time history at Ardmore, OK (ARDM) with two high wind events identified. The horizontal black line indicates the wind speed threshold V_T and the red dots indicate the independent maxima wind gusts or "parent records". Records between each pair of dashed lines indicate discrete high wind "events" used throughout the remainder of this study.

Since the values chosen for V_T and t_{int} directly impacted the number of high wind events identified for each station (and thus, the sample size of subsequent analyses), a sensitivity analysis was performed for each variable. The parameter spaces were defined as 18 to 65 m/s for V_T and 30 minutes to 1.5 days for t_{int}, with the base case for each being 20 m/s and 6 hours, respectively. For each parameter, the event identification scheme was repeated using various values within its parameter space; the number of events identified at each OKM station was recorded for each iteration. The results of these two sensitivity analyses are shown in Figure 4.14 and Figure 4.15.

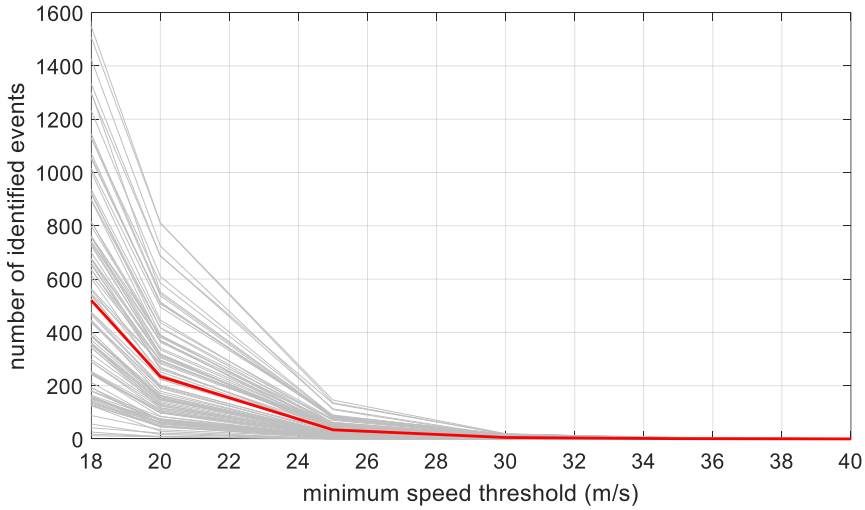

Figure 4.14. Sensitivity of event count on wind speed threshold V_T for all 108 OKM stations. The average of all stations is presented as a red line.

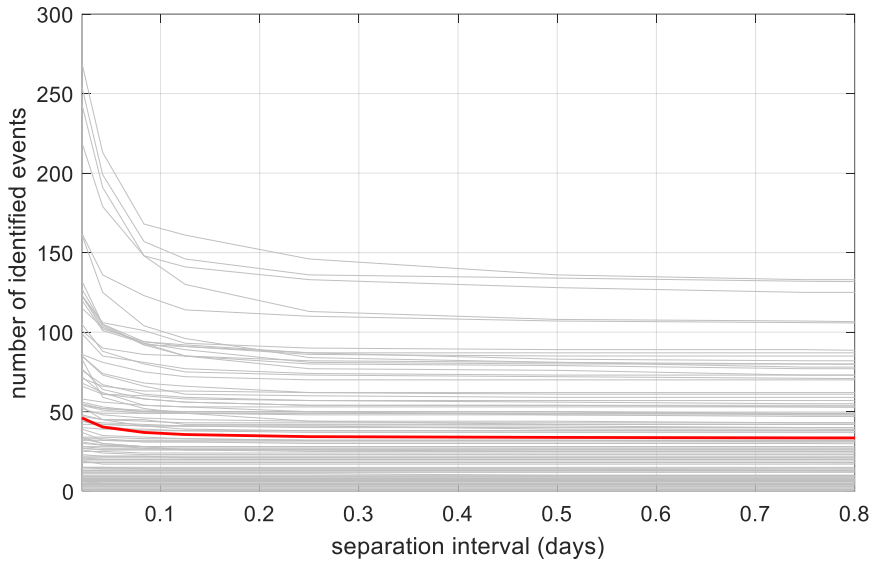

Figure 4.15. Sensitivity of event count on separation interval t_{int} for all 108 OKM stations. The average of all stations is presented as a red line.

It was apparent from these results that event counts at all stations were highly sensitive to the threshold speed V_T but only at some stations were they particularly sensitive to t_{int}. To ensure that each station used in the study had at least one identified event in its timeline, a threshold speed of 20 m/s was selected for use in subsequent analyses. This matches the threshold speed used in a similar study involving wind speeds data from the West Texas Mesonet (Zickar et al., unpublished manuscript) Since most stations were not highly sensitive to the t_{int} value chosen, a value of 0.25 days (equal to 6 hours) was selected in an attempt to balance event count with event duration. Using these chosen values of V_T and t_{int}, final high wind event timelines were generated for each OKM station; the results from this are summarized in Figure 4.16.

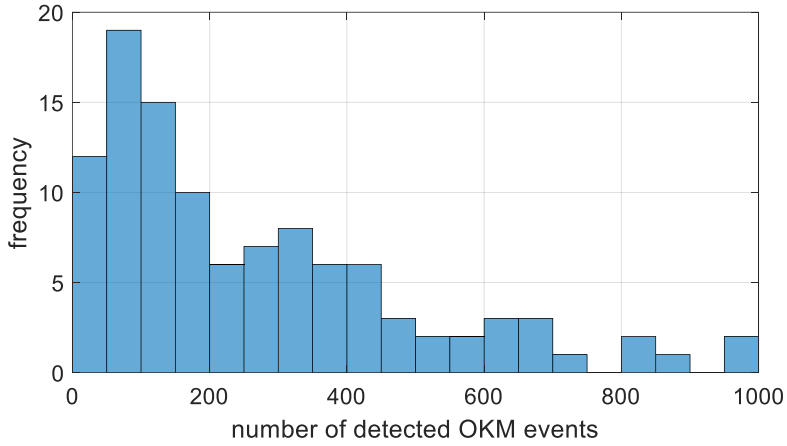

Figure 4.16. Distribution of number of identified high wind events across all 108 OKM stations.

4.2.4. Comparison to ISD 3505 Events

With the event timelines for each OKM station established, analysis proceeded to compare these events to the time histories recorded at ASOS stations within (and nearby) the state of Oklahoma. To select a set of ASOS stations to use in analysis, a sequential filtering system was applied to the finalized set of 2,447 ISD 3505 station groupings discussed in Chapter 3. For consistency and simplicity, these "groupings" are referred to as "ASOS stations" for the remainder of this chapter.

First, ASOS stations not located within the box formed by 33.25° N – 37.75°N -- 103.75°W – 93.75°W were excluded; this box forms a complete envelope around the state of Oklahoma with approximately 50 miles of buffer on the perimeter. This first filtering yielded 114 stations considered to be close enough to OKM stations to make reasonable comparisons. Next, stations were filtered out based on the temporal makeup of their time histories. Since the 108 filtered stations in the OKM have time histories spanning the entirety of each year from 1994 to 2017 inclusive, ASOS stations were selected that had time histories of the same character in both total duration and continuity. This second filtering yielded 39 ASOS stations, shown in Figure 4.17, with locations and time histories deemed suitable for comparison to OKM high wind events. Note this process did not account for the "prorupted" shape of Oklahoma—in

having a so-called western “panhandle”— so some stations in eastern New Mexico are also included despite being far away from the majority of Oklahoma.

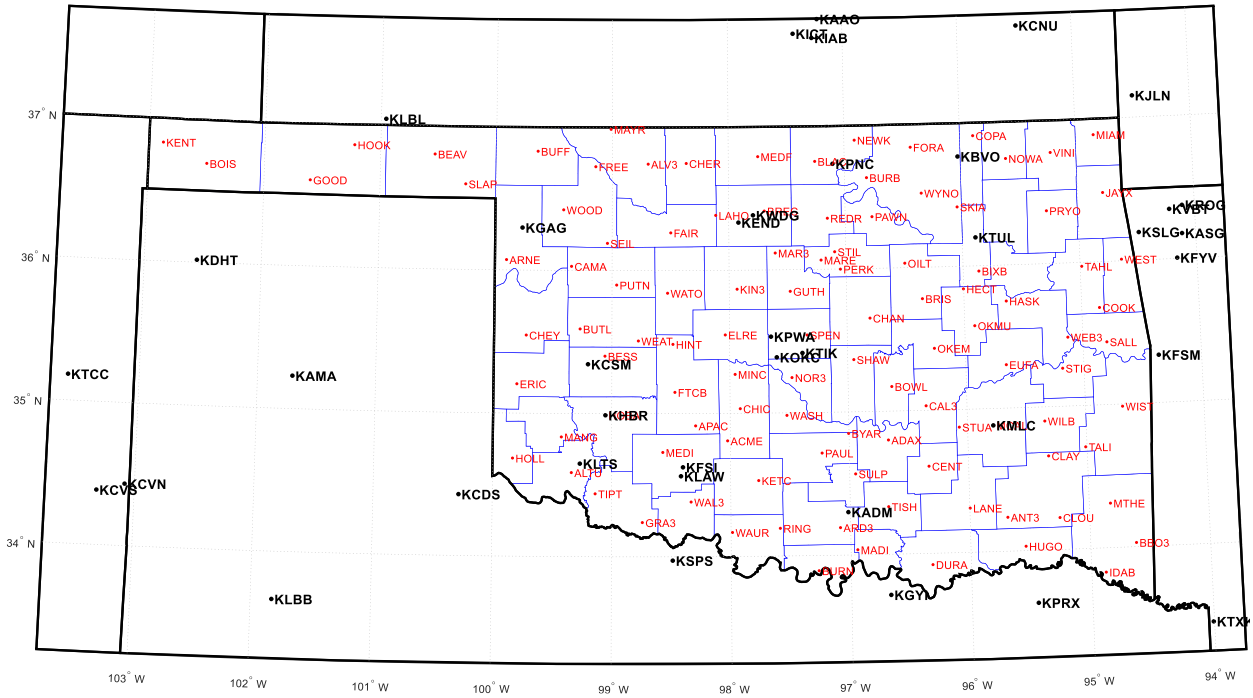

Figure 4.17. Final map of 108 OKM stations and 39 ASOS stations used for comparative analyses.

To compare high wind events from the OKM to records at ASOS stations, a multi-faceted “windowing” technique was employed. For each discrete OKM event, a timing window was established that spanned from span some time T_w before the event’s start time to T_w after the event’s end time. Since OKM gust records are reported at even five-minute intervals with no indication of when during the interval the gust occurred, an additional 2.5 minutes was added on either side of the established timing window to account for possible mid-interval times found in the ASOS records. So for example, an OKM high wind event consisting of a single wind speed recorded at time T (an isolated peak) would have a timing window spanning T-2.5-T_w to T+2.5+T_w. Using this timing window, time histories at all 39 ASOS stations were searched for wind gust records corresponding to the established timing window. If corresponding ASOS data

(referred to here as a "block") was found, additional determinations were made using the OKM event's wind speed and direction.

Since the "parent record" (see Section 4.2.3) of each discrete OKM event was the record containing the event's highest wind speed (U_{max}), this parent record was used for further windowing. First, a wind speed window was established encompassing all wind speeds from U_w below U_{max} to U_w above U_{max}, with U_w being a consistent percentage of U_{max}. Second, a similar wind direction window was created ranging from all wind directions D_w below the parent record's wind direction, D_{max}, to D_w above D_{max}; proper adjustments were made to accommodate the 359-to-0 degree discontinuity. The matched block of ASOS records was then analyzed using these windows. If any individual record (wind speed and direction) found in the matching ASOS block was within *both* the aforementioned windows of wind speed and direction, the OKM event was classified as "captured" or "hit" by that particular ASOS station. If no records within the ASOS block matched the windowed criteria, the OKM was classified as "not captured" or "missed" by the ASOS station. Assessments were made using this binary system only and with no tolerance ranges (i.e. an ASOS block wind speed of 29.99 m/s would be recorded as a "miss" if the OKM event window begins at 30 m/s).

For each of the 108 OKM stations, all high wind events on its timeline (number of events at each OKM station is hereby defined as k, which varies across stations) were compared against records from all 39 ASOS stations, yielding 39 x k hit-or-miss results for each OKM station, or 39 x 108 x k results overall. Out of this extensive process, a dichotomy of event-capturing logic emerged. Since each event was compared to multiple ASOS stations, it was entirely feasible that a single OKM event could be captured at multiple ASOS stations (i.e. multiple "hits" for a single event). A probability model based off of these results would therefore indicate the probability of

each ASOS station capturing an event separately, where the 39 total hits or misses for each OKM event constitute 39 independent trials. Since the focus of this study, however, is to compare the capabilities of the two networks as a whole (i.e. capturing wind events without regard for *which* station captures them), it is also relevant then to consider the probability of *any* ASOS station capturing a particular event. Thus, a reduction in the previous results was performed such that if a particular OKM event was classified as a hit at *any* of the 39 ASOS stations, the event overall was considered to be captured by the ASOS network. This reduction resulted in a secondary dataset of 108 x k hit or miss results for use in further analysis.

An example of this hit-or-miss scheme for a single high wind event at a single OKM station is exemplified in Figure 4.18. The OKM station selected, "ARDM", is depicted as a green star; all other plotted markers show the locations of ASOS stations to which the particular high wind event was compared. ASOS stations marked with a black circle (a "bullseye" marker) indicate that the station observed a wind event matching the windowing criteria previously described and is classified as a "hit". ASOS stations marked with a red X, conversely, did not record such an event and are classified as a "miss".

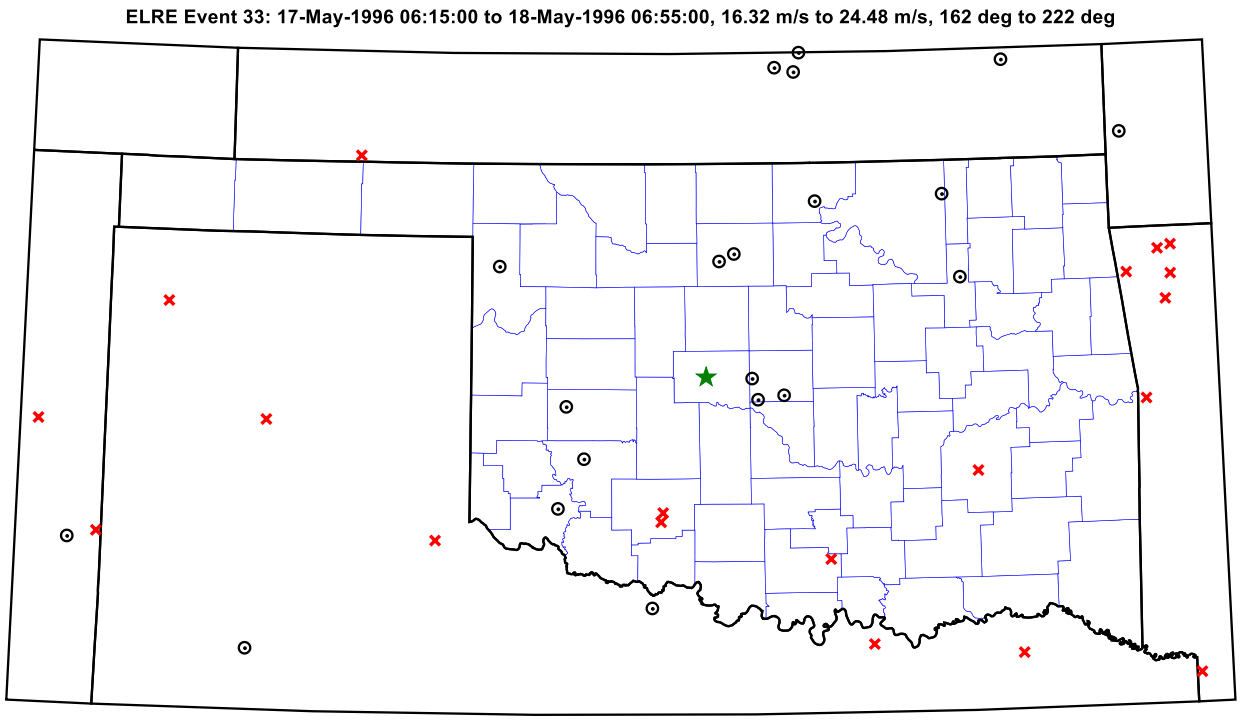

Figure 4.18. Example of the hit-or-miss analysis performed for one high wind event at one OKM station, ELRE, shown as a green star. Circles indicate hits and X's indicate misses among the 39 ASOS stations.

Using the first logical approach (referred to as the "all" approach in subsequent analyses), where each ASOS station is treated as an independent trial, this particular event at OKM station ELRE would be associated with 20 individual hits and 19 individual misses (an overall success rate of 51.2%). The other logical approach (referred to as the "any" approach), however, would consider that this particular OKM event was observed by at least one ASOS station (i.e. at least one hit by the ASOS network) and would therefore only associate this OKM event with a singular hit. This hit-or-miss procedure and the two distinct logical interpretations of its results form the basis for further ensemble-wide OKM analyses presented in Chapter 6.

CHAPTER 5: EXTREME VALUE ANALYSIS METHODS

While the construction of an accurate and comprehensive wind speed time history—as discussed in Chapters 4 and 5—is useful for detailing conditions of the past, perhaps its most powerful application is in the projection of future extreme wind events. Once observed extreme wind speeds within a time history are identified, they can then be used to generate a probability distribution capable of projecting the trend of extreme wind events into the future. In general, this statistical application is known as extreme value analysis (EVA). A number of well-established EVA methods for wind data exist that utilize varying procedures for identifying extrema and various methods of developing distributions. This chapter provides a brief overview of the EVA methods used in this study and further describes how these methods are implemented using the extensive datasets prepared in Chapters 3 and 4. Some representative results from these EVA methods are presented as well, though collected network-wide results are presented together in Chapter 6.

5.1. Overview of EVA Methods

The following three subsections describe three different methods of identifying extreme wind speeds within a time history: annual maxima (AM), method of independent storms (MIS) and peaks over threshold (POT). Within these categories exist numerous methods of EVA using the observed extrema. This study utilizes, in total, six such EVA methods in an attempt to capture the breadth of available techniques used in practice for modeling wind extrema. Table 5.1 concisely summarizes these methods. Thorough descriptions of all these methodologies and their limitations can be found in the cited references.

Table 5.1. Summary of extreme value methods used in this study.

Extrema Identification Method	Extrapolation Method
annual maxima (AM)	Generalized Extreme Value (GEV) distribution
	Gumbel distribution (GEV special case)
	Harris improved method (Gumbel fit)
method of independent storms (MIS)	Harris improved method (Gumbel fit)
peaks over threshold (POT)	Generalized Pareto Distribution (GPD)
	exponential distribution (GPD special case)

5.1.1. Annual Maxima (AM)

A traditional approach to identifying extreme events within a wind time history involves breaking down the record into even-length time segments known as "epochs". For records of considerable length, one convenient and oft-used way to define epochs is by using calendar years as the delineator. Extrema within the larger dataset, thus, can be easily defined as the single most extreme value within each of the years present in the record. For applications of extreme wind speeds where maximum values are of interest, this process entails selecting the highest wind speed recorded at each calendar year over the entire length of the time history. These selected wind speeds form a series of "annual maxima" (AM) observations that characterize the extreme wind climate at a particular location. It should be noted, however, that this method implicitly assumes that the annual maxima are statistically independent of one another. While this is likely to be true for year-long epochs, there are separation techniques available (as discussed in Chapter 3) that can further enhance independence as needed.

To fit annual maxima to a distribution suitable for extrapolation, an empirical cumulative distribution function (CDF) is generated. This is achieved by ordering the annual maxima by ascending wind speed and assigning each a rank ("lowest", "second lowest", "third lowest", etc.). Given the observations conform to a known probability distribution, the rank-ordered

annual maxima can then be plotted (as shown in Figure 5.1) and fit to a distribution using a number of fitting techniques.

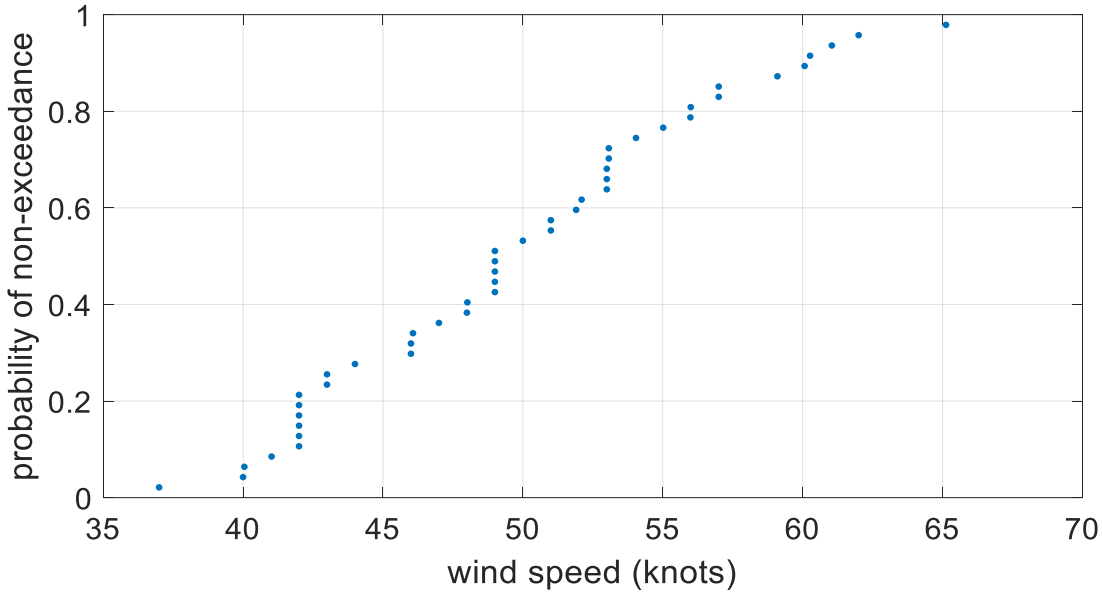

Figure 5.1. Example of rank-ordered wind speed annual maxima plotted as an empirical CDF.

Two of the extrapolation methods used in this study exclusively use the generalized extreme value (GEV) distribution, also known as the Fisher-Tippett distribution. The overall behavior of the GEV distribution is defined by its three parameters: shape (c), location (u), and scale (a). Of these three parameters, the shape parameter is perhaps the most influential on the distribution's tail behavior—a characteristic of high importance for long range extrapolation. The precise value of the shape parameter governs which "type" of GEV distribution is used, as shown in Table 5.2. Figure 5.2 (left side) shows these three versions of the GEV distribution CDF plotted in "standard space"—defined in this study as a basic, untransformed set of linearly-scaled axes—along with the sample data from Figure 5.1. The functional form of the CDF is given in Equation 5.1. The special case of the GEV distribution where the shape parameter equals zero—Type I GEV—is known as the "Gumbel" distribution. The CDF of the Gumbel distribution is given in Equation 5.2.

Table 5.2. Summary of GEV distribution characteristics by shape parameter value

Shape Parameter (c)	**GEV Type**	**Name**
c < 0	Type III	Reversed Weibull distribution
c = 0	Type I	Gumbel distribution
c > 0	Type II	Fréchet distribution

$$F(U) = \exp\left[-\left(1 + c\left(-\frac{U-u}{a}\right)\right)^{-\frac{1}{c}}\right] \quad , \quad c \neq 0 \qquad \text{(Eq. 5.1)}$$

Where

$F(U)$ = GEV CDF value, probability of non-exceedance

U = wind speed

c = shape parameter

u = location parameter

a = scale parameter

$$F(U) = \exp\left[-\exp\left(-\frac{U-u}{a}\right)\right] \qquad \text{(Eq. 5.2)}$$

Where

$F(U)$ = Gumbel CDF value, probability of non-exceedance

U = wind speed

u = location parameter

a = scale parameter

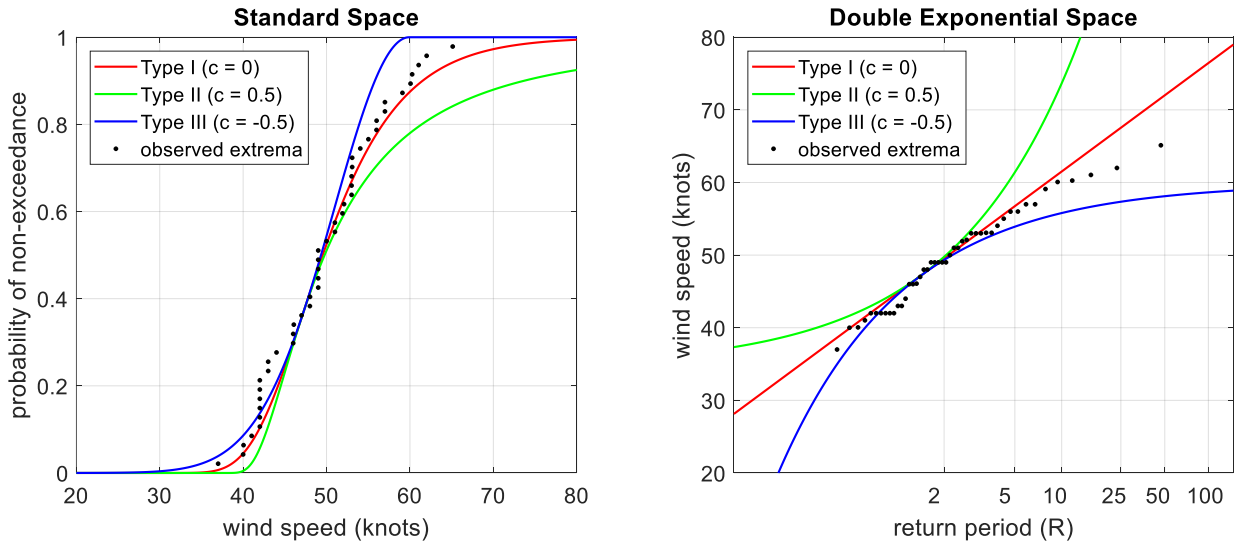

Figure 5.2. Left: Sample annual maxima plotted in standard space with three fitted GEV distributions. Right: Sample annual maxima plotted in double exponential space with three fitted GEV distributions.

While the GEV distribution CDF, as plotted in Figure 5.2 (left side), allows for easy interpretation of probabilities of non-exceedance for various wind speeds, internal mechanisms of the distribution are somewhat obscured. By making a few modifications to the plotting scheme, a more useful realization of observed annual maxima and fitted distributions can be obtained. First, since probability of non-exceedance is related to return period (R) according to Equation 5.3, wind speed can thus be related to a return period using Equation 5.1 instead of a cumulative probability. Second, since the GEV distribution takes the double exponential form, plotting the double log of the range (now return period) versus wind speed affords a direct visual interpretation of how the distribution's parameters govern its behavior. In this plotting space, the location parameter dictates the y-intercept, the scale parameter controls the slope, and the shape parameter governs the curvature. Finally, Harris (1996) suggests the inversion of plotting axes—such that wind speed is plotted as function of the double log of return period in this case—offers a more realistic interpretation of the data. Making this modification, along with the other two as described, yields the final plotting form shown in Figure 5.2 (right side), where return period (in

years) is plotted along the abscissa and wind speed is plotted as the ordinate. This plotting scheme is used for all iterations of EVA throughout this study; for distributions not conforming to the double exponential form, the plotting positions of the data and fitted distributions are converted accordingly for ease of comparison.

$$F(U) = 1 - \frac{1}{R} \quad \text{(Eq. 5.3)}$$

In this study, the GEV and Gumbel distributions comprise the first two (of six total) extrapolation methods performed with the datasets prepared in earlier chapters. For the GEV method, values for c, u, and a are estimated using the maximum likelihood (ML) method and are then used to predict an expected wind speed corresponding to a return period of 50 years (V50). The Gumbel method first assumes c equals zero, then estimates u, a, and V50 similarly. The third extrapolation method using annual maxima observations is a method introduced by Harris (1996) that implements specific improvements to the Gumbel method. These improvements reduce the systematic error in fitting the Gumbel distribution to observed annual maxima by varying the weights used in a least-squares fitting technique, rather than assigning an equal weight to each observation (Palutikof et al. 1999). This eliminates the need for conventional parameter estimation schemes, replacing u and a with analogous parameters pi (Π) and alpha (α) respectively. Harris also introduces updated plotting positions for observed annual maxima, which can be observed in the summary of all three annual maxima extrapolation methods displayed in Figure 5.3.

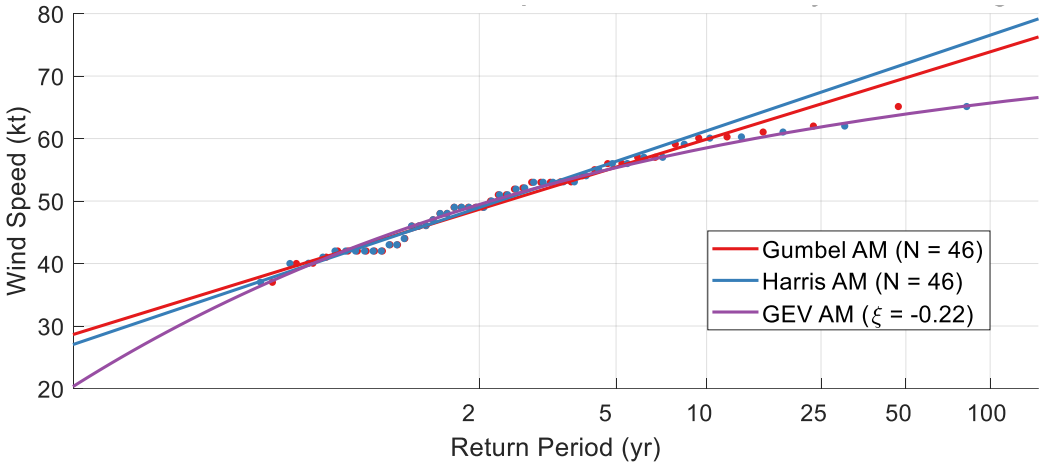

Figure 5.3. Example of wind speed annual maxima (46 years total) from Memphis, TN plotted with three different fitted distributions. Data points are the observed extrema to which the corresponding (by color) distributions are fit.

5.1.2. Method of Independent Storms (MIS)

While the epochal approach described in Section 5.1.1 is suitable for time histories of considerable length, this method presents a significant challenge for shorter sets of data. Cook (1982) argues that the annual maxima method eliminates many useful data points in the time history and should not be expected to yield adequate results for datasets spanning ten years or fewer. Noting that many of the stations' time histories identified in Chapter 3 span less than ten years of time, an approach that makes use of sub-annual epochs is necessary if these shorter time histories are to be useful. Cook (1982) provides a method for identifying extrema that (in many cases) significantly increases the number of observations available compared to the annual maxima approach. This is known as the "method of independent storms" (MIS) and is summarized as follows.

A wind speed time history is scanned to find downward crossings of an arbitrary wind speed threshold. Each crossing represents the end of a discrete and independent wind event or "storm" and the period after each crossing is considered a "lull" or non-storm period. Between each successive downward crossing, exactly one independent storm occurs. The maximum wind speed recorded in each storm then becomes a data point in the set of observed extrema found in

the time history. Preliminary analyses by Cook (1982) using a ten year long wind record found that the MIS yielded a typical storm frequency rate of around 100 events per year. To ensure a proper fit with an extreme value distribution such as Gumbel, Harris (1999) advises filtering these storms such that only the most extreme samples are retained. For the purposes of this study, storms identified using MIS are filtered such that only those ranked higher than "m", as defined in Equation 5.4 provided by Harris (1999), are utilized for analysis. This subset corresponds to roughly the top 2.5% most extreme storms identified and forms the basis for subsequent extrapolation methods.

$$\left(\frac{m}{N+1}\right)^{r} = \frac{1}{11} \qquad \text{(Eq. 5.4)}$$

Where

m = minimum rank for most extreme storms

r = rate of storms per year

N = total number of storms identified

Using this subset of independent storms, modified Gumbel distribution parameters (pi and alpha) are once again estimated using improved methods by Harris (1999). From this, a value for V50 is estimated, which comprises the fourth extrapolation technique utilized in this study. With regard to the empirical CDF generated from the observed extrema, this particular method makes use of updated plotting positions described by Harris (1996, 1999) which are similar to those used for annual maxima analyses in Section 5.1.1. An example of MIS data and a fitted distribution is presented in Figure 5.4.

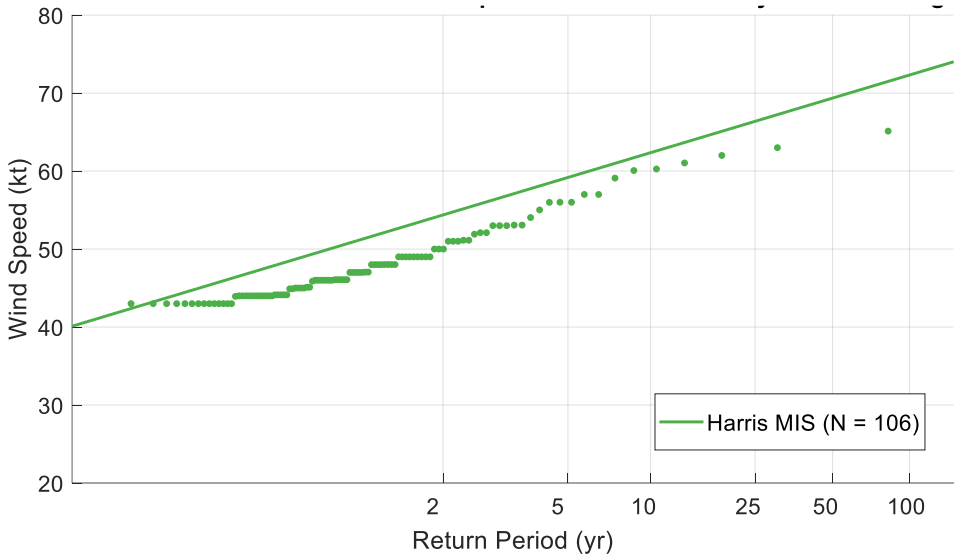

Figure 5.4. Example of wind speed extrema identified using the method of independent storms from Memphis, TN plotted with the accompanying fitted distribution.

5.1.3. Peaks Over Threshold (POT)

As an alternate method for increasing the sample size of extrema for shorter wind time histories, the peaks over threshold (POT) approach is shown to also be effective. Like the MIS, the POT method makes use of sub-annual extrema without regard for a pre-defined epoch length. Rather than looking at downward crossings of a certain wind speed, however, POT first considers all records, or "peaks", above a specific wind speed threshold. A number of advanced techniques exist for selecting a wind speed threshold suitable for identifying the peaks, such as a conditional mean exceedance (CME) graph presented by Davison and Smith (1990) and an extremal index discussed by Smith and Weissman (1994). Regardless of which threshold selection method is chosen, the resultant peaks must be statistically independent of one another. If they are thought not to be independent, a minimum separation time between successive peaks should be imposed to ensure their independence. This set of independent peaks thus becomes the set of observed extrema used in subsequent extrapolation methods.

The arrival of independent peaks over threshold can be appropriately modeled as a Poisson process having a mean annual arrival rate of lambda (λ). The magnitude of these peaks

can then be modeled using a generalized Pareto distribution (GPD), the maxima of which are shown to be GEV distributed (Palutikof et al. 1999). Similar to the GEV distribution, the behavior of the GPD is defined by a shape parameter (c), a scale parameter (a) and a location parameter (u), which in this case is the same quantity as the wind speed threshold. The functional form of the GPD CDF is presented in Equation 5.5 and several visualizations of it are shown in Figure 5.5. The special case of the GPD where the shape parameter approaches zero is simply an exponential distribution, as shown in Equation 5.6. Plotted in the same space as the other GEV plots, the exponential version of the GPD appears as a straight line just like the Gumbel.

$$F(U) = 1 - \left[1 - \frac{c}{a}(U - u)\right]^{\frac{1}{c}} \quad , \quad c \neq 0 \qquad \text{(Eq. 5.5)}$$

Where

$F(U)$ = GPD CDF value, probability of non-exceedance

U = wind speed

c = shape parameter

u = location parameter (wind speed threshold)

a = scale parameter

$$F(U) = 1 - \exp\left(-\frac{U-u}{a}\right) \qquad \text{(Eq. 5.6)}$$

Where

$F(U)$ = GPD, exponential version, CDF value, probability of non-exceedance

U = wind speed

u = location parameter (wind speed threshold)

a = scale parameter

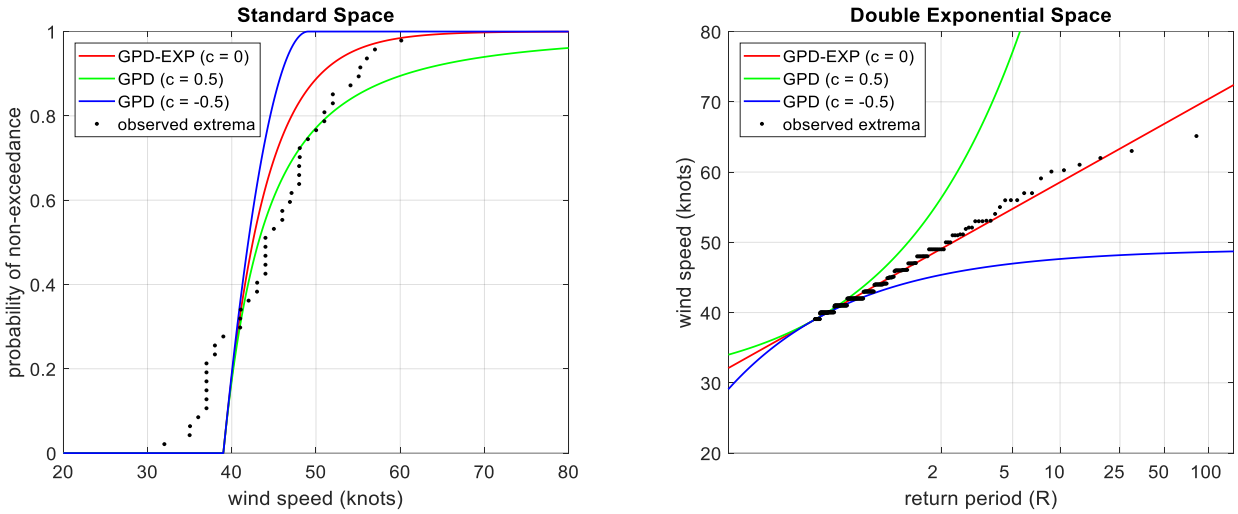

Figure 5.5. Left: Sample annual maxima plotted in standard space with three fitted GPD's. Right: Sample annual maxima plotted in double exponential space with three fitted GPD's.

Use of the GPD and GPD-exponential with POT form the final two (fifth and sixth) extrapolation methods used in this study. Compared to the MIS or AM methods, however, procuring V50 estimates using the POT method is slightly more involved. The procedure used in this study is briefly outlined as follows.

Due to the wealth of data processed, a simplified process of selecting a proper wind speed threshold is utilized. This involves setting a target value for lambda and finding, iteratively, a threshold wind speed such that the actual value of lambda matches the target value as closely as possible. This study sets a target lambda of 5 events per year for all storm types, which is just above the minimum value used prescribed by Pintar et al. (2015). Additionally, a wind speed threshold range from 10 knots to 80 knots is used for iteratively finding the closest matching lambda. The implications of these selections are discussed in Section 5.3. With the threshold value determined, estimates for the GPD shape parameter (c) and scale parameter (a) are made using a moment-based approach given by De Haan (1994); for the GPD-exponential case where c equals 0, a secondary estimate for a (a2) is also calculated. The two fitted CDFs are then written in terms of return period (R) using Equation 5.7 from Simiu and Heckert (1996), which

differs slightly from that used for AM and MIS. From there, two resultant estimates of V50 are calculated. Figure 5.6 provides an example of the POT approach, with plotting positions for the empirical CDF provided by Brabson and Palutikof (2000).

$$F(U) = 1 - \frac{1}{\lambda R} \quad \text{(Eq. 5.7)}$$

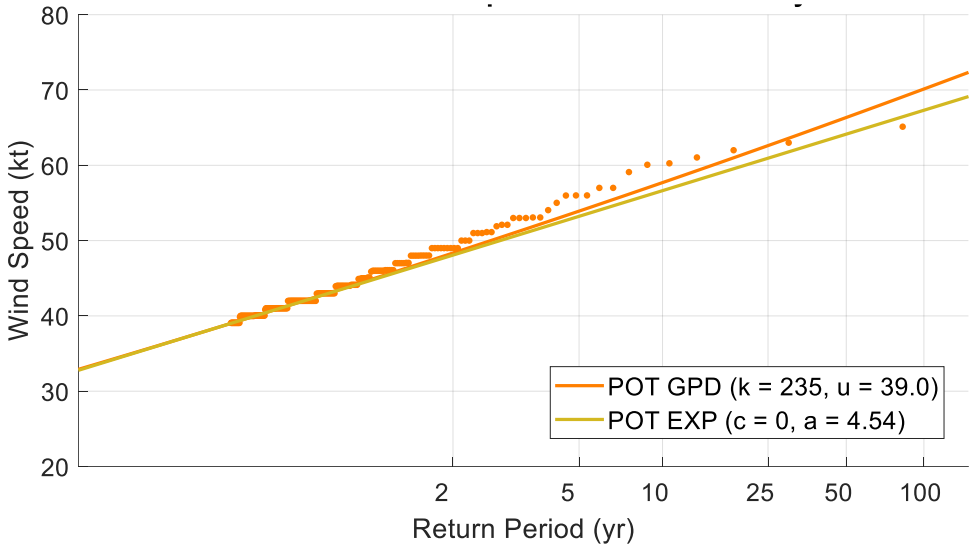

Figure 5.6. Example of wind speed extrema identified using the peaks over threshold method from Memphis, TN plotted with accompanying fitted distributions.

5.2. EVA Implementation

The following subsections detail the most relevant aspects of the EVA implementation process used in this study. For a visualization of these steps in the form of a flow chart, see Appendix A.

5.2.1. Data Selection

The six EVA procedures described in Section 5.1 were used to analyze wind speed time histories from all United States nationwide datasets considered (and available) in this study. This included data from previous iterations of the extreme wind database (Chapter 2), data from the DS 6405 set (Chapter 4) and data from the updated ISD 3505 set (Chapter 3). To streamline this process, the six extrapolation procedures were collected into a single, unified MATLAB program capable of simultaneously processing these EVA methods using any generic wind speed

time history inputted. Therefore, time histories from any data set and of any storm type could all be evaluated using consistent techniques and protocols. Table 5.3 describes each of the six nationwide datasets used for extreme value analysis in this study. Table 5.4 lists out the full suite of 18 time history types analyzed that were analyzed using the unified EVA program.

Table 5.3. Summary of extreme wind datasets used for extreme value analyses

Dataset Name	**Description**	**Location Count**
DS 6405 Non-QC	Cleaned 1-min resolution data before quality control procedures were applied	888
DS 6405 Unified Time History (UTH)	Cleaned and quality controlled 1-min resolution data in accordance with the procedures in Section XX	816
ISD 3505 Unified Time History (UTH)	Portion of the ISD 3505 Improved set matched with DS 6405 in time; has same overall length as DS 6405	888
ISD 3505 Sep 12 QC	Quality controlled version of older dataset	1,195
ISD 3505 US L48	Less quality controlled version of older dataset with two more years of data	1,180
ISD 3505 Improved	Expanded and updated version of older databases as described in Chapter XX	2,447

Table 5.4. Summary of all time history types used for extreme value analyses

DS 6405 Non-QC Non-Thunderstorm	DS 6405 Non-QC Thunderstorm	DS 6405 Non-QC Commingled
DS 6405 Unified Time History Non-Thunderstorm	DS 6405 Unified Time History Thunderstorm	DS 6405 Unified Time History Commingled
ISD 3505 Unified Time History Non-Thunderstorm	ISD 3505 Unified Time History Thunderstorm	ISD 3505 Unified Time History Commingled
ISD 3505 Sep 12 QC Non-Thunderstorm	ISD 3505 Sep 12 QC Thunderstorm	ISD 3505 Sep 12 QC Commingled
ISD 3505 US L48 Non-Thunderstorm	ISD 3505 US L48 Thunderstorm	ISD 3505 US L48 Commingled
ISD 3505 Improved Non-Thunderstorm	ISD 3505 Improved Thunderstorm	ISD 3505 Improved Commingled

To perform the analysis, the unified EVA program began by iterating through all 2,447 geographic locations found in the ISD 3505 Improved dataset (from the station groupings

established in Chapter 3). At each location, each of the 18 time history types displayed in Table 5.4 was analyzed. Results for each location were cataloged in a size 6x3 MATLAB-style data structure organized identically to Table 5.4. For each of these analyses, raw, unstandardized wind gust time histories (all in knots) were used.

To best match locations across different datasets, the ISD History Document and the station groupings developed in Chapter 3 were used extensively. This made it possible to connect ISD 3505 data—organized by USAF-WBAN pair—to DS 6405 data which is organized by call sign. In some cases, however, there was ambiguity as to which time history should be used at a particular location, especially when more than one option was available. For these cases, subjective judgment was used to select the most appropriate time history for each location with a focus on selecting the longest set of data possible. A tabulated list of specific selections is provided in Appendix A.

5.2.2. Storm Type Identification

Wind event storm types (non-thunderstorm versus thunderstorm) were identified previously within all of the ISD 3505-based datasets, though by slightly differing methods. To control for the differences in storm type identification scheme across datasets, a more streamlined procedure was implemented for this study. When thunderstorm events were identified for the improved ISD 3505 database in Chapter 3, a series of thunderstorm beginning and end times was created for each of the 2,447 groups (if thunderstorm information was available). Since these beginning and end times comprised the most robust and comprehensive set of thunderstorm times available at observation stations in the contiguous United States, these times were applied to all six of the data sets. To do this, a thunderstorm flagging function was used to assimilate pre-identified thunderstorm times with any generic, wind speed time history. All wind records were assumed to be associated with non-thunderstorm events, unless otherwise

flagged by the function. Thus, thunderstorm time histories (column 2 of Table 5.4) were composed of all wind records flagged by this function and non-thunderstorm time histories (column 1) were composed of all un-flagged records. Commingled time histories were comprised of the original time history without any flagging function applied. The nuances and implications of this classification system are discussed in Section 5.2.3.

Additionally, wind records associated with tropical versus non-tropical events were not identified for the EVA portion of this study. Despite the availability of this information, the presence of tropical events in time histories was assumed to be insignificant in the context of solely comparing results between datasets.

5.2.3. Elimination Criteria

Despite that the unified EVA program was designed to evaluate all 18 time history types at each of the 2,447 locations, this was not entirely possible due to a number of reasons. The primary reason was that at many locations, some data was simply unavailable. This was to be expected, however, since the 2,447 locations analyzed was more than double the number of locations represented by either of the two older datasets. A complete list of situations in which EVA was not conducted at any particular location is presented below:

1) *No wind data available* – if no wind data was found for a particular dataset, analysis was skipped for all storm types (an entire row in Table 5.4) at that location
2) *No thunderstorm beginning and end times available* – if wind data was found but thunderstorm times were not available, only the "commingled" storm type (third column in Table 5.4) was analyzed at that location; this implied that thunderstorm events could have existed within the time history, but were just not recorded
3) *Timestamp error* – if timestamps were corrupted or miscoded such that they lacked hour and minute specificity, analysis was skipped for the entire dataset (an entire row

in Table 5.4) at that location; this error was found to occur sporadically throughout the older datasets

4) *Thunderstorm flag error* – if thunderstorm beginning and end times existed but no thunderstorms events were flagged within the time history, analysis was skipped for thunderstorm time histories only; this implied that thunderstorms were physically not present at that location (as is found to be likely for many stations in the western United States) and that the non-thunderstorm time history was identical to the commingled time history
5) *Insufficient data length for EVA* – certain EVA methods for a particular time history were skipped if the extrema identified were too few in number; thresholds for skipping analysis were fewer than 2 years for AM, fewer than 1 independent storm for MIS, and fewer than 3 peaks for POT

5.3. EVA Results

Using the EVA methods described in Section 5.1 and the implementation strategy outlined in Section 5.2, the unified EVA program was successfully run, producing a large number of V50 estimates. The quantities of these estimates produced—corresponding to the dataset and storm type shown in Table 5.4—are given in Table 5.5. Percentages depict the amount of V50 estimates produced out of the total number of V50 estimates theoretically possible for each type of time history (i.e. number of locations from Table 5.3 times 6 EVA methods). Higher percentages indicate that fewer time histories were eliminated from analysis using the elimination criteria described in Section 5.2.3.

Table 5.5. Number of V50 estimates produced for each time history type across all locations

5,212 ~ 97.82%	5,061 ~ 94.99%	5,314 ~ 99.74%
4,890 ~ 99.88%	4,673 ~ 95.45%	4,890 ~ 99.88%
5,314 ~ 99.74%	5,016 ~ 94.14%	5,314 ~ 99.74%
6,406 ~ 89.34%	5,883 ~ 82.05%	6,543 ~ 91.26%
6,226 ~ 87.94%	5,669 ~ 80.07%	6,239 ~ 88.12%
12,358 ~ 84.17%	11,212 ~ 76.37%	14,340 ~ 97.67%

Figure 5.7 shows example results of all six EVA methods used with a single dataset (Improved ISD 3505) and a single storm type (commingled) in Champaign, IL. Empirical CDFs, representing the observed extrema, are plotted as discrete points along with the smoothed curves representing their fitted distributions. It is clear from this single example how some extrapolation methods diverge from one another as return period increases, even when analyzing the same dataset.

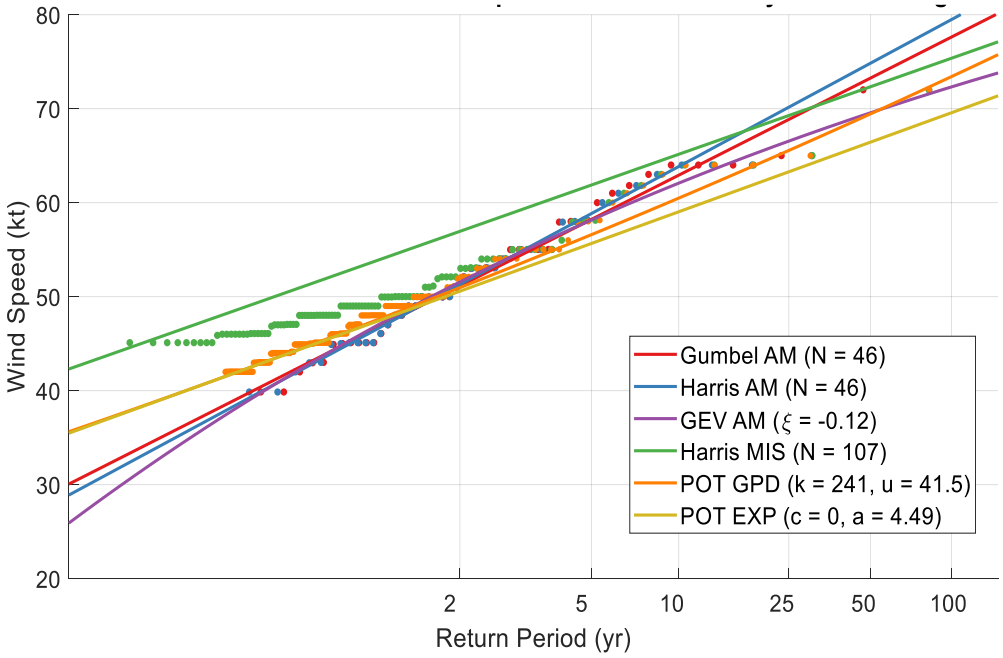

Figure 5.7. Example results of all six EVA methods for the Improved ISD 3505 dataset and commingled storm type in Champaign, IL.

Figure 5.8 expands the view slightly to include commingled storms from all six datasets in Champaign, IL. This figure highlights the disparate nature of each of the datasets with regard to how they are able to model extrema—a topic that is further explored in Chapter 6.

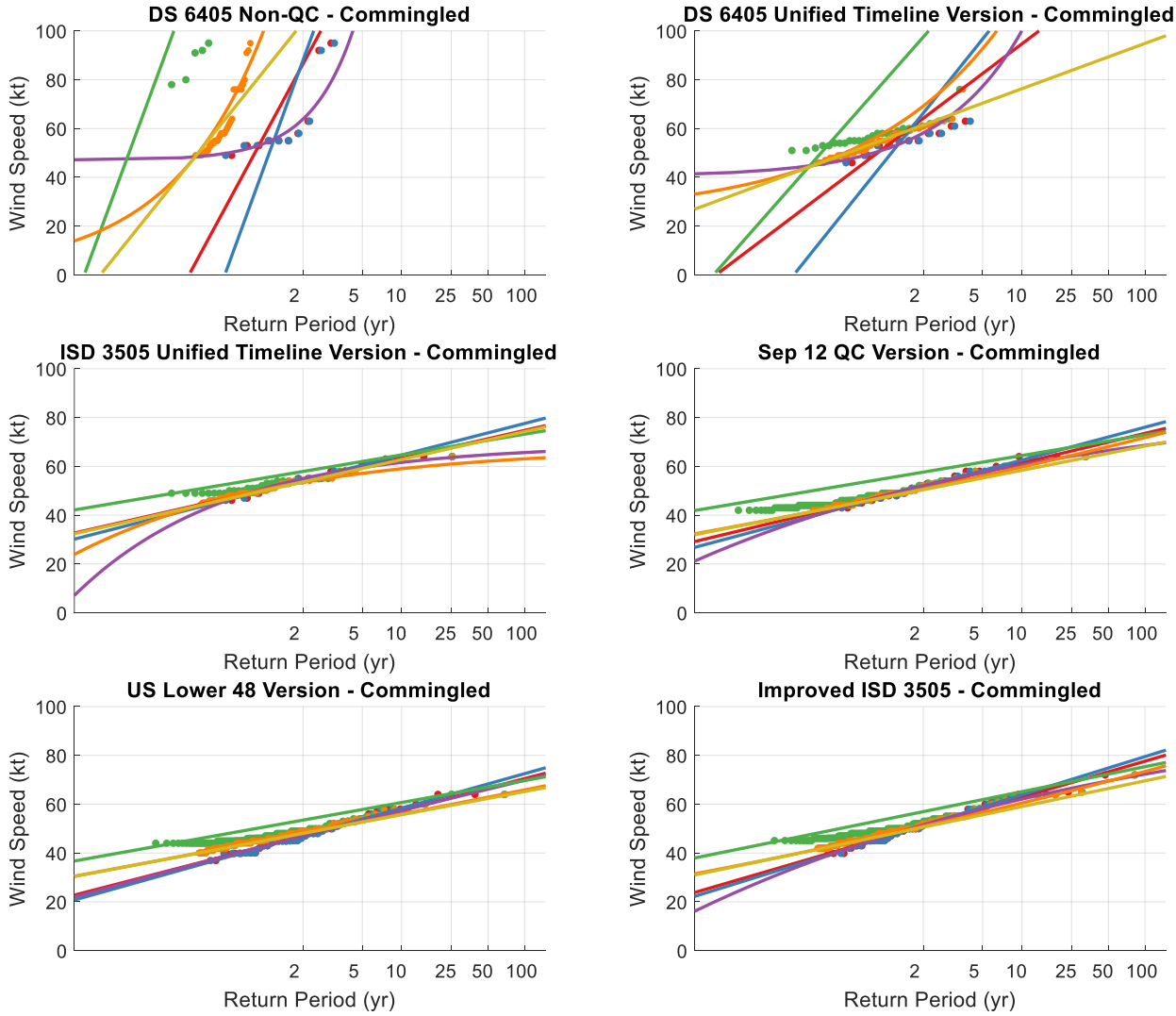

Figure 5.8. Example results of all six EVA methods using all six datasets for commingled storms in Champaign, IL.

Upon inspecting results at other locations, however, it became clear that challenges persisted with some of the EVA methods. The MIS, while yielding fairly consistent results across most locations, produced in some instances a fitted distribution with a negative slope. Further investigation of this issue revealed that a special mathematical case of Harris's method (1999) could yield a best fit line with a negative alpha value (indicator of slope) for data that, by

inspection, should clearly be fitted by a positive alpha value. An example of this phenomenon is shown in Figure 5.9, where the solid line depicts the distribution as fitted and the dashed line shows the same distribution but with sign of alpha forcibly flipped from negative to positive.

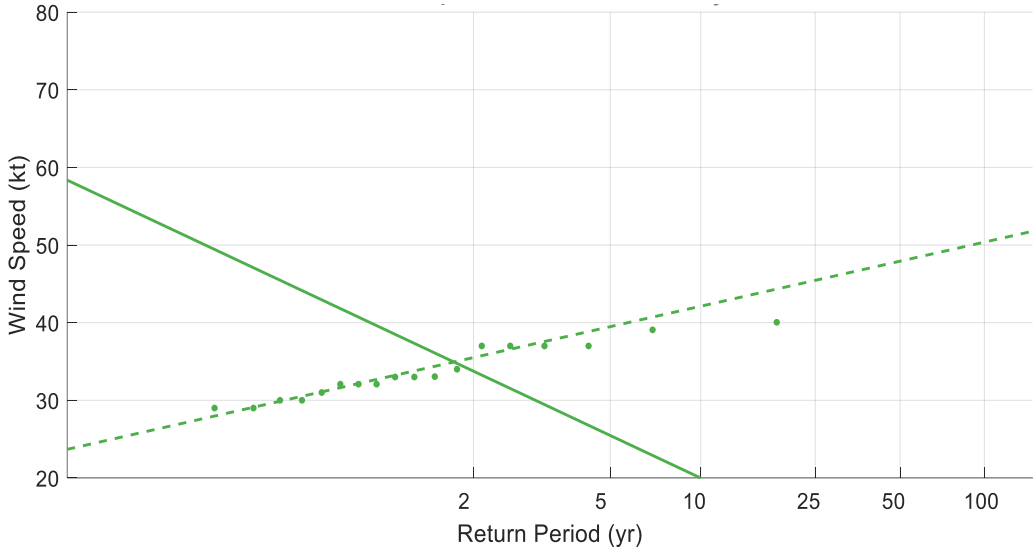

Figure 5.9. Scenario where the MIS fit of the wind extrema produces a negative slope in the fitted distribution when a positive slope is clearly the better fit.

For POT, instances where the target lambda could not be matched by further lowering the wind speed threshold (ostensibly due to a lack of data) yielded some highly questionable results as well. Fitted distributions for both POT extrapolation methods where the threshold speed (u) iteratively converged to the lower boundary of the threshold parameter space (10 knots) were found to be, by inspection, quite poor in most cases. In many of these cases, the estimated shape parameter (c) was so extreme that a V50 value was impossible to calculate because its theoretical "value" would have to exist beyond the asymptote of the GPD. This circumstance clearly indicated that the average annual arrival rate (lambda) was chosen too high for the particular time history and that the fitted distributions as calculated were unsuitable for estimating V50. Figure 5.10 depicts this issue clearly.

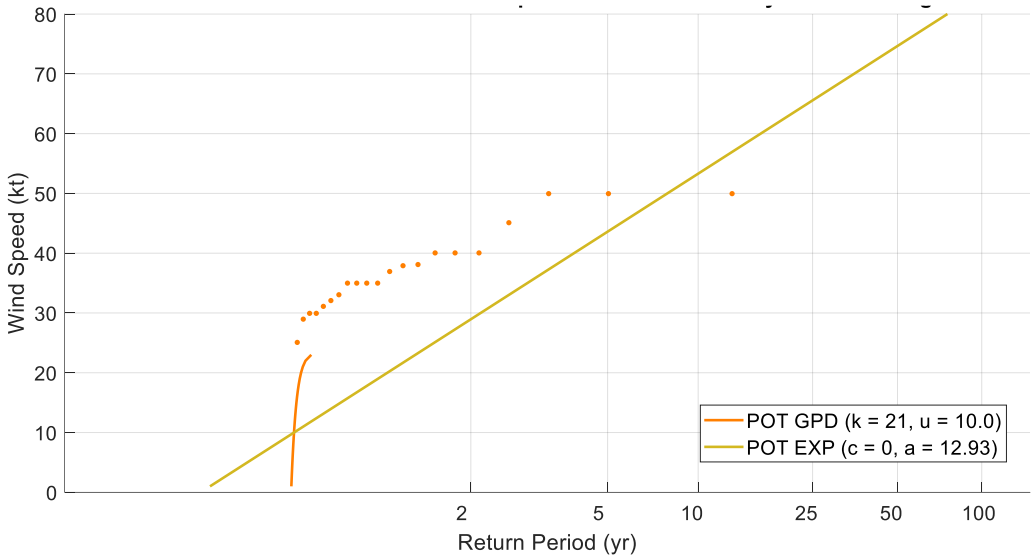

Figure 5.10. Scenario where the GPD fits of the data were unsuitable because the wind speed threshold was not low enough to accommodate the dataset properly.

The presence of these issues within the EVA results indicated overall that while performing EVA with the thousands of time histories used in this study was indeed possible, the viability of the results was not readily guaranteed. For time histories where the two chronic issues already described were known to exist, the EVA results were simply excluded from further analyses. To accommodate for other undetected issues that could highly skew ensemble-wide EVA results, however, a simple filter was applied such that only V50 values between the 5th and 95th percentiles of a particular time history type were retained. The implicit result of these "quasi quality control" procedures is given in Table 5.6, which provides updated and final V50 estimate quantities for all 18 time history types analyzed. The ensemble-wide analyses presented in Chapter 6 utilize only EVA results that pass this final set of quality checks and 5th to 95th percentile filtering step.

Table 5.6. Updated number of V50 estimates produced for each time history type across all locations

4,895 ~ 91.87%	4,582 ~ 86.00%	4,979 ~ 93.45%
4,423 ~ 90.34 %	4,222 ~ 85.23%	4,426 ~ 90.40%
4,839 ~ 90.82%	4,570 ~ 85.77%	4,823 ~ 90.52%
5,827 ~ 81.27%	5,407 ~ 75.41%	5,946 ~ 82.93%
5,653 ~ 79.84%	5,214 ~ 73.64%	5,686 ~ 80.31%
11,176 ~ 76.12%	10,261 ~ 69.89%	13,005 ~ 88.58%

5.4. EVA for OKM

Because the locations of Oklahoma Mesonet (OKM) observation stations were incompatible with those of the ISD 3505 and DS 6405 stations, EVA was performed separately for OKM data using a much narrower scope. Only one incarnation of the OKM time histories was used and thunderstorm event times were not determined for this network. Therefore, only one time history type (corresponding to the "commingled" storm type) was analyzed for all 108 OKM locations established in Chapter 4. At each of these locations, all six EVA methods were implemented. Since the length of each OKM time history was known to be 24 years and the overall quality of the wind data was known to be good, no elimination criteria were used to exclude certain analyses or results. An example of EVA results plotted for a single OKM station is shown in Figure 5.11.

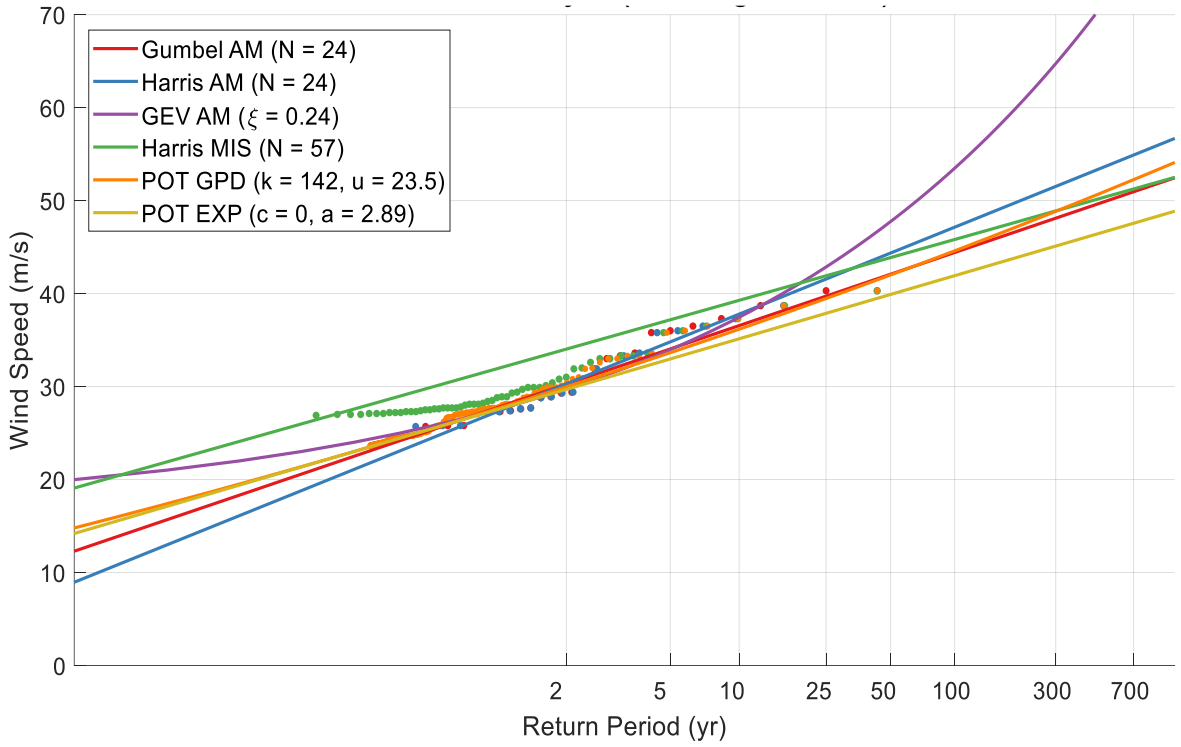

Figure 5.11. Example results of all six EVA methods evaluated for the wind speed time history at Freedom, OK (FREE).

CHAPTER 6: ENSEMBLE RESULTS FOR ALL ANALYSES

Results presented in Chapters 3, 4, and 5 focused solely on the wind conditions at single locations, rather than across any particular area or observation network. While a thorough understanding of a single location is useful in some applications, it is perhaps more useful overall to interpret these results in a broader context. Hence, this study aims to evaluate the impact of various extreme wind database improvements and augmentations on the overall understanding of United States extreme wind climatology. To better accommodate this objective, results from each previous analysis were compiled across all geographic locations to generate network-wide (or "ensemble") results. These results are interpreted using a number of tools, including a geospatial (mapping) scheme, a practical scheme, and numerous graphical means.

6.1. Geospatial Interpolation Scheme

Data from thousands of discrete locations in the contiguous United States were analyzed in accordance with the procedures outlined in Chapter 5. The subsequent result was a multitude of V50 estimates, each associated with a specific observation station where the data originated. To visualize these results spatially, V50 values could simply be mapped using their corresponding locations to show their geographic distribution. While such a map would depict only the true results obtained in this study, it would also neglect any locations not associated with analyzed data (i.e. anywhere lacking an observation station). Therefore, this study makes use of a geographic interpolation tool developed in by Lombardo et al. (2016) that uses these discrete values to estimate additional values across a grid that completely covers the contiguous United States. The tool then smooths the gridded values using a cubic spline smoothing algorithm and produces a colorized contour map as exemplified by Figure 6.1.

While there are a number of different operational parameters available for this mapping algorithm, the results mapped in this chapter, unless otherwise specified, make use of a single set of parameters that balance computational requirements with overall precision. For the interpolation grid, a spacing of 0.2 degrees (latitude and longitude) is used. A smoothness parameter (sp)—which controls the coarseness of the applied smoothing (Lombardo et al. 2016)—of 0.5 is used as it produces modestly-smoothed contours. To illustrate these methods, a map is presented in Figure 6.1 that depicts smoothed V50 wind speed results from the Sep 12 QC database calculated using the GEV annual maxima method and commingled storms. Data from 971 stations are spatially arranged in their corresponding locations (shown as black dots) and grid boxes between them are subsequently populated using interpolation. The results shown in Figure 6.1 also serve as the control group for subsequent comparisons made in this Chapter.

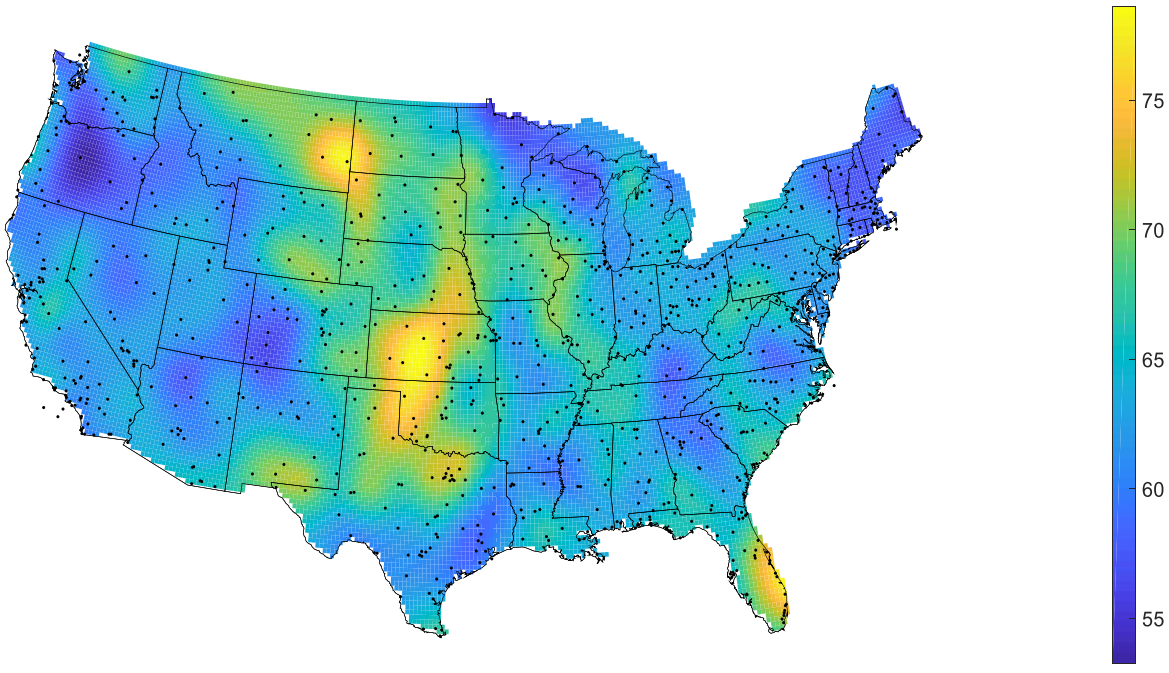

Figure 6.1. Example of the geospatial (mapping) interpretation of ensemble EVA results. Presented is V50, in knots (1 knot = 1.15 mph), estimated using GEV, annual maxima, commingled storms from the Sep 12 QC database.

6.2. Practical Interpretation Scheme

In addition to a geospatial interpretation of the results, a more practical approach was included to show how V50 estimates vary as a result of different changes made to the databases. To do this, a set of 20 cities across the contiguous United States (given in

Table 6.1 and mapped in Figure 6.3) was hand-selected in approximate correspondence to the 10 climatological regions identified by Lombardo and Zickar (in press) and shown in Figure 6.2. These regions are each shown to have a distinct climatological identity with respect to extreme convective wind speeds and provide a means for identifying representative climatology locations throughout the United States. In each region, two cities were selected: one representing a populous location where wind observation data are known to exist (i.e. containing an observation station) and one representing an area known to not have wind observation data (i.e. where geospatial interpolation is therefore necessary).

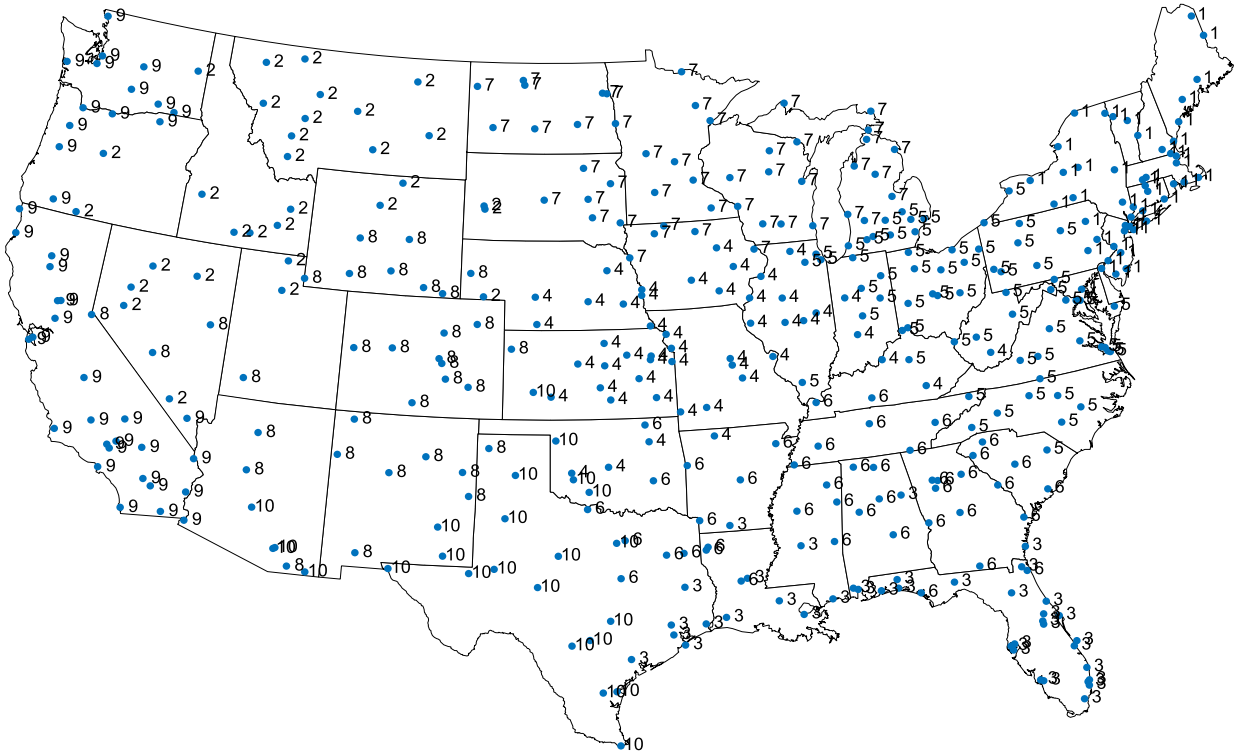

Figure 6.2. Map of ten extreme wind climatological regions.

Table 6.1. Names and coordinates of 20 cities selected for analysis

Cluster	City (with station)	Coordinates	City (interpolation)	Coordinates
1	Hartford, CT	41.765, -72.673	Skowhegan, ME	44.765, -69.719
2	Great Falls, MT	47.505, -111.300	Glenns Ferry, ID	42.954, -115.300
3	Baton Rouge, LA	30.451, -91.187	Arcadia, FL	27.215, -81.858
4	Decatur, IL	39.840, -88.954	Red Cloud, NE	40.089, -98.519
5	Columbus, OH	39.961, -82.998	Keysville, VA	37.040, -78.483
6	Augusta, GA	33.473, -82.010	Kosciusko, MS	33.057, -89.587
7	Fargo, ND	46.877, -96.789	Ontonagon, MI	46.871, -89.314
8	Colo. Springs, CO	38.833, -104.821	Duchesne, UT	40.163, -110.402
9	Sacramento, CA	38.581, -121.494	South Bend, WA	46.663, -123.804
10	Roswell, NM	33.394, -104.523	Guthrie, TX	33.620, -100.322

Figure 6.3. Map of the 20 cities presented in Table 6.1.

These 20 cities form a set of running evaluation locations corresponding to the smoothed contour maps presented in this chapter. Evaluating changes in V50 at these locations is practical in that it shows how various manipulations of the extreme wind database would potentially affect

design wind speeds around the country. To provide a baseline (control group) for comparisons, V50 was first evaluated at each of the 20 cities using both of the older extreme wind databases—"Sep 12 QC" and "US L48". A sample of these results using commingled storms and the GEV annual maxima extrapolation method is given in Table 6.2; a full suite of baseline values using all three storm types and all six extrapolation methods for these 20 cities is provided in Appendix A. Given that (1) the V50 values for both the Sep 12 QC and US L48 databases are very similar at these locations and (2) that the Sep 12 QC database is known to be more rigorously quality controlled, all subsequent comparisons of V50 are made with reference to the Sep 12 QC values presented in Table 6.2.

Table 6.2. V50 results for selected cities using both the Sep 12 QC and US L48 databases, GEV annual maxima method, and commingled storm type.

City	**V50: Sep 12 QC (kt)**	**V50: US L48 (kt)**	**City**	**V50: Sep 12 QC (kt)**	**V50: US L48 (kt)**
Hartford	58.1	58.2	Skowhegan	57.4	57.1
Great Falls	68.1	68.1	Glenns Ferry	60.6	60.1
Baton Rouge	65.6	64.5	Arcadia	69.9	70.5
Decatur	64.9	63.3	Red Cloud	72.7	70.4
Columbus	63.2	63.1	Keysville	58.6	60.3
Augusta	62.4	60.9	Kosciusko	63.0	62.3
Fargo	68.8	69.0	Ontonagon	58.5	55.8
Colo. Springs	65.7	66.2	Duchesne	61.2	60.5
Sacramento	62.9	61.5	South Bend	62.2	61.0
Roswell	66.7	68.1	Guthrie	71.0	71.0

6.3. Improving the ISD 3505 Database

6.3.1. Breadth of Data

Of all the improvements made to the ISD 3505 extreme wind database described in Chapter 3, the two most significant are the inclusion of additional reporting stations and the extension of existing time histories. The increase in reporting stations is visualized in Figure 6.4, where the 1,195 stations comprising the Sep 12 QC database are plotted alongside the 2,447 station groupings comprising the Improved ISD 3505 database. Assuming the total land and water area of the contiguous United States is approximately 3.12 million square miles (Owen et al. 2019) and ignoring any spatial clustering tendencies of the reporting locations, the overall network density is calculated to be approximately 0.0004 sites per square mile (roughly one per 2,610 square miles) for the Sep 12 QC database and approximately 0.0008 sites per square mile (roughly one per 1,275 square miles) for the Improved ISD 3505 database. As a first-level estimation, these metrics indicate that the inclusion of additional reporting stations in the Improved ISD 3505 database roughly doubles the overall network density compared to the Sep 12 QC database. This comparison holds true with regard to the US L48 database as well, which is comprised of a similar number of reporting locations as Sep 12 QC (1,180).

Figure 6.4. Comparison of observation network densities between the Sep 12 QC database (left) and the Improved ISD 3505 database (right).

The augmentation of time history lengths across the network is quantified by the histograms in Figure 6.5, which show the distribution of time history lengths for both the Sep 12 QC and Improved ISD 3505 datasets. Each bin of the histogram is normalized by the total number of observation stations to yield a percentage of total stations. In the Sep 12 QC set, nearly 100% of all stations observed less than 40 years of wind data. This contrasts to the Improved ISD 3505 set, where nearly 25% of all stations observed 40 years of data or more. This difference is attributed not only to the years of elapsed time between the formation of each dataset, but to the detailed geographic grouping scheme employed by the Improved ISD 3505 dataset. For instance, two stations in the Sep 12 QC database that are nearby in space but still considered to be separate reporting locations could each have 15 mutually exclusive years of recorded wind data. If these stations were subsequently grouped (due to their location) in the Improved ISD 3505 database, their resultant time history could easily be over 40 years in length when also accounting for the elapsed time. This mechanism likely explains the surge in reporting locations with 46 years of data in the improved dataset.

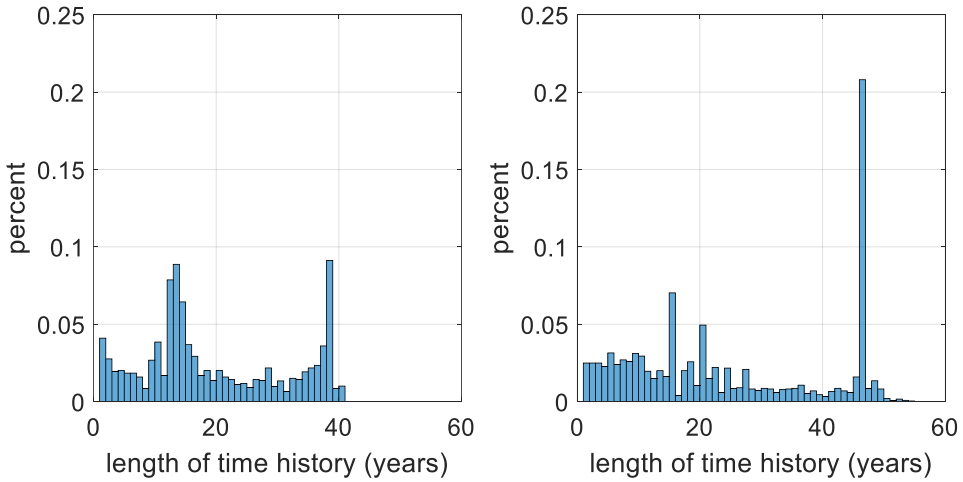

Figure 6.5. Normalized histograms showing the comparison of time history lengths between the Sep 12 QC database (left) and the Improved ISD 3505 database (right).

For both datasets, however, the distribution of time history lengths appears to be bimodal, with a concentration of reporting stations containing "long" time histories and a concentration containing "short" time histories. The cause of this is likely attributed to uneven commissioning cycles of reporting stations (such as ASOS) and other irregularities regarding how stations' data were brought into the ISD 3505 database. This bimodal nature, however, does suggest that the utilization of two different treatments of wind speed extrema, as a function of time history length, might be appropriate across the network.

To show geographically which areas are impacted most by the augmented time history lengths, Figure 6.6 shows smoothed color contours (similar to the process described in Section 6.1) depicting the net change in time history length between the Sep 12 QC and Improved ISD 3505 datasets. Red shading indicates a net increase in total time history length, blue shading indicates a net decrease, and white indicates no change. While spatial averaging of time history lengths is largely non-sensical in principle, Figure 6.6 nonetheless indicates overwhelmingly that most areas of the country observe an overall increase in time history length.

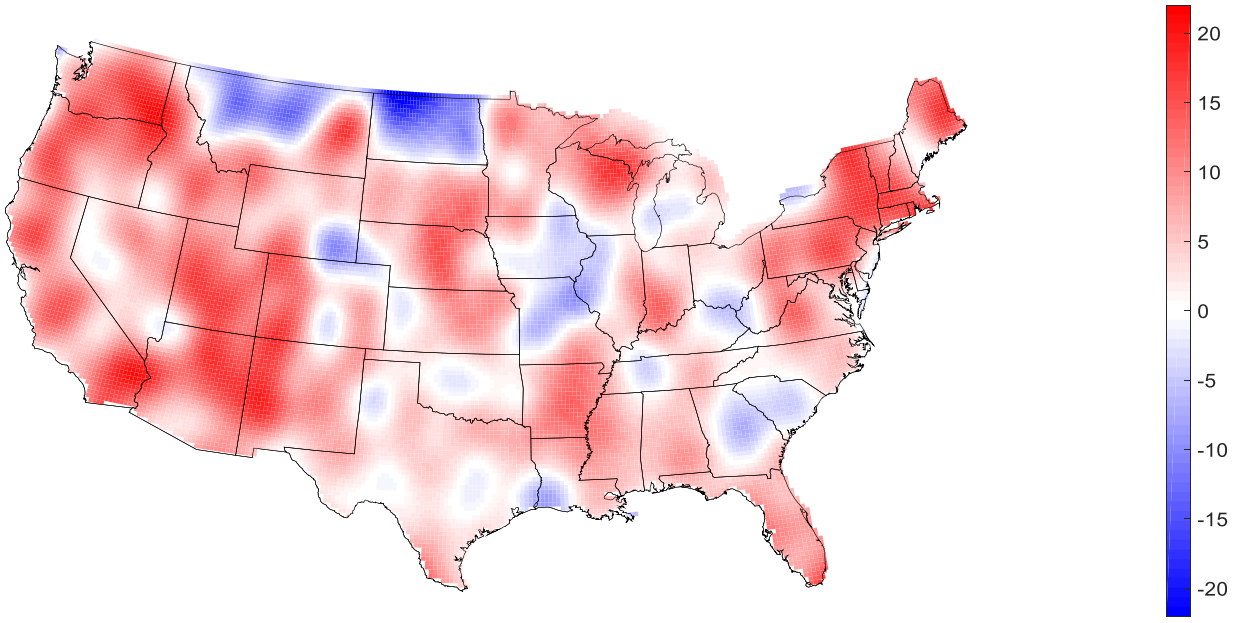

Figure 6.6. Spatially-smoothed net change in time history length between the Sep 12 QC and Improved ISD 3505 databases. Units are years.

Time histories in New England, the Intermountain West, and the Pacific Coast are the most benefited on average by the improved database, whereas parts of the far northern plains of North Dakota and Montana are seemingly least benefited. Further examination of the reporting locations in Figure 6.4, however, shows a distinct correlation between locations where many observation sites were added and areas with a net decrease in spatially-averaged time history lengths. This indicates, intuitively, a presence of many newer observation locations—with consequently shorter time histories—in these areas. Therefore, the map in Figure 6.6 can alternatively be viewed as a rough indicator of which areas in the United States show the greatest increase in spatial network density with the Improved ISD 3505 database.

6.3.2. Extreme Value Analysis

As discussed in Chapter 5, six different extreme value analysis techniques were implemented on the multitude of datasets prepared in this study. The wind speed corresponding to a 50-year return period, V50, was calculated for each method, which serves as the primary result metric used in this chapter. To initially compare the Improved ISD 3505 results to those from the Sep 12 QC database (the control set), V50 values from each database were plotted against one another on a series of scatter plots shown in Figure 6.7. Only locations with valid V50 results from both databases are presented, effectively limiting the plotted data to only locations found in the Sep 12 QC database. As with the gust comparison plot shown in Figure 4.8, both a 1:1 line (solid gray) and a linear regression line (dashed black) are constructed to show theoretical perfect agreement and actual agreement, respectively.

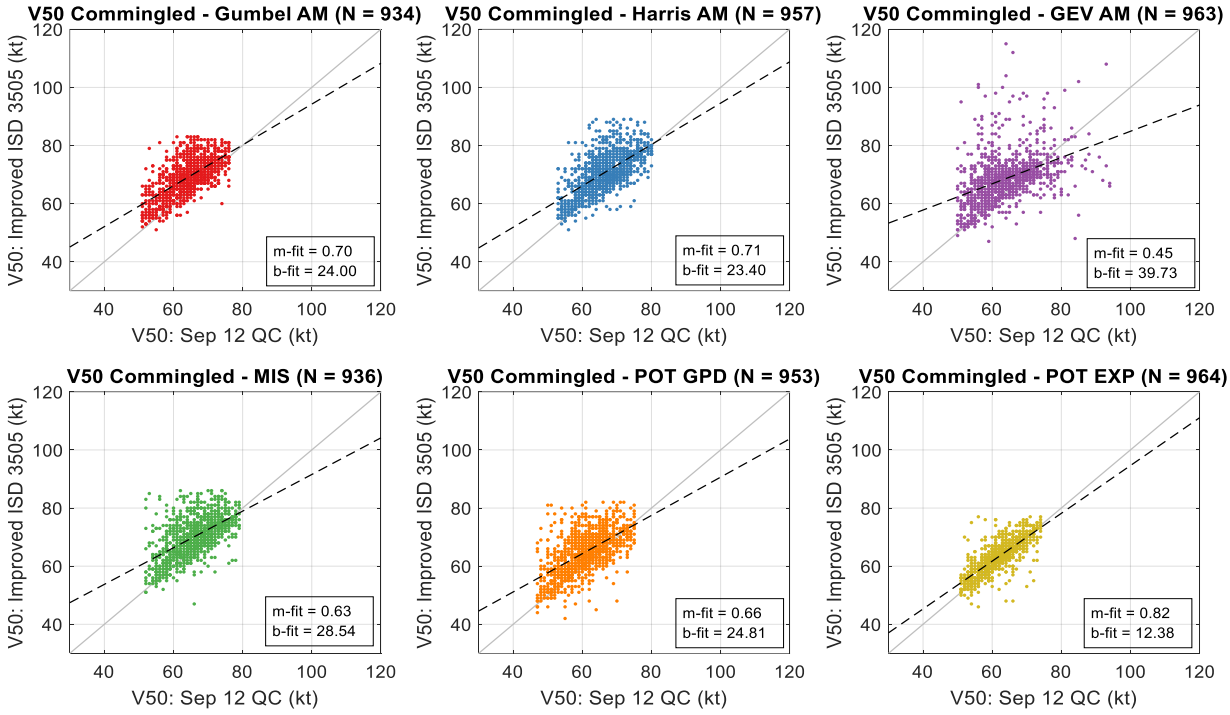

Figure 6.7. Scatter plots comparing V50 values (GEV annual maxima, commingled storms) obtained using the Sep 12 QC database to those obtained using the Improved ISD 3505 database. The linear fit line is shown as a dashed line and fitted parameters are given in the plots' legends.

It is evident from Figure 6.7 that V50 estimates calculated using the Improved ISD 3505 database tend to be larger than those calculated using the Sep 12 QC database over the range of available data. Departures from the control values are minimized using the peaks over threshold exponential distribution method and are maximized when using a GEV fit of annual maxima. There is overall very little difference in how the V50 estimates compare, as an ensemble, among the other four extreme value methods. What is consistent among all six methods, however, is the apparent tendency of the Improved ISD 3505 V50 estimates to approach perfect agreement with the Sep 12 QC estimates with increasing V50 wind speed. This is evidenced, in part, by the intersection of the regression line with the 1:1 line being situated neatly at the upper extent of the plotted data in all six plots. Thunderstorm and non-thunderstorm V50 estimates largely follow

the same behavior as those of commingled storms; corresponding scatter plots for these other storm types are presented in Appendix A, for reference.

To get a better sense of how the entirety of the improved database results compare to the control set, V50 estimates from the Improved ISD 3505 database were mapped and spatially smoothed as described in Section 6.1. The results—corresponding to the commingled storm type and GEV annual maxima extrapolation method—are shown in Figure 6.8 and can be directly compared to the smoothed contours shown in Figure 6.1 which were computed similarly. Figure 6.8 displays results from 2,158 out of the 2,447 total station groupings, indicating that approximately 12% of the station groupings were filtered out based on any of the criteria discussed in Chapter 5. A full set of V50 maps made using commingled storms and all EVA methods is presented in Appendix A.

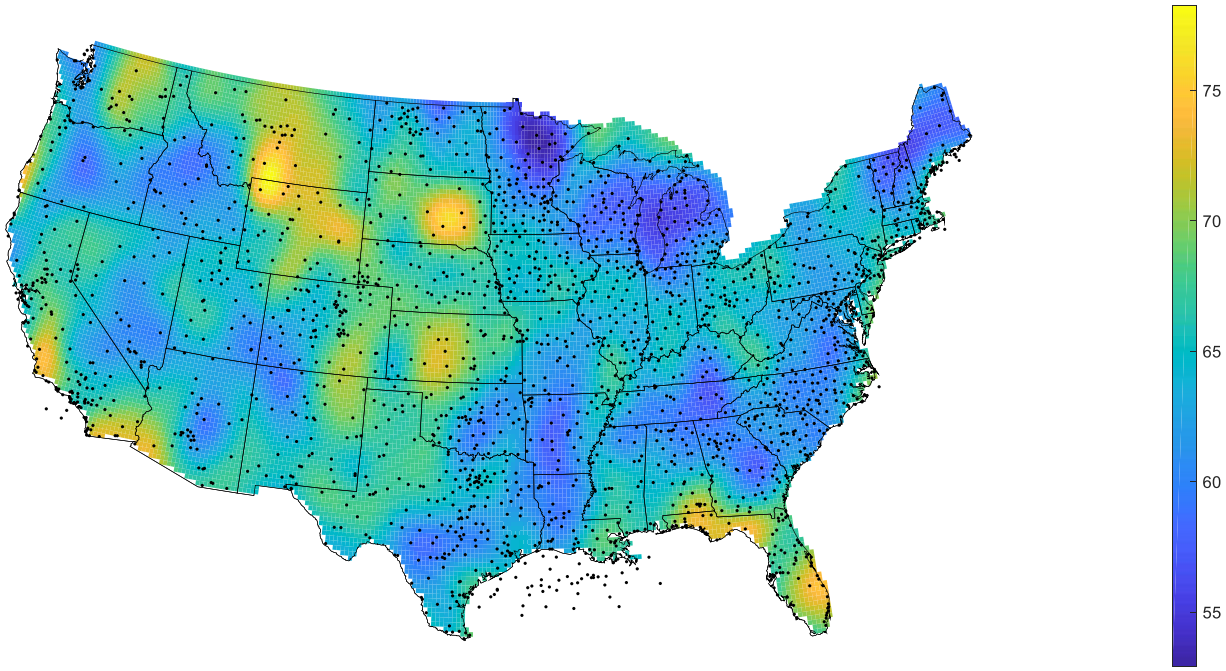

Figure 6.8. V50 mapped using the Improved ISD 3505 database, GEV annual maxima method and commingled storms. Number of stations plotted is 2,158. Units are knots (1 knot = 1.15 mph).

Observing both Figure 6.1 and Figure 6.8, it is evident initially that the overall character of the two sets of results is the same. V50 wind speeds tend to be higher in the middle of the

country and lower in areas like the Great Lakes, New England, and Intermountain West. Elevated V50 speeds are estimated in south Florida in both instances, likely owing to the persistence of extreme winds from tropical events in the area. What is most different, however, between the two maps is the presence of more isolated areas of high V50 speeds in the Improved ISD 3505 dataset results. Figure 6.9 depicts these areas by mapping the net difference in V50 wind speed between the two datasets at each smoothed grid point. Among the most noteworthy areas of increased V50 speed are those near the West Coast in southern California, southern coastal Oregon, and eastern Washington. Also of note are the significant departures observed in the panhandle region of Florida and in the south-central part of Montana.

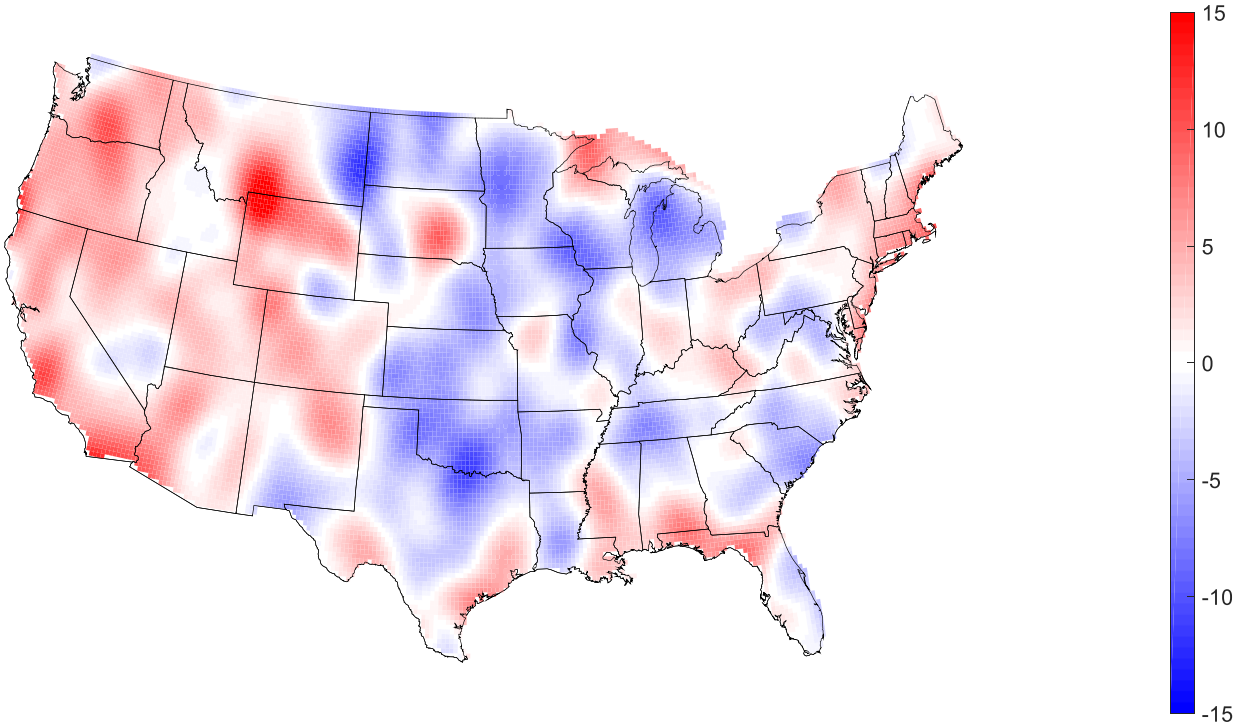

Figure 6.9. Residual V50 map showing the net change in V50 between the Sep 12 QC and Improved ISD 3505 databases (i.e V50 Improved ISD 3505 minus V50 Sep 12 QC). Red shading indicates an increase from current database to improved and blue shading indicates a decrease. Units are knots (1 knot = 1.15 mph).

Table 6.3 presents V50 estimates from the Improved ISD 3505 database evaluated at the 20 cities identified in Section 6.2. These estimates are all calculated using the spatially-smoothed contour values, regardless if direct V50 calculations are possible at the location.

Evaluations using all six extreme value methods are presented along with percent changes, which depict the change in V50 wind speed from the Sep 12 QC dataset using the same extreme value method. The results are color coded to match the contours in Figure 6.9 for continuity and the GEV AM column is shaded to indicate the values directly corresponding to Figure 6.1, Figure 6.8, and Figure 6.9. Table 6.4 further summarizes these results by averaging across locations as well as by city type and by extrapolation method. Version of these tables corresponding to Thunderstorm and Non-Thunderstorm events are included in Appendix A for reference.

Table 6.3. V50 results for selected cities using the Improved ISD 3505 database, all EVA methods, and commingled storm type. Percentages show comparisons to Sep 12 QC V50 estimates of the same storm type and EVA method.

City	Improved ISD 3505 V50 Est. for Commingled Storms (in knots) By Extrapolation Method					
	Gum. AM	Harris AM	GEV AM	MIS	POT GPD	POT Exp
Hartford	64.0 (+9%)	65.5 (+8%)	63.8 (+10%)	65.3 (+8%)	59.3 (+9%)	58.2 (+1%)
Great Falls	73.1 (+11%)	77.1 (+16%)	70.1 (+3%)	76.1 (+12%)	70.1 (+11%)	71.1 (+9%)
Baton Rouge	63.9 (0%)	66.7 (0%)	66.8 (+2%)	67.9 (-1%)	61.2 (-5%)	56.0 (-9%)
Decatur	64.8 (-3%)	66.6 (-3%)	63.8 (-2%)	65.7 (-3%)	62.3 (-1%)	60.6 (-6%)
Columbus	64.4 (-1%)	66.0 (-1%)	64.8 (+3%)	65.8 (0%)	61.7 (+1%)	61.2 (-2%)
Augusta	58.0 (-2%)	59.5 (-3%)	60.0 (-4%)	58.8 (-5%)	52.8 (-7%)	52.8 (-11%)
Fargo	65.8 (-6%)	65.5 (-6%)	62.3 (-9%)	66.9 (-5%)	58.2 (-13%)	60.7 (-4%)
Colo. Springs	69.0 (0%)	76.2 (+6%)	67.9 (+3%)	73.7 (+9%)	67.6 (+6%)	66.9 (+1%)
Sacramento	64.0 (+1%)	66.5 (0%)	67.9 (+8%)	66.0 (+1%)	59.4 (-3%)	59.5 (-2%)
Roswell	68.8 (+2%)	73.2 (+5%)	66.0 (-1%)	68.9 (0%)	66.6 (+8%)	66.2 (+1%)
Skowhegan	57.3 (-2%)	59.2 (-1%)	58.5 (+2%)	58.8 (-1%)	55.8 (-1%)	56.3 (-3%)
Glenns Ferry	62.2 (+1%)	63.3 (-2%)	61.0 (+1%)	63.3 (-2%)	59.9 (+1%)	58.5 (-3%)
Arcadia	65.2 (-2%)	67.7 (-3%)	70.4 (+1%)	69.0 (+1%)	64.0 (-6%)	59.3 (-3%)
Red Cloud	70.8 (+0%)	73.9 (+1%)	69.2 (-5%)	72.6 (-1%)	66.5 (-2%)	66.1 (-2%)
Keysville	57.2 (-5%)	59.0 (-7%)	59.2 (+1%)	60.1 (-1%)	54.9 (-1%)	52.7 (-7%)
Kosciusko	64.2 (0%)	66.5 (0%)	64.9 (+3%)	67.1 (+2%)	62.8 (+4%)	57.5 (-6%)
Ontonagon	62.4 (0%)	61.2 (-5%)	65.3 (+12%)	60.9 (-5%)	55.1 (-11%)	57.1 (-10%)
Duchesne	67.0 (+4%)	69.9 (+4%)	64.1 (+5%)	67.1 (+5%)	62.5 (+6%)	62.9 (-1%)
South Bend	66.0 (+5%)	67.8 (+3%)	65.1 (+5%)	65.5 (+1%)	60.3 (+2%)	62.8 (+1%)
Guthrie	70.0 (-2%)	70.6 (-3%)	67.8 (-5%)	70.3 (-1%)	65.2 (-3%)	68.1 (+1%)

Table 6.4. Summary of V50 statistics presented in Table 6.3.

City (with station)	Avg. V50 (kt)	Average Departure	Closest Match Method	City (interp.)	Avg. V50 (kt)	Average Departure	Closest Match Method
Hartford	62.7	+8%	GEV AM	Skowhegan	57.7	-1%	Gumbel AM
Great Falls	72.9	+10%	Gumbel AM	Glenns Ferry	61.4	-1%	GEV AM
Baton Rouge	63.8	-2%	Gumbel AM	Arcadia	65.9	-2%	Gumbel AM
Decatur	64.0	-3%	GEV AM	Red Cloud	69.9	-2%	GEV AM
Columbus	64.0	0%	Gumbel AM	Keysville	57.2	-3%	Gumbel AM
Augusta	57.0	-5%	Gumbel AM	Kosciusko	63.8	+1%	Gumbel AM
Fargo	63.2	-7%	GEV AM	Ontonagon	60.3	-3%	MIS
Colo. Springs	70.2	+4%	Gumbel AM	Duchesne	65.6	+4%	Gumbel AM
Sacramento	63.9	+1%	Gumbel AM	South Bend	64.6	+3%	GEV AM
Roswell	68.3	+3%	Gumbel AM	Guthrie	68.7	-2%	POT Exp.
City (with station) overall	N/A	+0.77%	N/A	City (interp.) overall	N/A	-0.67%	N/A
Gumbel AM overall	N/A	+0.50%	N/A	Harris AM overall	N/A	+0.45%	N/A
GEV AM overall	N/A	+1.65%	N/A	MIS overall	N/A	+0.70%	N/A
POT GPD overall	N/A	-0.25%	N/A	POT Exp overall	N/A	-2.75%	N/A

Table 6.4 also shows a selected "closest match" extreme value analysis method for each location. This was calculated to be the method producing the V50 wind speed closest to the arithmetic average of all six V50 estimates at each location. Overall, the Gumbel annual maxima method prevails among the 20 cities with 12 closest matches. GEV annual maxima is the second most common with 6 closest matches and the MIS and POT exponential methods have one match each. The table also provides some indicators of relative sensitivity of V50 wind speed estimation to a particular extreme value method. Averaged over all 20 cities, V50 estimate changes between the Sep 12 QC dataset and the Improved ISD 3505 dataset are found to be less drastic when using the Gumbel annual max, Harris annual max, MIS and POT GPD methods than they are when using the GEV annual max and POT exponential methods. The latter two methods also appear to act significantly in opposite directions, such that use of the GEV annual max method tends to increase V50 estimates between databases and the POT exponential method tends to decrease them.

6.3.3. GEV Shape Parameter

While the areas of high V50 wind speed—or "high points"—identified in Figure 6.9 are not necessarily errant simply because they appear anomalous, they are nonetheless the subject of further consideration and refined analyses. In Chapter 5, a set of elimination criteria was established such that, among other things, only time histories of long enough duration to perform EVA routines were used. Post-EVA criteria also filtered out results from identified errant analyses as well as any values lying outside the 5^{th} and 95^{th} percentiles. What these filtering steps did not remove, however, were locations with mathematically-possible results yet comparatively short time histories. Both Cook (1982) and MEASNET (2016) suggest that annual maxima-based analyses are not reliable for records bearing less than ten years' worth of annual maxima; it is found that over 450 of the data points plotted in Figure 6.8 fail to meet that

criterion alone. Furthermore, the indication of a bimodal distribution of time history lengths—with the lower mode centered between 15 and 20 years, albeit higher than 10 years—indicates that the data presented thus far is likely saturated with results stemming from numerous short-duration time histories. Given that this is the case, a second set of analyses was run using data only from locations reporting more than 20 years of observations (i.e. 21 or more recorded annual maxima wind speeds). This filtering step, thus, reduced the number of plotted locations from 2,158 to 1,086 (a 50% decrease). For brevity, only the mapped results from this set of analyses (shown in Figure 6.10) are presented.

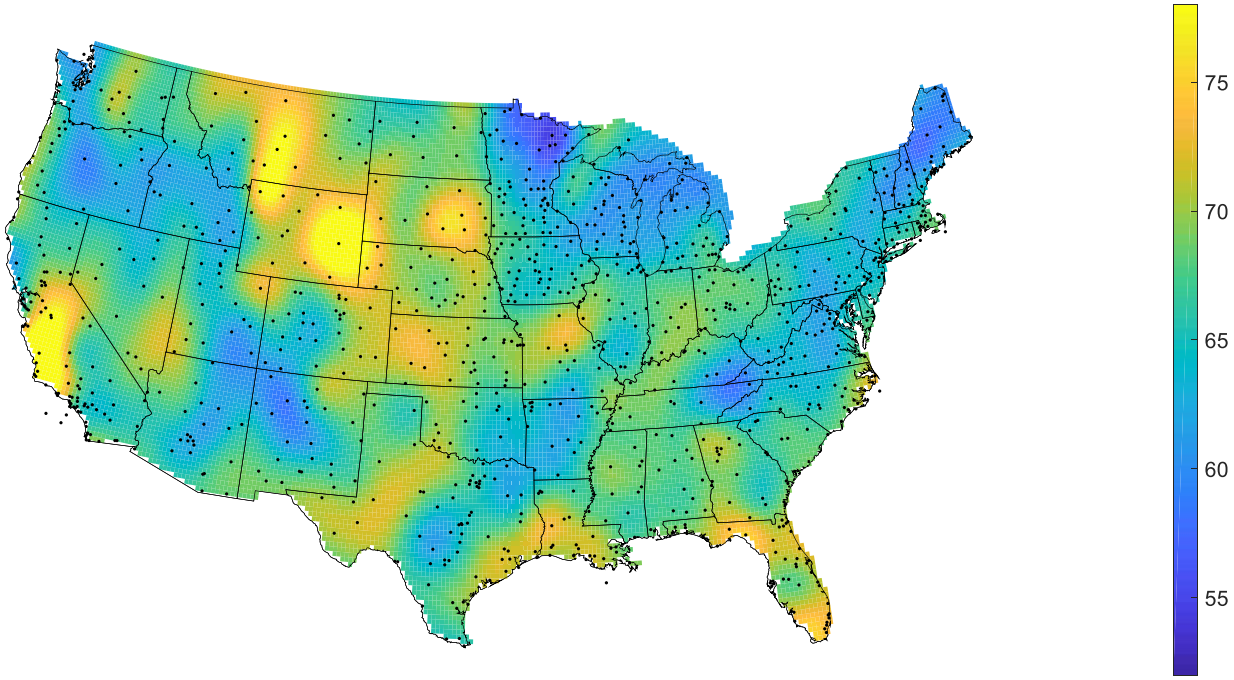

Figure 6.10. V50 mapped using the Improved ISD 3505 database, GEV annual maxima method and commingled storms using only stations reporting more than 20 years of data. Number of stations plotted is 1,086. Units are knots (1 knot = 1.15 mph).

With the color scale adjusted to match that of Figure 6.8, it is evident still that despite filtering out stations with shorter time histories, several of the same high points found in Figure 6.8 dominate the map (and perhaps more so). Since Figure 6.10 depicts about half as many data points as Figure 6.8, the effect of spatial averaging is diminished. This allows locations with extremely high V50 values to effectively dominate the surrounding areas' interpolated results, as

appears to be the scenario in eastern Wyoming and central California. These exact high points do not appear in the mapped results from other EVA methods (including others using annual maxima), indicating that the fitted shape parameter—to which the distribution's end behavior is known to be highly sensitive—is likely driving the observed results. To evaluate this claim, the map in Figure 6.10 is subsequently annotated in Figure 6.11 with corresponding data (direct from observation stations, before smoothing) at some areas of interest. The plots in Figure 6.12, where the annotated locations are also identified, depict the behavior of shape parameters across all 1,086 locations with over 20 years of annual maxima.

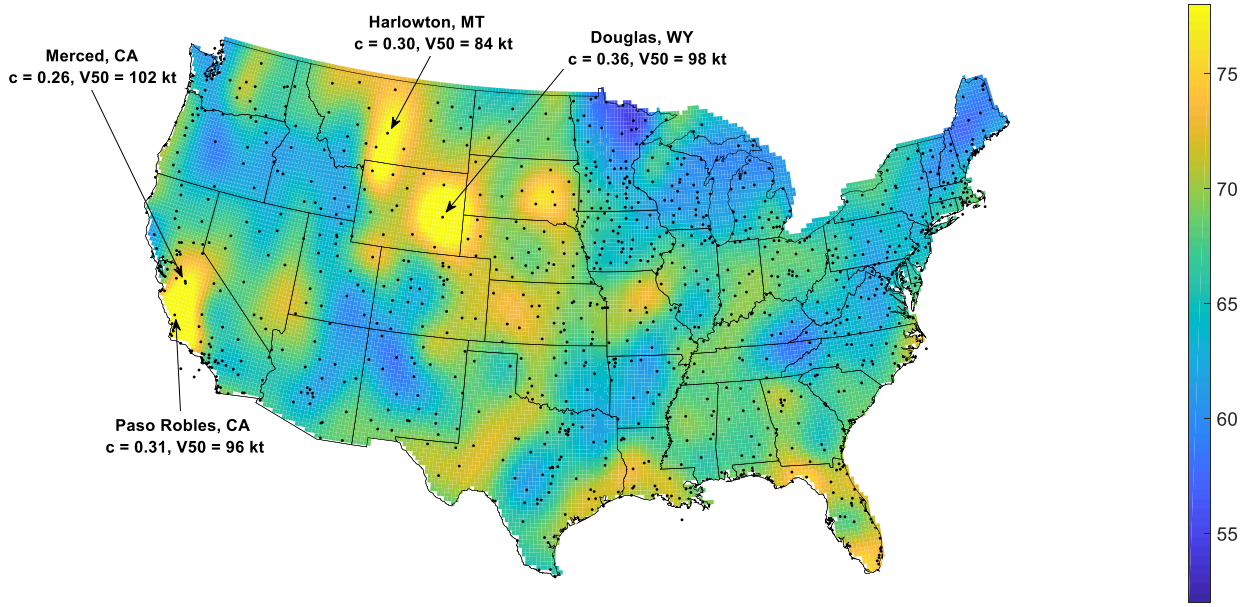

Figure 6.11. Map from Figure 6.10 with four notable high points annotated. Units are knots (1 knot = 1.15 mph).

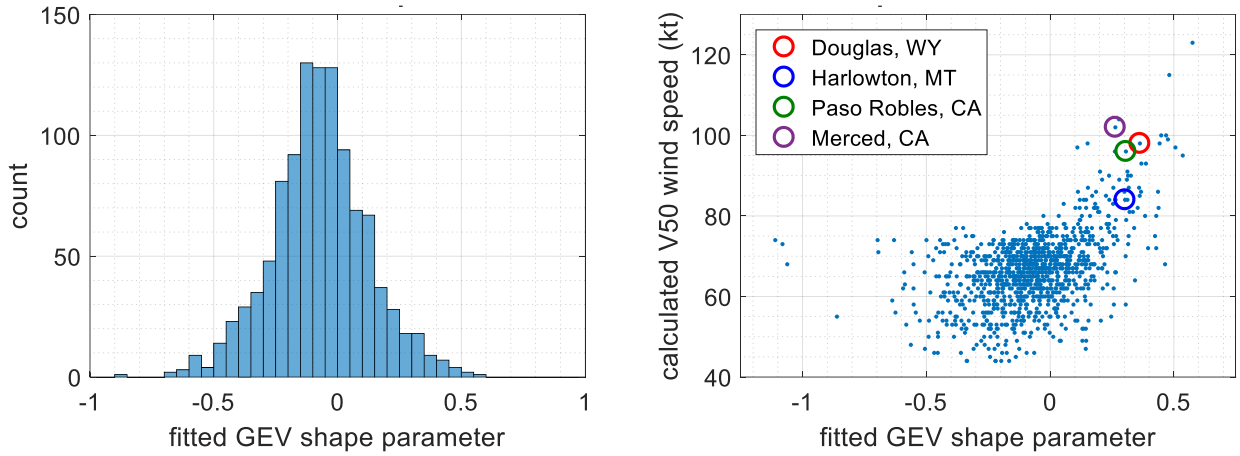

Figure 6.12. Right: distribution of GEV shape parameters for stations plotted in Figure 6.10. Left: GEV shape parameter versus V50 estimate for stations plotted in Figure 6.10.

Figure 6.11 asserts that, even by rudimentary spot checking of mapped data, there is indeed a correlation between high points on the V50 map and elevated local values of the GEV shape parameter, c. Despite the rather Gaussian distribution of shape parameters shown in the histogram in Figure 6.12, it is evident from the accompanying scatter plot that shape parameters of increasing value (mostly where $c > 0$) correlate well with dramatically-increasing V50 wind speeds. These four selected high points in California, Montana and Wyoming—despite being chosen largely by inspection—in fact belong to the right-hand tail of the shape parameter distribution. For extreme value methods where the shape parameter is fixed at zero (i.e. Gumbel annual maxima), the anomalous increase in V50 at these four areas is not readily observed, as shown in Figure 6.13 where V50 estimates are presented using the Gumbel annual max method and a comparable set of stations with over 20 annual maxima recorded.

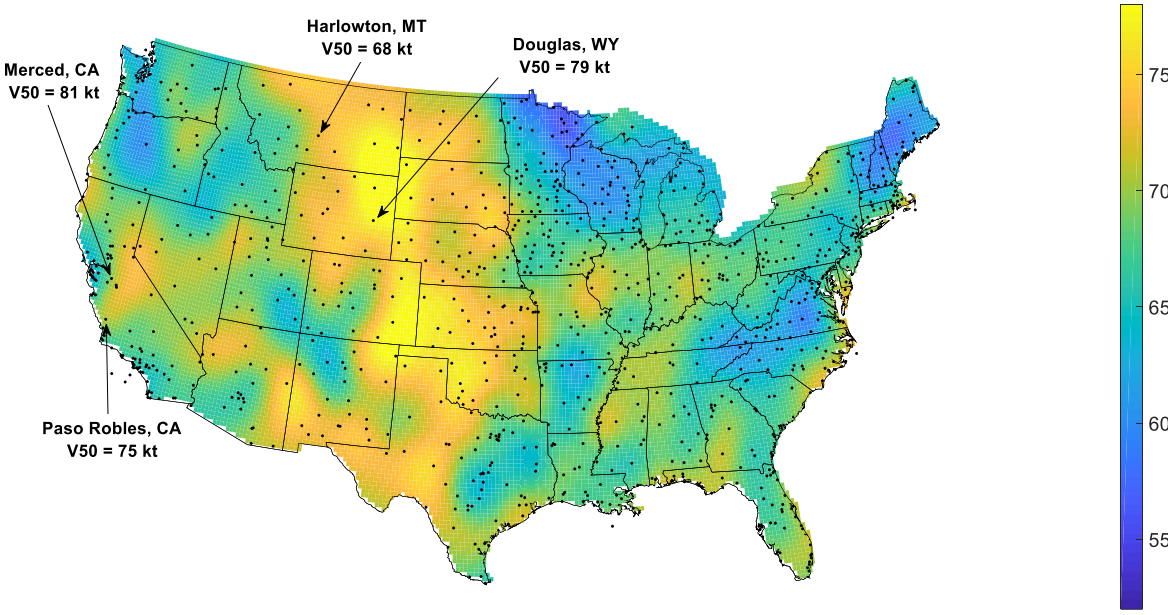

Figure 6.13. V50 mapped using the Improved ISD 3505 database, Gumbel annual maxima method and commingled storms using only stations reporting more than 20 years of data. Annotated high points from Figure 6.11 are shown as a comparison. Units are knots (1 knot = 1.15 mph).

6.4. Improving Temporal Resolution – DS 6405 Study

6.4.1. Gust Comparison Analysis

Gust comparison plots and regression analyses, as shown in Figure 4.8, were generated for all 888 stations with useable high resolution DS 6405 data. The ensemble results presented in this section consist of 816 stations where quality control procedures were applied and 72 stations that did not meet the criteria for quality control (e.g. no wind speeds above 70 knots in the time history). Figure 6.14 shows the ensemble-wide distribution of match percentages (percentage of DS 6405 gusts where an ISD 3505 temporal match could be made), fitted slope values, and fitted intercept values. The extremes of each histogram have been truncated for ease of display and the median value of each is shown in red.

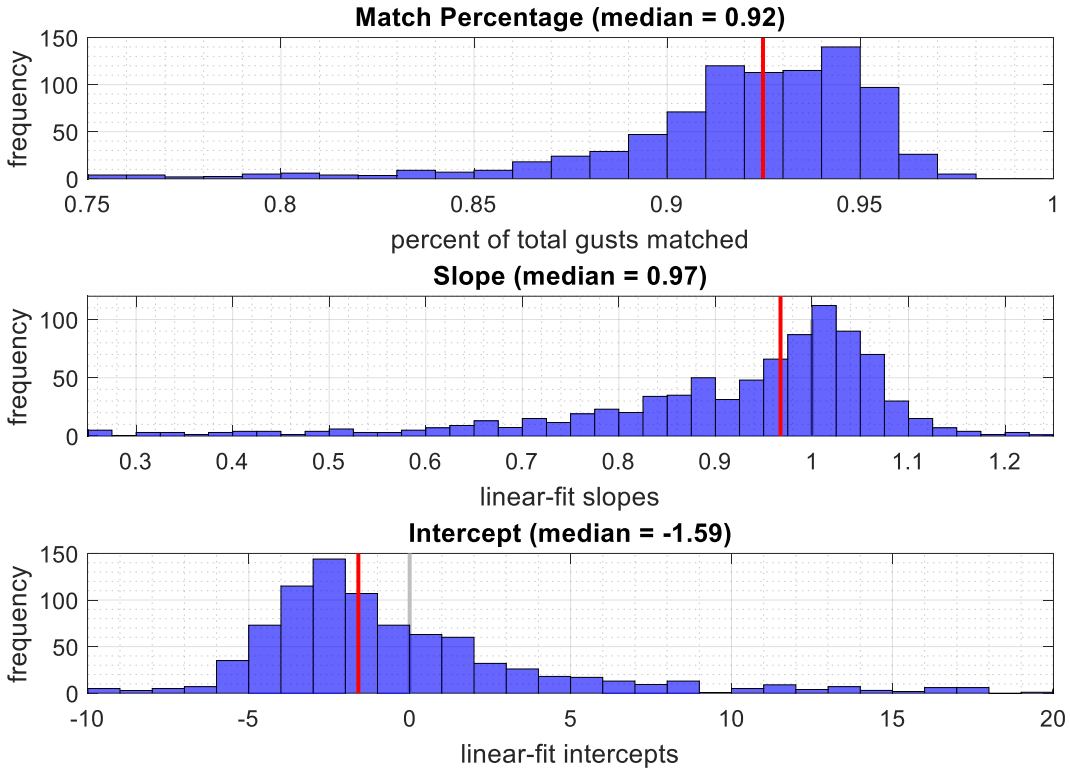

Figure 6.14. Histograms showing the ensemble distribution of match percentage (top), regression slope (middle) and regression intercept (bottom) with median values of each distribution shown as a red line.

A perfect match between datasets would yield an ensemble-wide match percentage of exactly 1 (indicating a complete temporal match) and slope and intercept values of exactly 1 and 0, respectively (indicating congruency of wind speeds between the datasets). The results shown in Figure 6.14 indicate that these perfect-match "objectives" are largely unmet as an ensemble. Most stations' DS 6405 time histories provided matches to at least 90% of the ISD 3505 gusts analyzed, but at no station out of 888 were 100% of gusts perfectly matched. Furthermore, if the median slope and intercept values were used to "predict" a DS 6405 wind speed using a known ISD 3505 wind speed and a linear fit, the result would differ by over 6% (over 3 knots) for a wind speed as low as 50 knots. To better visualize the slope and intercept results together, Figure 6.15 displays a scatter plot of all 888 stations' slopes and intercepts plotted. Again, extremities are removed for ease of display and median values are shown as red lines. Perfect match values for slope and intercept are shown as bold black lines intersecting at (1,0).

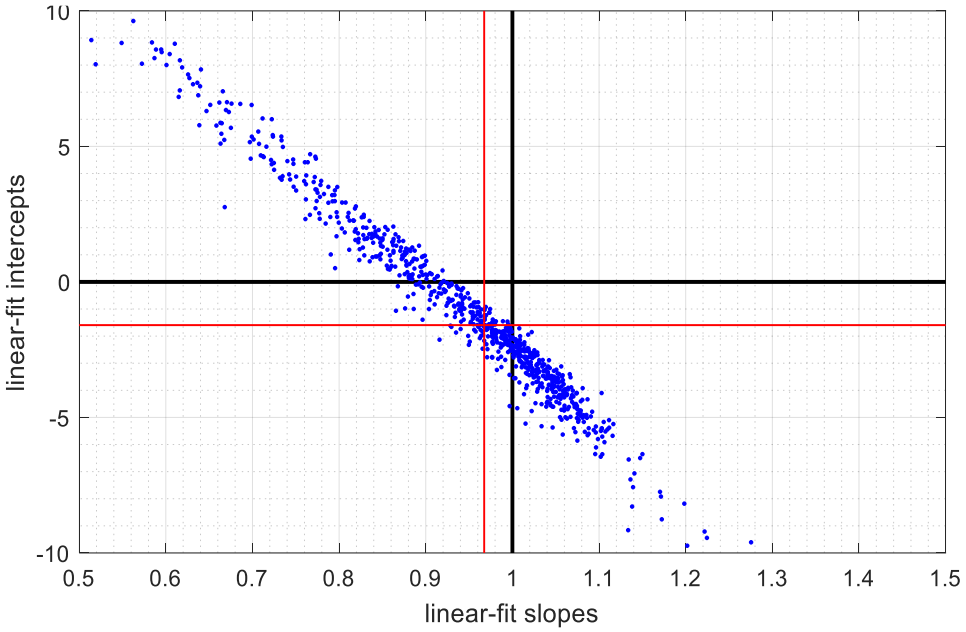

Figure 6.15. Scatter plot of each station's fitted slope versus its fitted intercept. Median values for each are shown with red lines and perfect agreement values are shown with black lines.

The scatter plot in Figure 6.15 not only reaffirms the relative mismatch between the ISD 3505 and DS 6405 datasets but also offers some interpretation of how the datasets differ. Suppose, for this example, that the plot's "quadrants" are defined by the perfect match lines x = 1 and y = 0, where each quadrant has a slope above 1 (>S) or below 1 (<S) and an intercept above 0 (+I) or below 0 (–I). Where slope and intercept are both below the perfect match quantities (in the [<S, –I] quadrant), reported DS 6405 wind speeds are on average lower than ISD 3505 wind speeds across all wind speed magnitudes. In the [>S, –I] and [<S, +I] quadrants, DS 6405 wind speeds could be above or below ISD 3505, depending on the wind speed considered and the exact values of slope and intercept. The [>S, +I] quadrant would indicate that DS 6405 wind speeds are on average above those reported by ISD 3505 for all wind speed magnitudes. Of the 888 stations analyzed, 234 lie within the [<S, –I] quadrant, 334 lie within the [>S, –I] quadrant, and 320 lie within the [<S, +I] quadrant. Of note, however, is that none of the stations lie within the [>S, +I] quadrant where DS 6405 wind speeds are expected to be higher overall.

Figure 6.16 illustrates the potential predictive power of this relationship by adding lines plotted at selected wind speeds of 50, 60 and 70 knots. These lines indicate all the possible combinations of slope and intercept that produce the wind speed indicated. Areas to the left of each line indicate an overall downward bias at that wind speed by the DS 6405 dataset, assuming that the control group of ISD 3505 wind speeds are "correct". This figure clearly shows that for the three wind speeds selected, most stations in the DS 6405 network exhibit significant downward bias of wind speeds when compared to the same wind speeds in ISD 3505. In other words, the DS 6405 network chronically reports lower wind speeds than the ISD 3505 for the same physical wind events observed.

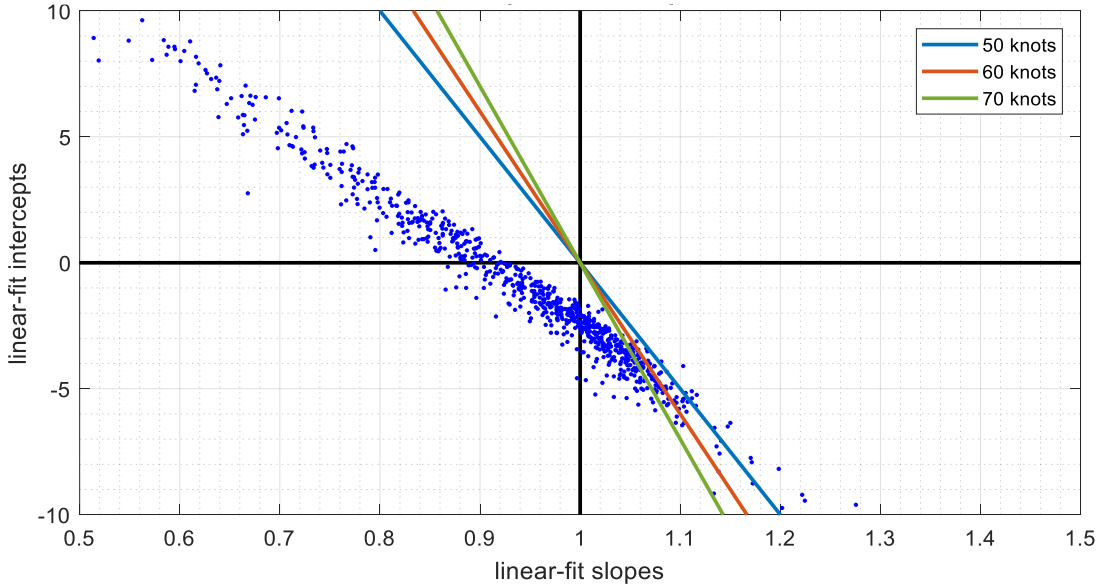

Figure 6.16. Scatter plot from Figure 6.15 with three wind speed reference lines added. Points (stations) to the left of each line can be said to underestimate wind speeds of that particular magnitude.

6.4.2. Extreme Value Analysis

Ensemble results of EVA using the high resolution DS 6405 data were produced in a similar fashion to the Improved ISD 3505 database methods described in Section 6.3. In this section, two resultant databases—DS 6405 Non-QC and DS 6405 Unified Time History (UTH)—are compared to one control database, ISD 3505 Unified Time History (UTH). As

described in Chapter 4, the ISD 3505 UTH database contains wind speed time histories from the Improved ISD 3505 database that have been matched in time to the DS 6405 data and have also been truncated to match the length of available DS 6405 data at the corresponding location. It should be noted also that, unlike the gust comparison plots analyzed in Chapter 4, the EVA ensemble results do not blend the two DS 6405 databases in order to utilize all 888 stations with suitable, quality controlled data. Rather, the two databases remain separate such that analyses pertaining to the DS 6405 Non-QC database incorporate results from all 888 stations and analyses using the DS 6405 UTH database only utilize results from the 816 stations where quality control procedures were applied.

Figure 6.17 displays comparisons of V50 wind speed estimates between the DS 6405 Non-QC database and the ISD 3505 UTH database for commingled storms. Subsequently, Figure 6.18 depicts this same comparison between the two UTH databases. A 1:1 line (solid gray) and a linear regression line (dashed black) are again constructed to show theoretical perfect agreement and actual agreement, respectively. Corresponding figures for other storm types are presented in Appendix A, though the general behavior of the results is largely similar across storm type.

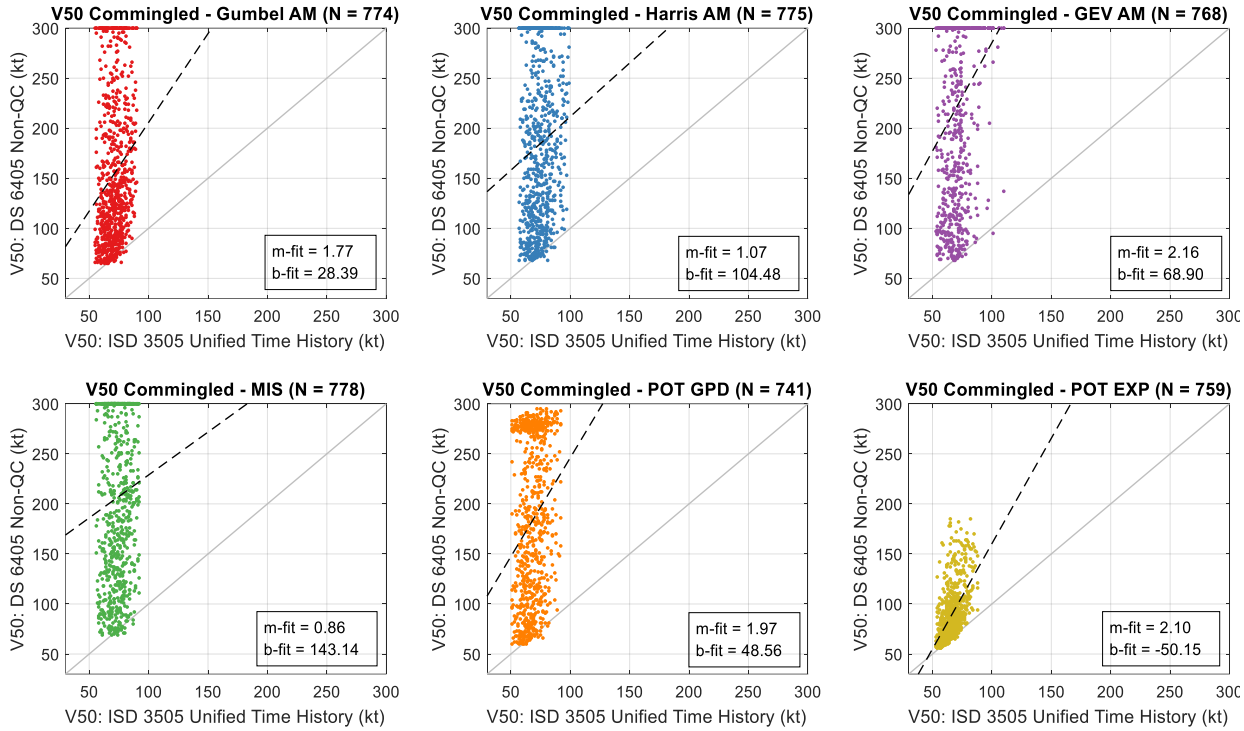

Figure 6.17. Scatter plots comparing V50 estimates created using the DS 6405 Non-QC and ISD 3505 UTH databases, GEV annual maxima method, and commingled storms.

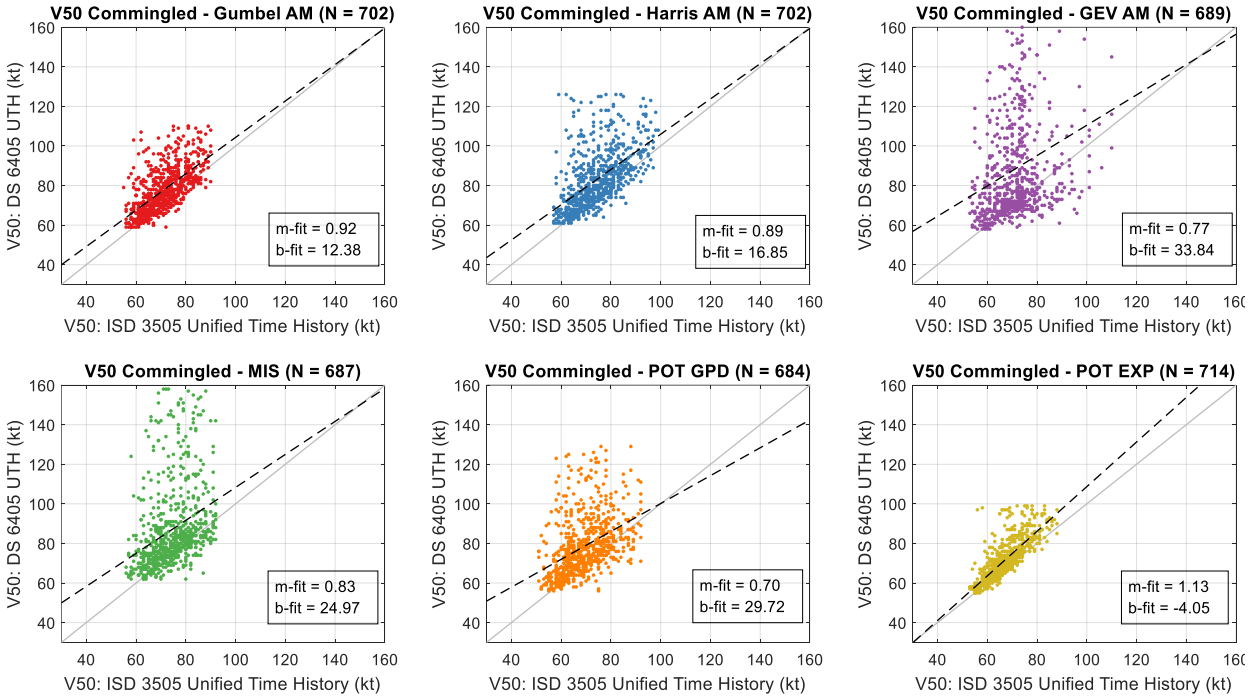

Figure 6.18. Scatter plots comparing V50 estimates created using the DS 6405 UTH and ISD 3505 UTH databases, GEV annual maxima method, and commingled storms.

Figure 6.17 indicates a quite poor agreement between the ISD 3505 UTC database results and the DS 6405 Non-QC database results across all EVA methods. A number of data points in most plots are situated exactly at 300 knots on the y-axis, which is the upper extent of the wind speed parameter space used to evaluate V50 from the fitted distribution. Therefore, it is likely that the regression lines would show an even worse fit overall if the V50 estimates were unbridled by the 300 knot cap. The EVA method with the most reasonable results, POT exponential, still indicates roughly a 2:1 relationship between the DS 6405 Non-QC V50 wind speed and the V50 calculated from ISD 3505 UTH. Given that the DS 6405 Non-QC results deviate so greatly from the control set and that its constituent wind speed records are consistently and improbably high, this dataset is not utilized in subsequent analyses.

Figure 6.18, comparatively, shows a much improved agreement between the two datasets, suggesting the effectiveness of implementing a quality control routine on the DS 6405 time histories. While the DS 6405 UTH V50 estimates are still higher overall, the Gumbel annual maxima method shows a particularly close match of slope (0.92) to the 1:1 line, demonstrating a level of consistency across all wind speeds. The GEV annual maxima and MIS plots, however, both still show significant “upward scattering” trends (similar to those depicted in Figure 6.7) which may indicate some lingering issues persist in the quality control process.

The V50 estimates were then plotted geospatially using the process defined in Section 6.1. Estimates corresponding to a GEV annual maxima method and commingled storms are presented for both resultant datasets in Figure 6.19. Similarly, a residual map was (Figure 6.20) constructed to show the difference between Figure 6.19 and a smoothed contour map of corresponding ISD 3505 UTH dataset V50 values (not shown).

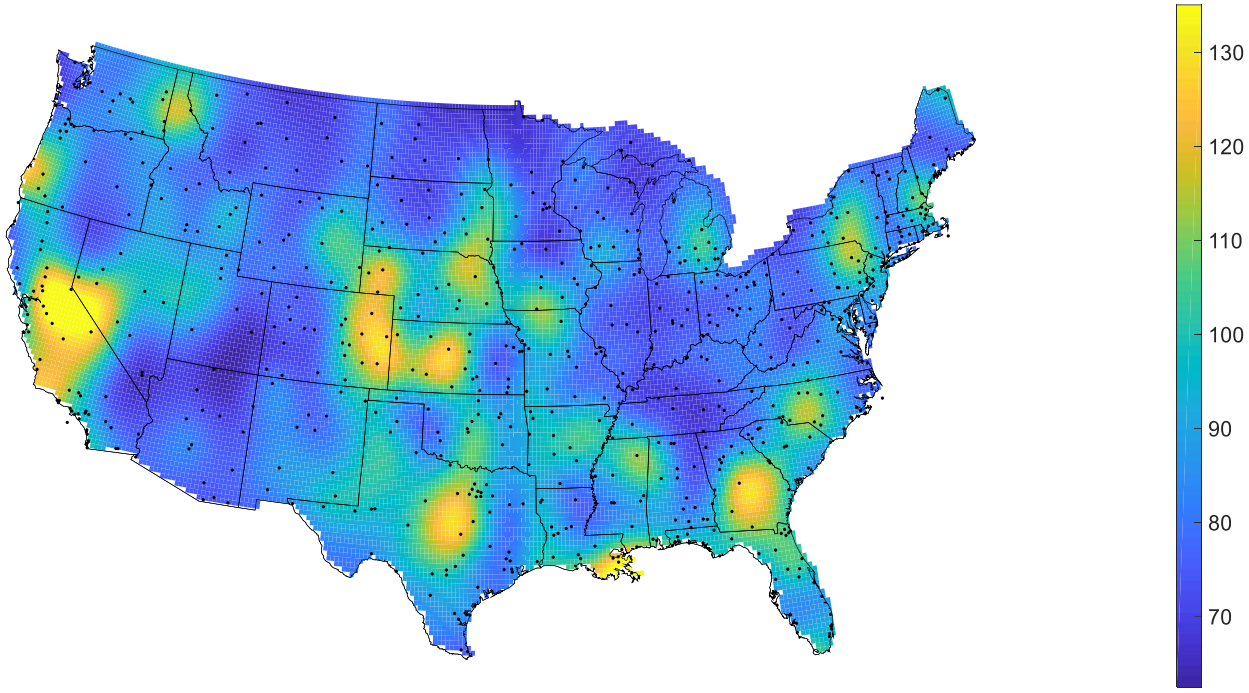

Figure 6.19. V50 mapped using the DS 6405 UTH database, GEV annual maxima method and commingled storms. Number of stations plotted is 736. Units are knots (1 knot = 1.15 mph).

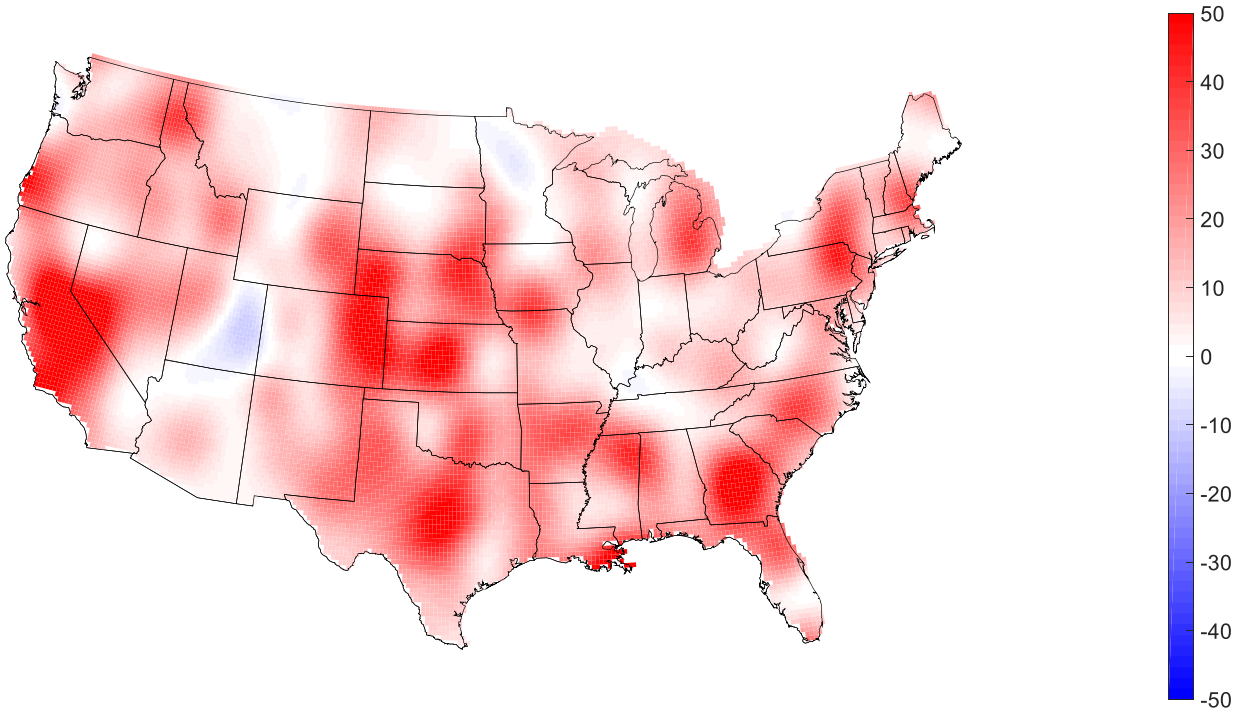

Figure 6.20. Residual V50 map showing the net change in V50 between the ISD 3505 UTH and DS 6405 UTH databases. (i.e DS 6405 UTH minus ISD 3505 UTH). Red shading indicates an increase from control database to experimental and blue shading indicates a decrease. Units are knots (1 knot = 1.15 mph).

The V50 estimates and residuals shown in **Error! Reference source not found.** and REF _Ref13559772 \h Figure 6.20 give rise to a similar conclusion to that obtained from the scatter plots in Figure 6.18: use of the DS 6405 UTH database results in an overall increase in V50 estimates throughout most of the country.

Next, the 20 cities identified in Section 6.2 were analyzed for changes in V50 between the two UTH databases, with values obtained using the ISD 3505 UTH set serving as the control. It was decided ultimately not to directly compare the DS 6405 UTH set to the Sep 12 QC set used in Section 6.3.2, despite that such a comparison was indeed feasible. Instead, comparisons (namely the percent changes) were kept with reference to the ISD 3505 UTH database to ensure time histories of identical length were being compared. The comparison using Sep 12 QC results, however, can be made indirectly by comparing the values in Table 6.5 and Table 6.2, which both calculate V50 using the GEV annual maxima method and commingled storms. As with the previous Improved ISD 3505 database analysis, an accompanying summary table of all methods and cities is also provided in Table 6.6; the "closest match methods" were determined in the same manner as described previously for the Improved ISD 3505 version.

Table 6.5. V50 results for selected cities using the DS 6405 UTH database, all EVA methods, and commingled storm type.

City	DS 6405 UTH V50 Estimate for Commingled Storms (in knots) By Extrapolation Method					
	Gum. AM	Harris AM	GEV AM	MIS	POT GPD	POT Exp
Hartford	70.8 (+10%)	77.4 (+13%)	82.2 (+17%)	83.6 (+19%)	76.0 (+23%)	64.6 (+5%)
Great Falls	74.9 (+1%)	82.4 (+6%)	73.0 (+5%)	96.2 (+29%)	70.0 (+1%)	74.0 (+3%)
Baton Rouge	80.0 (+8%)	88.2 (+12%)	94.8 (+22%)	80.5 (-1%)	75.2 (+5%)	78.4 (+22%)
Decatur	76.5 (+7%)	80.8 (+9%)	72.9 (+6%)	76.5 (+7%)	74.4 (+8%)	75.4 (+10%)
Columbus	74.6 (+8%)	77.8 (+10%)	77.5 (+8%)	80.7 (+11%)	74.4 (+11%)	68.7 (+5%)
Augusta	76.0 (+14%)	81.4 (+16%)	104.7 (+52%)	91.3 (+32%)	83.4 (+26%)	64.6 (+4%)
Fargo	71.1 (+1%)	74.2 (0%)	82.5 (+8%)	74.9 (0%)	69.7 (-1%)	68.1 (0%)
Colo. Springs	81.7 (+12%)	83.9 (+11%)	102.2 (+42%)	95.5 (+29%)	77.1 (+10%)	75.4 (+5%)
Sacramento	86.9 (+14%)	99.2 (+24%)	134.8 (+85%)	106.2 (+37%)	94.7 (+29%)	69.9 (+7%)
Roswell	78.3 (+13%)	86.4 (+20%)	90.6 (+37%)	105.8 (+54%)	74.8 (+18%)	73.8 (+5%)
Skowhegan	67.9 (+4%)	72.5 (+8%)	74.6 (+6%)	74.2 (+5%)	63.3 (+4%)	62.0 (+4%)
Glenns Ferry	78.6 (+13%)	83.3 (+15%)	86.0 (+19%)	86.8 (+19%)	79.1 (+15%)	76.5 (+17%)
Arcadia	81.5 (+5%)	88.3 (+5%)	84.6 (+5%)	86.4 (+5%)	81.2 (+7%)	71.3 (+5%)
Red Cloud	84.6 (+6%)	88.8 (+7%)	102.5 (+42%)	92.1 (+13%)	90.1 (+18%)	77.2 (+1%)
Keysville	74.8 (+6%)	80.0 (+6%)	88.7 (+26%)	88.2 (+29%)	86.0 (+37%)	74.0 (+13%)
Kosciusko	88.5 (+26%)	95.0 (+30%)	95.0 (+30%)	98.8 (+34%)	91.0 (+32%)	76.8 (+18%)
Ontonagon	68.9 (+8%)	72.0 (+10%)	74.4 (+19%)	73.9 (+13%)	66.3 (+11%)	61.9 (+3%)
Duchesne	72.1 (-2%)	74.7 (-4%)	74.7 (-6%)	73.9 (-7%)	68.8 (-3%)	70.7 (+4%)
South Bend	74.8 (+6%)	78.2 (+6%)	70.7 (-5%)	77.0 (+6%)	75.6 (+12%)	72.0 (+6%)
Guthrie	83.8 (+12%)	88.0 (+13%)	93.6 (+33%)	101.2 (+36%)	87.6 (+23%)	80.7 (+10%)

Table 6.6. Summary of V50 statistics presented in Table 6.5.

City (with station)	Avg. V50 (kt)	Average Departure	Closest Match Method	City (interp.)	Avg. V50 (kt)	Average Departure	Closest Match Method
Hartford	75.8	+15%	Harris AM	Skowhegan	69.1	+5%	MIS
Great Falls	78.5	+8%	Harris AM	Glenns Ferry	81.8	+16%	Harris AM
Baton Rouge	82.9	+11%	Harris AM	Arcadia	82.3	+5%	Gumbel AM
Decatur	76.1	+8%	POT GPD	Red Cloud	89.3	+15%	MIS
Columbus	75.7	+9%	Gumbel AM	Keysville	82.0	+20%	GEV AM
Augusta	83.6	+24%	POT GPD	Kosciusko	90.9	+28%	Gumbel AM
Fargo	73.5	+1%	Gumbel AM	Ontonagon	69.6	+11%	POT GPD
Colo. Springs	86.0	+18%	Gumbel AM	Duchesne	72.5	-3%	POT GPD
Sacramento	98.7	+33%	MIS	South Bend	74.7	+5%	Gumbel AM
Roswell	85.0	+24%	Harris AM	Guthrie	89.2	+21%	POT GPD
City (with station) overall	N/A	+15%	N/A	City (interp.) overall	N/A	+12%	N/A
Gumbel AM overall	N/A	+8.62%	N/A	Harris AM overall	N/A	+10.88%	N/A
GEV AM overall	N/A	+22.64%	N/A	MIS overall	N/A	+18.46	N/A
POT GPD overall	N/A	+14.36%	N/A	POT Exp overall	N/A	+7.46%	N/A

The results of the 20 city analysis largely reflect those already described by the geospatial interpretation and scatter plots: that use of the DS 6405 UTH dataset results in an overall predictable increase in V50 estimates compared to an ISD 3505-based control. Despite that the values displayed in Table 6.5 were spatially smoothed, increases of over 20% were still observed frequently among all EVA methods and were found to be as high as 85% in the most extreme scenario. Within each location, V50 estimates (and percent changes) tended to vary widely across EVA methods. This was not unexpected, however, since the time history length of all DS 6405-based records was under 20 years and the extreme value methods all extrapolated out to a return period of 50 years. Nonetheless, because of this high degree of scatter among the methods, the set of "best match methods" presented in Table 6.6, as well as other data quantifying EVA methods, should not be considered ultimately conclusive.

6.5. Improving Spatial Resolution – OKM Study

6.5.1. Logistic Regression Analysis

The hit-or-miss analysis described in Chapter 4 was performed using all identified extreme wind events at all 39 OKM stations. As discussed previously, extreme wind events within OKM station time histories were defined using the parameters V_T = 20 m/s and t_{int} = 0.25 days. Parameters defining windows for comparison with ASOS records were identified as T_w, U_w, and D_w but were not explicitly defined to allow for multiple iterations of analysis to be presented in this chapter. Table 6.7 summarizes all of the parameters and provides window parameter values for the first set of ensemble results presented subsequently.

Table 6.7. Parameters used for the first run of the OKM hit-or-miss analysis.

Type	Parameter Name	Symbol	Value	Units
OKM Wind Event Identification	threshold speed	V_T	20	m/s
	separation interval	t_{int}	0.25	days
Windowing for Hit-or-Miss Analysis	timing window	T_w	0.5	days
	wind speed window	U_w	20	% of U_{max}
	wind direction window	D_w	30	degrees

The results of the hit-or-miss analysis were interpreted using a logistic regression model that computes the tendency of OKM events to be hit or missed (the response) as a function of some quantity of interest (the predictor). This type of analysis allows for the ensemble results of all OKM stations to be combined such that simple relationships may be identified. Overall, the guiding question of this study is whether or not ASOS stations can adequately capture intense, yet small-scale, extreme wind events that are known to occur. Two convenient metrics for assessing these types of events are wind speed (a decent analog of intensity) and event duration (an acceptable, yet not ideal, analog of spatial scale). Therefore, the logistic regression procedure was implemented using both wind speed and event duration as predictor variables as shown in Figure 6.21. Results corresponding to both logical treatments of the results are indicated as “any” and “all” (as discussed in Chapter 5) and the number of independent trials considered in each regression, n, is provided in the legend.

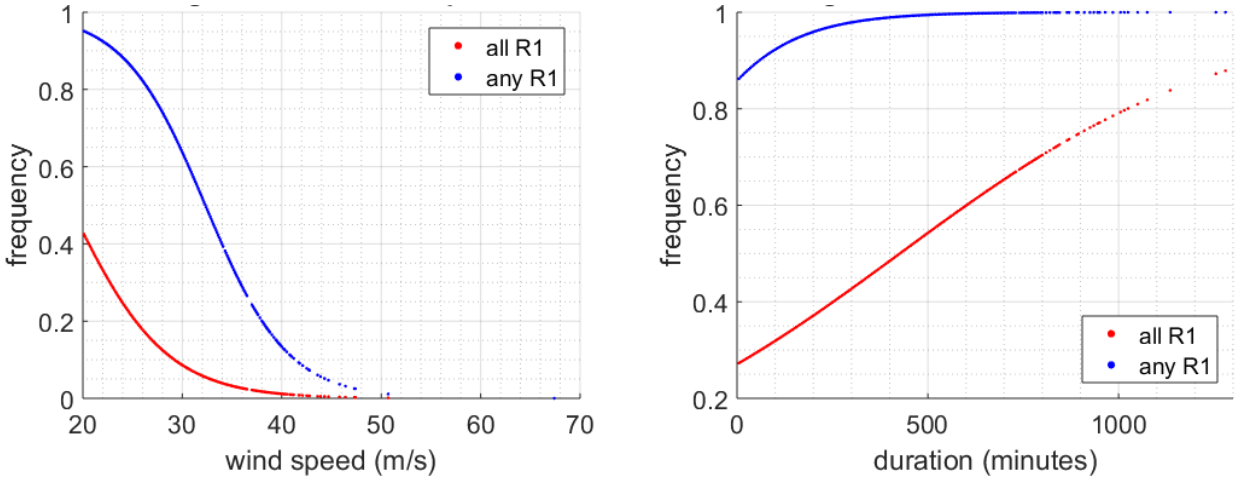

Figure 6.21. Left: logistic regression performed using wind speed as the predictor and probability of an event "hit" as the response variable. Right: logistic regression performed using event duration as the predictor and probability of an event "hit" as the response variable.

The regression of wind speed suggests overall that OKM wind events of increasing wind speed are less likely to also be observed at ASOS stations than events of more modest speeds. Likewise, the regression of wind event durations suggests that shorter-duration events are also less likely to be captured by the ASOS network, though to a less dramatic degree. That the regressions of both "any" and "all" logical treatments behave similarly in each plot helps reinforce these claims. Figure 6.22 combines the information from both regressions into a single plot, where the duration regression is again plotted but using various subsets of the data partitioned by wind speed. The partitions were selected such that each set of wind speeds included at least 100 data points and are thus of unequal size. The original "any" and "all" curves from Figure 6.22 are shown for reference.

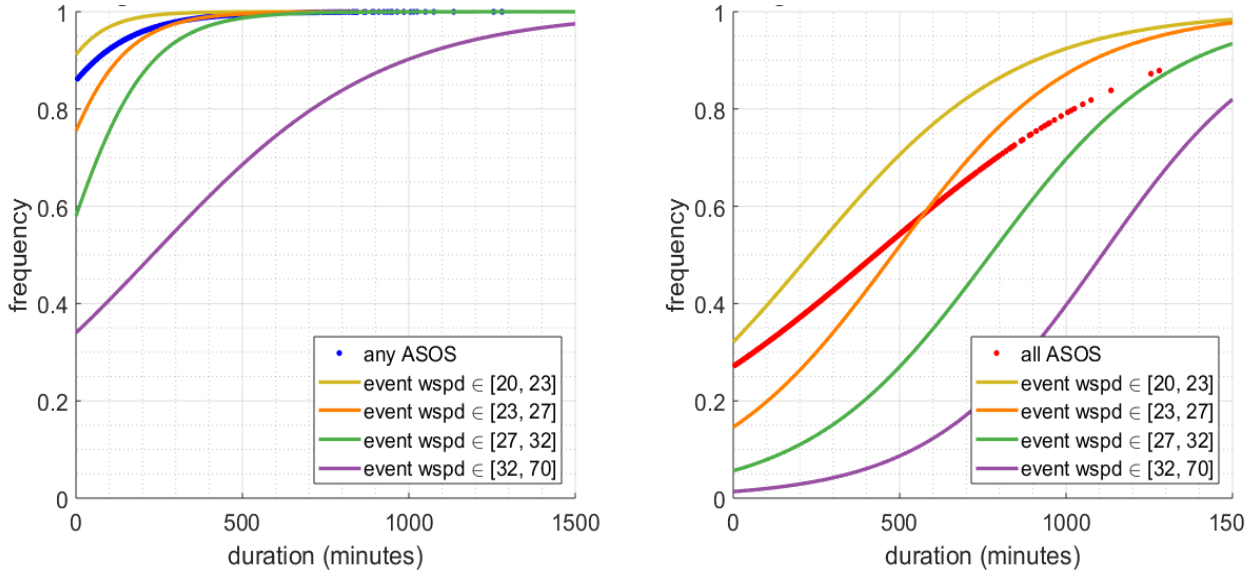

Figure 6.22. Left: logistic regression on event duration partitioned into four discrete wind speed bins showing the probability of event capture for any ASOS station. Right: logistic regression on event duration partitioned into four discrete wind speed bins showing the probability of event capture for all ASOS stations.

Figure 6.22 shows that, in general, OKM events with higher wind speeds and shorter durations tend to be less frequently observed by ASOS networks. The gold-colored curve, representing the lowest wind speed partition (and consequently the most data points), appears to control the overall behavior of both the "any" and "all" regressions. Regressions performed with data at higher wind speeds (the orange, green, and purple curves) diverge significantly downward from the unpartitioned regression as duration approaches zero. Overall, these results imply that the spatially-dense OKM network is likely more capable of detecting intense, small-scale wind events than its coarser ASOS counterpart.

To further embellish this claim, the windowing parameters given in Table 6.7 were manipulated for additional runs of the hit-or-miss analysis. The values used for the first iteration were considered to be the most generous, so additional runs used reduced values in order to narrow the windows for comparison. Values used for the second and third runs of the analysis are given in Table 6.8; while it is known that some parameter adjustments are likely more impactful than others, these more detailed relationships are beyond the scope of this study.

Using these parameters, the hit-or-miss analysis was performed twice more. The results from these additional runs are presented in Figure 6.23 along with those from Run 1.

Table 6.8. Parameters used for all three runs of the OKM hit-or-miss analysis, progressing from widest windows to narrowest windows.

Parameter Name	**Run 1 – Wide Window**	**Run 2 – Medium Window**	**Run 3 – Narrow Window**
timing window	0.5 days	0.25 days	0.125 days
wind speed window	20%	15%	10%
wind direction window	30°	20°	10°

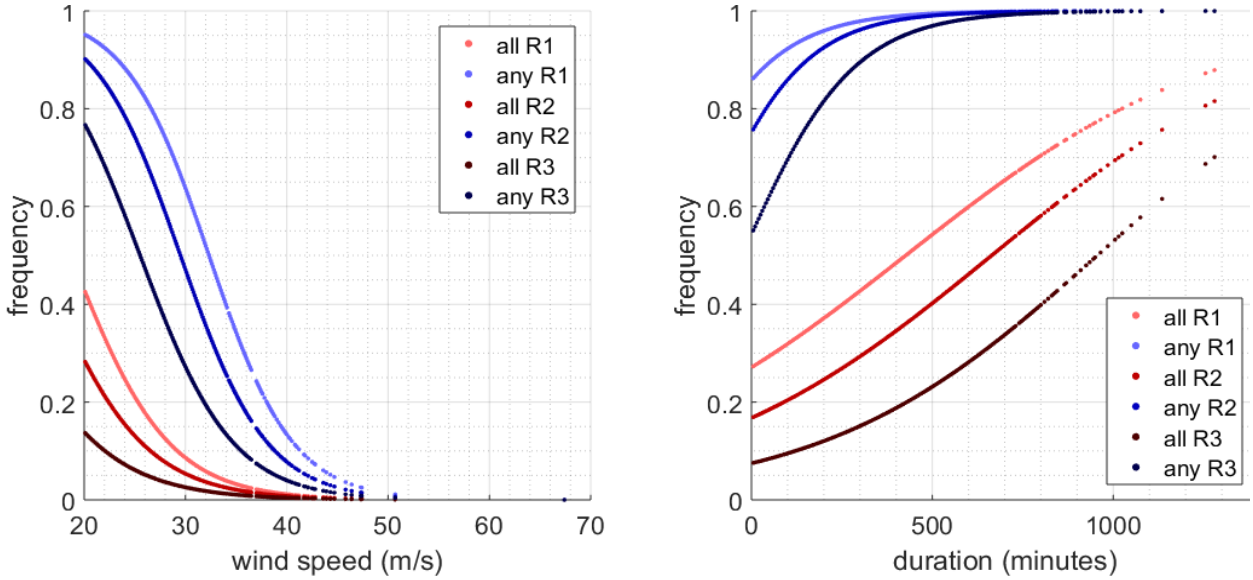

Figure 6.23. Left: logistic regression from all three runs using wind speed as the predictor. Right: logistic regression from all three runs using event duration.

Perhaps not surprisingly, narrowing the comparison windows results in a perceivable drop in overall likelihood of OKM event capture by ASOS stations. This drop was observed consistently in both the wind speed and duration indicators as well as for both logical treatments. Most importantly, however, Figure 6.23 asserts that the overall behavior of the regressions—that is, the tendency toward zero with increasing wind speed and decreasing duration—is largely independent of the size of the comparison windows used. In other words, even as the

comparison method becomes more selective, the analysis still supports the conclusion that the denser OKM network captures small-scale extreme wind events more completely than the ASOS network.

6.5.2. Extreme Value Analysis

As with the other sets of data evaluated in this study, EVA results from OKM data are collected across all locations for ensemble-wide comparison analyses. The notion of a true control set with which to compare, however, is less obvious since the observation stations in the ISD 3505/DS 6405 networks do not correspond geographically to OKM stations locations. This renders a direct point-by-point comparison, such as a scatter plot, untenable. One way to circumvent this issue is to compare values of mapped grid boxes across datasets, as is done with the residual maps in previous sections. Thus, EVA result comparisons of OKM data rely largely on geospatial interpretations.

Figure 6.24 and Figure 6.25 show a maps of Oklahoma created using the mapping scheme described in Section 6.1; Figure 6.24 maps the data using the same grid spacing and smoothing parameter used in the full United States maps presented previously, whereas Figure 6.25 incorporates tighter grid spacing (0.05 degrees) and a higher smoothing parameter (0.9). V50 estimates computed using the GEV annual maxima method are presented in both maps, and since no storm type identification was performed for OKM data, all results are considered to represent winds of commingled storm type. Note that all grid boxes outside the state boundary of Oklahoma are generated using extrapolation and should not be considered valid.

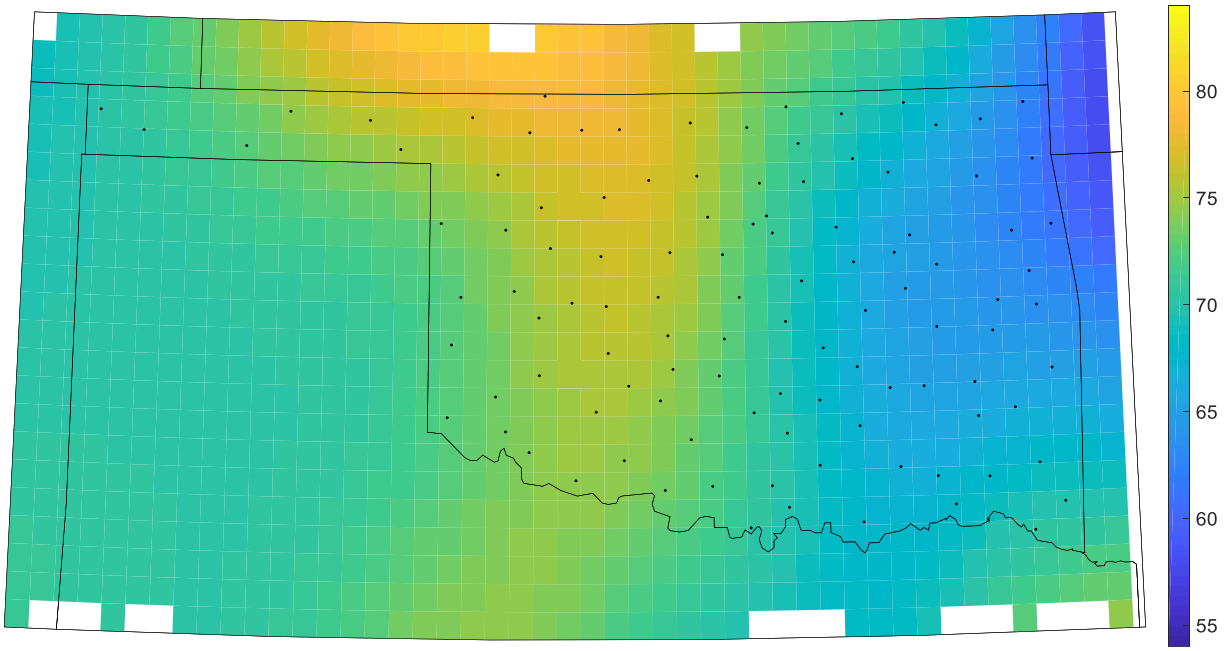

Figure 6.24. V50 mapped using data from 108 OKM stations and the GEV annual maxima method. A grid spacing of 0.2 degrees and a smoothness parameter of 0.5 are used. Units are knots (1 knot = 1.15 mph).

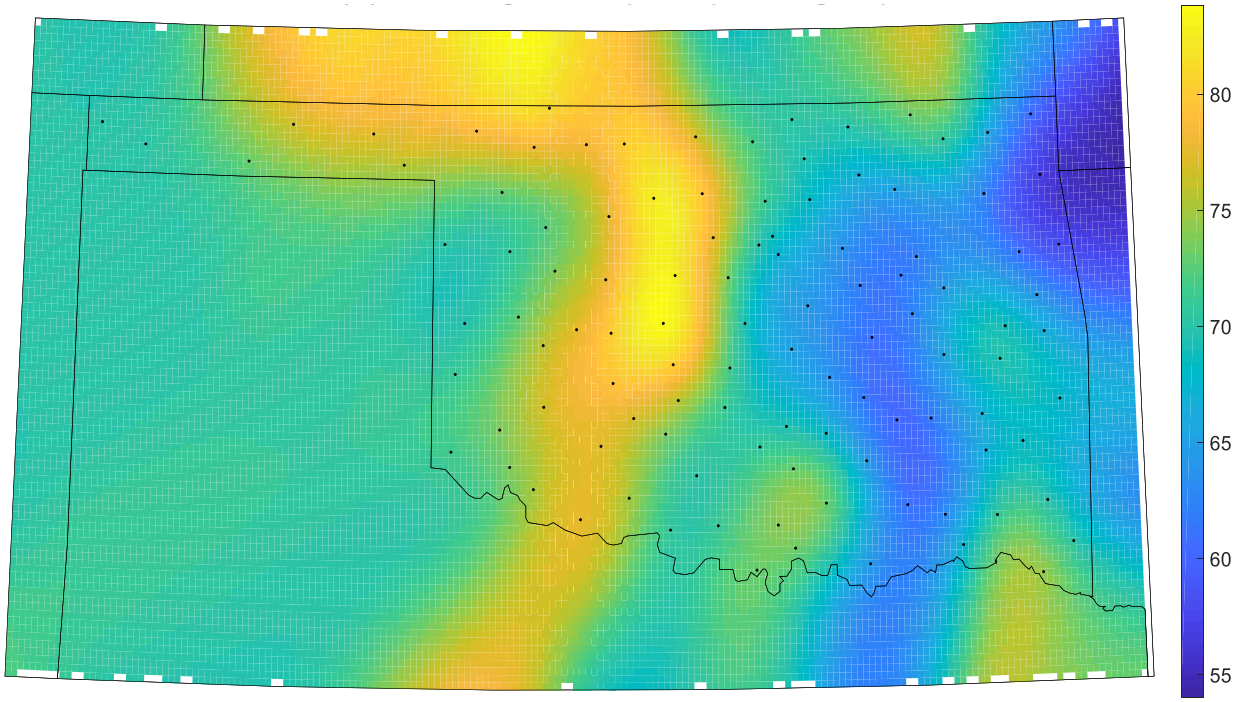

Figure 6.25. V50 mapped using data from 108 OKM stations and the GEV annual maxima method. A grid spacing of 0.05 degrees and a smoothness parameter of 0.9 are used. Units are knots (1 knot = 1.15 mph).

These two figures suggest that a substantial east-west gradient in V50 wind speed exists across the state of Oklahoma, with an overall maxima occurring in the western third of the state (not including the panhandle). With a tighter grid spacing and higher smoothing parameter used, spatial intricacies of the V50 results are much more apparent. This is because each of these features of the mapping scheme directly affect the degree of area averaging incorporated into the final map. While reducing area averaging is likely permissible when using data from a denser network, it should nonetheless be approached with caution as effects of statistical outliers become much more pronounced. This is evidenced perhaps most clearly by the specific orientation of the 80 knot (brightest yellow) contour in Figure 6.25. The southern extent of the contour is fixed directly over the ELRE (El Reno, OK) station, which is known to have observed a direct tornado passage in its time history (OM 2019a). Indeed, the ELRE station contains the all-time maximum wind speed observed across the entire OKM network (67.4 m/s, 131 kt).

To get a sense of how these OKM-based V50 maps compare to those from an established extreme wind database, V50 estimates from the Improved ISD 3505 database were utilized as a control set. Data corresponding to the 39 ASOS stations employed in the hit-or-miss analysis in Chapter 4 were retrieved and mapped in the same fashion as Figure 6.24 and Figure 6.25. Residual maps showing the change from the ASOS-based maps to the OKM-based maps were also created to better quantify and depict the spatial nature of the changes. These maps are presented together in Figure 6.26, where each column of maps constitutes a different area averaging scheme. Figure 6.24 and Figure 6.25 are reproduced in the middle row for ease of comparison.

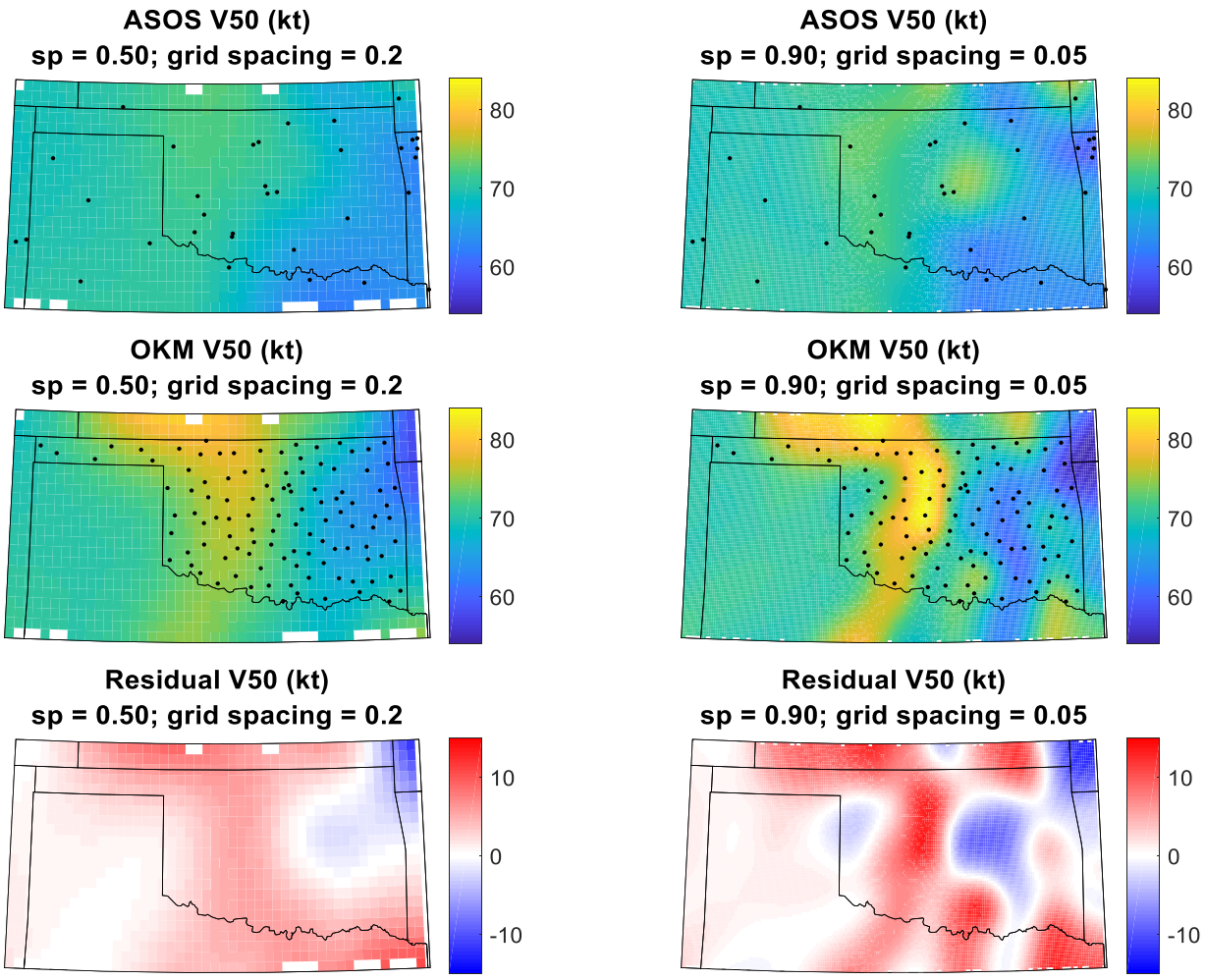

Figure 6.26. Comparison of V50 between the OKM network and ASOS network in Oklahoma. Lower resolution maps are shown in the left column while higher resolution maps are shown on the right. The top row introduces maps created using ASOS station data only, and the bottom row shows the difference between the ASOS maps and the OKM maps. Units are knots (1 knot = 1.15 mph).

The plots in Figure 6.26 demonstrate both some general trends and highly specific changes in V50 across Oklahoma. Regardless of the area averaging technique used, it is evident that the western part of the state observes a noted increase in V50 wind speeds with the OKM EVA results. Locations in the eastern half of the state observe the greatest decrease in V50 overall. What is most noticeable in the less-smoothed plots in the right column is an overall locational shift in the state's maximum V50 wind speeds. While the ASOS map suggests that a local maxima is located near the center of the state, the mapped OKM data produces no such maxima and rather places the state's highest V50 values further to the west. Additionally,

smaller-scale pockets of increased V50 are evident elsewhere around the state that do not appear on either of the ASOS-based maps—likely due to extreme wind events not captured by ASOS stations. Of note are regions in south central Oklahoma (just north of Texas) and east central Oklahoma (just west of Arkansas). These specific departures present in the OKM maps imply overall that a more spatially refined view of extreme wind climatology is possible with higher density observation networks than with the existing ASOS network.

CHAPTER 7: CONCLUSIONS AND IMPLICATIONS FOR EXTREME WIND CLIMATOLOGY OF THE UNITED STATES

7.1. Discussion of Results

The extreme wind database improvements evaluated in this study largely centered on improving either the quality, quantity, or scale of wind data used. Improving the existing ISD 3505 database largely capitalized on improved quantity (additional years of data) and enhanced geographic scale (more locations represented). The additional techniques of incorporating high-resolution DS 6405 data and higher density networks such as the Oklahoma Mesonet focused mainly on improvements of temporal and spatial scale, respectively. Data quality was improved as necessary throughout each analysis, by way of various quality control mechanisms or filtering processes. Despite the manifold improvements that were implemented or explored in this study, it was nonetheless innately difficult to compare the impacts of quality, quantity, and scale improvements due to the disparate nature of the datasets used. This issue necessitated the development of a standardized extreme value analysis (EVA) tool that could evaluate generic wind speed time histories and produce results, such as V50, capable of being compared across datasets of differing nature. While V50 estimates did provide a stable metric for analysis, these results by themselves were not capable of distinguishing one mode of database improvement over others. Therefore, the conclusions obtained by this study focus more on the viability of the techniques employed and provide some insight as to their potential impacts on extreme wind climatology of the United States.

7.1.1. Improvements to the ISD 3505 Database

The increase in number of reporting stations brought about by improvements to the older ISD 3505 extreme wind database was found to be most directly beneficial to geospatial interpretations of the data. With more observation stations (i.e. data points) included on the

contiguous United States grid, fewer overall locations must rely on interpolation for a site-specific estimation of V50. For locations that still require interpolation, however, use of a tighter grid spacing and lower degree of area averaging is likely warranted. This realization, while not explicitly illustrated for the Improved ISD 3505 scenario, is supported by the improved spatial resolution found in the OKM analysis results.

Overall, the increased density of reporting stations in the Improved ISD 3505 database demonstrates that a refinement of the spatial characterization of extreme wind climatology in the United States is not only possible, but is also necessary. Large-scale smoothing and overgeneralization are likely to occlude some of the more regional (state-scale) aspects of the extreme wind climate that this study revealed. This phenomenon is best exemplified by the GEV scale parameter analysis in Chapter 6, which identified several geographic regions with anomalous V50 values. Despite that the identified stations all had time histories of over 20 years in length, their shape parameter values (over 0.25) were all considerably higher than more typical values found in the literature and yet still below the 95th percentile of all values generated. While a more rigorous quality control procedure would certainly need to be employed for these time histories to ensure the veracity of identified wind extrema, the presence of potentially realistic results like these should not be immediately ignored or "averaged out" as is effectively done by fixing the scale parameter to zero (for a Gumbel fit) or over-smoothing the mapped contours.

The major caveat of increased network density, however, is the consistency of time history durations (or lack thereof) in similar geographic areas. This issue is alluded to in Figure 6.6, which depicts the change in spatially-averaged time history lengths between the older and new ISD 3505 databases. In the state of North Dakota, for example, average time history lengths

across the state dropped significantly from the old database to the new one, brought on by the inclusion of nearly three times as many reporting locations in the new database. The resultant change in V50 across North Dakota, as depicted in Figure 6.9, is universally negative. It follows, thus, that these "younger" reporting stations significantly influenced the extreme wind climate characterization of North Dakota despite providing additional geospatial density to the area. This result is not unexpected, however, since it is well-established that shorter time histories are not suitable for the annual maxima-type EVAs used in that comparison.

So while an increase in network density was found to be effective at revealing the finer details of wind climate regionality, its overall effect is still largely governed by the statistical quality of the data that is actually added. This notion is well-illustrated by comparing the results observed in the OKM analysis to those observed in North Dakota. In Oklahoma, an increase in network density from ASOS stations to OKM stations resulted in a more-or-less geographic "redistribution" of V50 maxima locations (i.e. some locations observed an increase in V50, some observed a decrease). In this case, the wind speed time history of every OKM and ASOS station considered was at least 24 years in length. By contrast in North Dakota, long-established ISD reporting locations (30+ years of data) were intermingled with much newer stations (< 20 years of data) to arrive at the improved spatial density. The result was a blanket decrease in V50 values across the state, which is likely less indicative of true wind phenomena than it is of the nature of the data used.

As a separate, yet related, improvement to the ISD 3505 database, the extension of time histories at "existing" reporting locations was found to be directly beneficial to EVA methods. It is well-noted in statistics that a set of samples drawn from a given population (assuming the population remains stationary in character) tend to represent the population more accurately as

the number of samples increases. The same principle applies with wind speed extrema, where annual maxima (or peaks over threshold or independent storms) constitute a set of samples from a broader population of extreme wind speeds spanning time beyond the era of modern recordkeeping. As shown in the histogram in Figure 6.5, most observation stations used in the previous Sep 12 QC extreme wind database have logged no more than 40 years of wind observations through 2010; many have logged far fewer. The problem with this is that useful predictions for extreme winds (in the context of engineering applications, at least) are those corresponding to return periods of 50 to 100 years and beyond. To make these predictions responsibly with the data available, statistical extrapolation is thereby required.

The dependence on extrapolation, however, is reduced if the number of samples can be increased. The MIS and POT extrapolation methods (as discussed in Chapter 5) were developed to serve this very purpose; they identify extrema sub-annually and thereby increase the sample size by resampling the population. On the contrary, extrapolation dependence can also be reduced in this context if the time history lengths being considered are extended, which is exactly what the improvements to the existing ISD 3505 database provided. Indeed, some time histories were extended by as much as 8 years by virtue of elapsed time and others were stitched together as a result of the geographic grouping procedure. The effects of extending these time histories, as opposed to simply reverting to POT and MIS methods, are twofold: (1) annual maxima approaches almost certainly become practicable and (2) agreement among the suite of results from all EVA methods is likely improved, enhancing the certainty of a particular V50 estimate. To expand upon number (1), consider Cook's (1982) recommendation that at least 10 years of data be available for adequate annual maxima extrapolation. In the Sep 12 QC dataset, 234 (20%) of the 1,195 stations had time histories spanning less than 10 years; 49 (4%) had time

histories spanning less than 2 years. Assuming that all Sep 12 QC stations' time histories were extended by 8 years, it follows that all but 49 stations (96%) of the original 1,195 would thus be able to make reasonable predictions using annual maxima.

The effects of this particular improvement are somewhat muted in the ensemble analyses, however, due to the fact that other "younger" stations were intermingled with these 1,195 stations to form the 2,447 groupings. As long as newer observation stations continue to come online, the issue of young stations with limited time histories will continue to persist. While it conceivable that a single EVA method may not be suitable for every time history in the database, it is likely true that at least one EVA method can be applied to any time history (of sufficient length) with a reasonable degree of success. This was demonstrated in a number of cases where MIS and POT were able to produce reasonable V50 estimates when annual maxima methods did not. These observations together imply that a hybrid extreme value analysis scheme could be utilized effectively, where short-duration time histories are analyzed using any of the MIS or POT methods and longer-duration time histories are treated using annual maxima (or any other better performing method). Doing so would maximize the number of stations used (i.e. maximize network density) without compromising the quality of V50 estimates by remaining bound to a particular EVA method.

As discussed in Chapter 6, the 20 cities selected for running V50 evaluations throughout this study were chosen so because they represent the 10 previously-identified extreme wind climate regimes found to exist in the contiguous United States by Lombardo and Zickar (in press). Evaluating climatology changes in this way is useful because it distills the multitude of results and otherwise unquantifiable graphical interpretations into a practical and digestible form, albeit with some loss in specificity. If these 10 regimes, however, are considered to be wholly

representative of the country's extreme wind climatology, then Table 6.4 suggests overall that a modest increase in V50 values was observed due to improvements made to the older ISD 3505 dataset. This conclusion, however, is somewhat dependent on the EVA method chosen, since evaluations using both POT methods were found to result in an overall decrease in V50 among the 20 cities analyzed. V50 values from the 10 cities co-located with observation stations were found on average to mimic this overall nationwide increase, whereas the 10 cities in interpolated areas observed an average decrease instead. It is not immediately evident, though, if the reliance on interpolation is the sole cause of this discrepancy since only 10 samples comprise each set. Table 6.4 also implies that, nationwide, the Gumbel annual maxima extrapolation method is perhaps the most centered approach of the six methods evaluated. The GEV annual maxima was found to be the second most centered, but is also capable of producing extreme results as discussed in Chapter 6. For situations where it is not feasible to evaluate V50 using all six methods (or more), estimates produced with the Gumbel annual maxima method should be considered most reliable and least extreme (in any direction). This is not surprising though, given the extensive body of literature (such as Lombardo et al. (2016)) that suggests this same trait. Still it is nonetheless important to maintain accuracy of V50, and averaging a suite of six or more co-located estimates produced with differing methods is a practical way to accomplish this.

7.1.2. Additional Techniques to Improve Database Robustness

The techniques described in Chapter 4 aimed to further improve the spatial and temporal resolution of the established ISD 3505 database. Given that these methods were largely unexplored in the context of an extreme wind database prior to this study, the presented conclusions address two general issues: (1) if the given technique should be considered viable and (2) how a possible implementation of the technique would alter the current understanding of extreme wind climatology in the United States.

The two datasets used to potentially enhance temporal resolution, DS 6405 Non-QC and DS 6405 Unified Time History (UTH), both demonstrated a troubling lack of quality and consistency. This fact alone made comparisons to ISD 3505-based datasets difficult and made extreme value analyses highly impractical, for the most part. The plot in Figure 4.4 shows a DS 6405 Non-QC time history for New Bern, North Carolina that contains several observed wind gusts over 200 knots—a highly unrealistic scenario. While the quality control process described in Chapter 4 was able to produce the less-anomalous New Bern time history shown in Figure 4.5, this process itself introduced additional uncertainty because it relied on a number of embedded (and potentially dubious) assumptions. Furthermore, the extremely anomalous wind speeds (over 200 knots) were not found in all of the DS 6405 time histories, suggesting a level of inconsistency among the reporting schemes that is difficult to accommodate in post-processing. That only 72 out of 888 analyzed time histories did not have any wind gusts over 70 knots (the threshold required for quality control to be applied) is also just cause for suspicion.

Perhaps the most convincing argument of all for the DS 6405 data's lack of integrity is the scatter plot shown in Figure 6.15. Even with the extensive cleaning and quality control processes applied, it was found that not a single DS 6405 time history could be perfectly matched with its corresponding ISD 3505 time history. Overwhelmingly, wind speeds in DS 6405 data were shown to be chronically lower than those recorded in ISD 3505 at the same time. This is especially troubling because wind speed data found in both the DS 6405 and ISD 3505 databases originate from the same observation station and are reported by the same physical anemometer. Therefore, since the higher resolution time histories could not effectively reproduce the observed wind gusts found in lower resolution time histories, it was concluded that the DS 6405 data, as cleaned and quality controlled in this study, was not a viable substitute for

ISD 3505-based wind data. While the general principle of using higher resolution wind data to enhance the existing extreme wind database is likely still possible, doing so with DS 6405 data was found to be impracticable.

Despite this initial finding, DS 6405 data was nonetheless evaluated using EVA and results were presented in Chapter 6. The presence of additional (and likely erroneous) extreme wind speeds in either set of DS 6405 data was made especially evident by the scatter plots given in Figure 6.17 and Figure 6.18. The geospatial interpretations of DS 6405 data showed blanket increases in V50 across the country of roughly 20-50 knots as compared to the ISD 3505 UTH database. By comparison, the observed changes between the older and updated ISD 3505 databases were generally between -15 and + 15 knots as shown in Figure 6.9. The 20 city analysis performed using the DS 6405 UTH database revealed similar findings: every city but one observed an increase in V50 (many of which were significant) when averaged across all six EVA methods. Further complicating the DS 6405 EVA comparisons was the fact that all DS 6405 time histories, regardless of their level of quality control, have a duration of no more than 18 years. Many of these, as noted in Chapter 4, span a mere 13 years. While this means that annual maxima EVA approaches were technically feasible (by a 10-year standard), it also means that agreement between the DS 6405 and ISD 3505 results was less guaranteed. The extra uncertainties stemming from a small sample size undoubtedly contributed to the significant V50 percent changes provided in Table 6.5.

In contrast to the high temporal resolution techniques explored, the evaluation of a denser spatial network was found to be more promising. In analyzing a large number of extreme wind events observed by the Oklahoma Mesonet and comparing them to time histories at nearby ASOS stations, it was found that wind events of increasing speed and decreasing duration were

overall less likely to be observed at ASOS stations. This notion is well illustrated by the ensemble-wide regression analyses depicted in Figure 6.22 and Figure 6.23. Assuming that wind speed and duration are suitable analogs for an event's intensity and size, respectively, it follows that highly intense but small scale wind events (such as tornadoes, supercell thunderstorms, downbursts and dust devils) are more frequently observed by high resolution networks such as OKM than by coarser networks such as ASOS. It is likely that the increase in network spatial density, above all, is the cause of this increased tendency to capture these events. Therefore, this study concludes that use of only ASOS stations in climatology characterization likely neglects some important and highly influential small scale extreme wind events that are known to occur. Incorporation of higher-density network observations into the extreme wind database is indeed a viable technique for improving the spatial interpretation of wind extrema.

The increased ability to capture small-scale extreme wind events was found to be highly influential on EVA results produced by the OKM data. Figure 6.26 indicates a geographic "rearrangement" of V50 estimate contours across the state of Oklahoma was observed when moving from a coarse ISD 3505 database to a finer OKM database. While some generalized magnitude differences may exist between the two maps overall, it is clear that some areas observed a significant increase in V50 while others observed a significant decrease. This result, coupled with the reasonable reliability of the 24 year long time histories used, indicates that a finer resolution characterization of extreme wind climate for Oklahoma is in order. As with the ISD 3505 database improvements, additional network density enables the use of smaller grid spacing and less area averaging. This allows localized pockets of higher (or lower) V50 values to appear on the map, thereby creating the small-scale climatological intricacies that are so desired.

7.2. Limitations of Study

Despite the incredible breadth of information obtained and dissected in this study, there were still a number of limitations encountered during its course. Some of these are alluded to in the previous chapters, but this section summarizes them by general topic.

7.2.1. Data Standardization and Quality Control

The ability to properly standardize and quality control data of any type is a well-established difficulty in experimental studies. Most of the datasets used in this study were of extremely large size, adding a further element of difficulty to these procedures. As a result, very crude measures, such as speed thresholding, were taken to standardize and filter some of the datasets *en masse* before use. Using a wind speed threshold, as was done to quality control the Improved ISD 3505 data, meant that all records above 75 knots were automatically excluded from analyses. No further measures were taken to re-investigate these records owing to the extraordinary amount of time required to conduct such a procedure. It is thus highly probable that truly observed wind speeds over 75 knots were excluded and erroneous wind speeds below 75 knots were inadvertently included in the final database.

DS 6405 records were first cleaned by removing duplicates (taking record of higher wind speed) and gaps then were quality controlled using the underlying assumption that high wind events are usually coupled with a shift in some other meteorological parameter. It was concluded previously that this quality control process was likely deficient, as the agreement between ISD 3505 and DS 6405 time histories remained poor even after quality control was applied. Furthermore, the averaging time shift encountered when switching between a standard cup anemometer to a sonic anemometer was not accommodated in the DS 6405 datasets, which undoubtedly affected to some degree the EVA results computed with those datasets.

Oklahoma Mesonet data was assumed to be fully quality controlled and standardized upon its acquisition, and no further checks were performed to evaluate its character. While this data indeed appeared by rough inspection to be of higher quality than that of other datasets, its true level of quality remains unevaluated.

Lastly, with regard to extreme value analyses, was the underlying assumption that the quality of results obtained was correlated solely with the duration of a particular time history, rather than both the duration and the quality of the data itself. Time histories were assumed to be complete and continuous (i.e. all annual maxima were determined from consecutive years) for all analyses, which presents an obvious fallacy if an "annual" maxima is actually determined from only a partial year's worth of data.

7.2.2. Unreconciled Systematic Errors

This study also identified some specific issues encountered that were managed but ultimately left unreconciled:

1) Errant distribution fits from the method of independent storms (MIS) were identified and removed from consideration, but the ultimate cause was not identified or remedied.
2) The parameter space for wind speed threshold used in peaks over threshold (POT) evaluations was lower bounded at 10 knots (or 10 m/s for OKM data). For extremely short time histories, a wind speed threshold below 10 knots would have been necessary but was not permitted in this analysis. Resultant fits to a distribution were thus flawed and removed from consideration. No attempt was made to re-analyze these time histories with a more appropriate parameter space.
3) V50 was calculated using a fitted distribution, but since the plotting axes were reversed, the distribution actually described return period as a function of wind speed.

The fitted distribution was evaluated for whole number wind speeds ranging from 1 to 300 knots. V50 was selected from this range as the wind speed corresponding most closely to R = 50. This also resulted in the ultimate 300 knot cap of V50 estimates shown with the DS 6405 Non-QC comparisons.

4) V50 results were filtered using the 5^{th} to 95^{th} percentile filter, which is an arbitrary set of bounds.
5) While the hit-or-miss analysis of OKM events used only time histories spanning from 1994 to 2017, extreme value analyses of the same stations did not have such consistency. Since ASOS station time histories used for EVA were drawn from the Improved ISD 3505 database, their durations could extend much further back than 1994. This means that EVA results of time histories of differing length were ultimately compared in this analysis.
6) Event duration was used as an analog for wind event physical size in the OKM event comparisons, which is a tenuous (yet convenient) claim. Storm motion is a significant confounding variable in this analysis but is much more difficult to address with stationary observation station data.
7) Thunderstorm identification was assumed to be complete and comprehensive in the preparation of the Improved ISD 3505 database. Thus, an observation station with thunderstorm times available but no identified thunderstorms in its time history was assumed to have no thunderstorms in its time history. This would theoretically be true in a general context but is not completely assured.
8) The spatial clustering of observation stations, especially with regard to mapping methods, was largely left unaddressed. Network density was considered solely in the

context of even spacing and minimized clustering, despite that conclusions made in this study with regard to network density also inherently account for some aspect of network clustering as well.

CHAPTER 8: RECOMMENDATIONS AND FUTURE WORK

The findings of this study should by no means be considered exhaustive, particularly because a number of simplifying assumptions and generalizing procedures as described in Chapter 7 were enacted in order to produce them. Improving these aspects, and thereby truly dedicating the time and resources required, is paramount to enhancing the clarity and accuracy of this kind of study.

Nowhere else is this is more necessary than in the data preparation process, which could easily be considered the greatest source of uncertainty in this study. Cleaning and quality control procedures should be refined further to increase the overall confidence in the databases' accuracy. This is probably most important for DS 6405 data, which does not receive any sort of quality treatment before being inputted to the online repository (in contrast with ISD 3505 data, which has baseline quality checks applied automatically). While the excessive volume of data required to produce these results makes multiple iterations of cleaning and quality control difficult, the ultimate reward for improving such efforts is significant and should be pursued further.

With regard to improving the existing ISD 3505 extreme wind database, future efforts should focus on continually expanding the both the number of reporting locations utilized and the length of time histories used, as these were both shown to be beneficial for characterizing the extreme wind climate. Methods of accommodating both long and short duration time histories in the same map also provide a promising avenue for improvement that incorporates as much of the available data as possible. Utilizing additional EVA methods, such as a penultimate Gumbel (Cook and Harris 2004), r-largest maxima (Palutikof et al. 1999), or a better-refined POT

technique, to expand the suite of V50 estimates is also recommended as a means of increasing the number of viable options for consideration.

Wind speed data from DS 6405 sources overall should be approached with caution, especially in the context of EVA. Maxima from these time histories are not completely accurate and would need intense verification before being fully trusted. Applications that do not rely on maxima, such as characterizing time histories for specific thunderstorm events or calculating gust factors, could still be plausible with this data if effective quality control measures are applied. A thorough investigation of duplicate wind records found in DS 6405 data would likely reveal some interesting results regarding its quality, as would a correlation study between these duplicate records and the observed highly anomalous extrema. The associated 2-minute average wind speeds with these 3-second gust records could also be a viable tool for investigation.

For analyses of higher spatial resolution networks like the Oklahoma Mesonet, avenues for improvement are wide. A study that quantifies network density and defines changes in V50 as a function of network density would certainly reveal the underlying relationship between these two variables and could further solidify that coarser networks are inadequate at capturing small-scale wind events. Further refinements to the hit-or-miss model are warranted, such as identifying and excluding any ASOS stations that report "misses" too consistently or deriving distance-dependent comparison windows. Work is ongoing for identifying thunderstorm wind events using reanalysis data (such as that from the North American Regional Reanalysis (NARR) database), which could provide a realistic control group of thunderstorm occurrence rates for comparison with ASOS and OKM. Additionally, other regional observation networks exist for which a similar hit-or-miss study could be conducted, including the Missouri Mesonet, and the Kentucky Mesonet. The West Texas Mesonet has already been the subject of similar analyses

(Zickar et al. unpublished manuscript) the results of which would provide intriguing comparisons to the Oklahoma Mesonet results obtained in this study.

REFERENCES

ASCE (American Society of Civil Engineers). (2017). *Minimum Design Loads and Associated Criteria for Buildings and Other Structures*, Standard ASCE/SEI 7-16. ASCE, Reston, VA.

Brabson, B. B., and Palutikof, J. P. (2000). "Tests of the generalized Pareto distribution for predicting extreme wind speeds." *Journal of Applied Meteorology*, 39(9), 1627-1640.

Cook, N. J. (1982). "Towards better estimation of extreme winds." *Journal of Wind Engineering and Industrial Aerodynamics*, 9(3), 295-323.

Cook, N. J., and Harris, R. I. (2004). "Exact and general FT1 penultimate distributions of extreme wind speeds drawn from tail-equivalent Weibull parents". *Structural Safety*, 26(4), 391-420.

Davison, A. C., and Smith, R. L. (1990). "Models for exceedances over high thresholds." *Journal of the Royal Statistical Society: Series B (Methodological)*, 52(3), 393-425.

de Haan, L. (1994). "Extreme value statistics." In *Extreme value theory and applications* (pp. 93-122). Springer, Boston, MA.

DeGaetano, A. T. (1997). "A quality-control routine for hourly wind observations." *Journal of Atmospheric and Oceanic Technology*, 14(2), 308-317.

Harris, R. I. (1996). "Gumbel re-visited: a new look at extreme value statistics applied to wind speeds." *Journal of Wind Engineering and Industrial Aerodynamics*, 59(1), 1-22.

Harris, R. I. (1999). "Improvements to the Method of Independent Storms". *Journal of Wind Engineering and Industrial Aerodynamics*, 80(1-2), 1-30.

Harris, I. (2005). "Generalised Pareto methods for wind extremes. Useful tool or mathematical mirage?" *Journal of Wind Engineering and Industrial Aerodynamics*, 93(5), 341-360.

Holmes, J. D. (2015). *Wind Loading of Structures, Third Edition*. CRC press, Boca Raton, FL.

Landsea, C., Franklin, J., and Beven, J. (2014). "The revised Atlantic hurricane database (HURDAT2)". <http://www.aoml.noaa.gov/hrd/hurdat/newhurdat-format.pdf> (Jul. 10, 2019)

Lombardo, F. T. & Zickar, A. S. (in press). "Characteristics of Measured Extreme Thunderstorm Near-Surface Wind Gusts in the United States." *Journal of Wind Engineering and Industrial Aerodynamics.*

Lombardo, F. T. (2012). "Improved extreme wind speed estimation for wind engineering applications." *Journal of Wind Engineering and Industrial Aerodynamics*, *104*, 278-284.

Lombardo, F. T., Main, J. A., and Simiu, E. (2009). "Automated extraction and classification of thunderstorm and non-thunderstorm wind data for extreme-value analysis." *Journal of Wind Engineering and Industrial Aerodynamics*, 97(3-4), 120-131.

Lombardo, F. T., Vickery, P. J., Pintar, A. L., Simiu, E., Sinh, H. N., Levitan, M., and Yeo, D. (2016). "Development of an updated US non-hurricane extreme wind climatology and wind maps for wind load design." In Preparation.

Lott, N. (2017). "Integrated Surface Data (ISD) FTP Access Point Readme File." <ftp://ftp.ncdc.noaa.gov/pub/data/noaa/readme.txt> (Jul. 10, 2019).

Masters, F. J., Vickery, P. J., Bacon, P., and Rappaport, E. N. (2010). "Toward objective, standardized intensity estimates from surface wind speed observations." *Bulletin of the American Meteorological Society*, 91(12), 1665-1682.

MEASNET (2016). "MEASNET Procedure: Evaluation of Site-Specific Wind Conditions". Version 2.

Nadolski, V. L. (1998). "Automated Surface Observing System (ASOS) User's Guide". National Oceanic and Atmospheric Administration, Department of Defense, Federal Aviation Administration, United States Navy.

National Centers for Environmental Information (NCEI [a]). "Automated Weather Observing System (AWOS)." *Land-Based Datasets and Products*, <https://www.ncdc.noaa.gov/data-access/land-based-station-data/land-based-datasets> (Jul. 10, 2019).

National Centers for Environmental Information (NCEI [b]). "Integrated Surface Database (ISD)." *Land-Based Datasets and Products*, <https://www.ncdc.noaa.gov/isd> (Jul. 10, 2019).

National Centers for Environmental Information (NCEI [c]). "Station Metadata." *Land-Based Datasets and Products*, <https://www.ncdc.noaa.gov/data-access/land-based-station-data/station-metadata> (Jul. 10, 2019).

National Centers for Environmental Information (NCEI) (2018). "Federal Climate Complex Data Documentation for Integrated Surface Data (ISD)." *NOAA - National Centers for Environmental Information.*

National Centers for Environmental Information (NCEI). (2006). "Data Documentation for Data Set 6405 (DSI-6405) ASOS Surface 1-Minute, Page 1 Data." <ftp://ftp.ncdc.noaa.gov/pub/data/asos-onemin/td6405.txt> (Jul. 10, 2019).

National Institute of Standards and Technology (NIST). (2012). "Standardized extreme wind speed database for the United States". *Extreme Wind Speeds*. <https://www.itl.nist.gov/div898/winds/NIST_TN/nist_tn.htm> (Jul. 10, 2019).

National Weather Service (NWS). “What is ASOS?” *Automated Surface Observing Systems,* <https://www.weather.gov/asos/asostech> (Jul. 10, 2019).

National Wind Institute (NWI). (2019). “West Texas Mesonet.” *Texas Tech University National Wind Institute,* < http://www.depts.ttu.edu/nwi/research/facilities/wtm/index.php> (Jul. 10, 2019).

Oklahoma Mesonet (OM) (2019a). *Mesonet,* <http://www.mesonet.org/index.php> (Jul. 10, 2019).

Oklahoma Mesonet (OM). (2019b). “Mesonet Files.” *Mesonet,* <http://www.mesonet.org/index.php/weather/mesonet_data_files> (Jul. 10, 2019).

Owen, W. and others. (2019). “United States.” *Encyclopedia Britannica*. <https://www.britannica.com/place/United-States> (Jul. 10, 2019).

Palutikof, J. P., Brabson, B. B., Lister, D. H., and Adcock, S. T. (1999). “A review of methods to calculate extreme wind speeds.” *Meteorological applications,* 6(2), 119-132.

Peterka, J. A., and Shahid, S. (1998). “Design gust wind speeds in the United States.” *Journal of Structural Engineering,* 124(2), 207-214.

Pintar, A. L., Simiu, E., Lombardo, F. T., and Levitan, M. L. (2015). “Maps of Non-hurricane Non-tornadic Wind Speeds With Specified Mean Recurrence Intervals for the Contiguous United States Using a Two-Dimensional Poisson Process Extreme Value Model and Local Regression.” [NIST Special Publication (NIST SP)-500-301].

Powell, M. D. (1993). “Wind Measurement and Archival Under the Automated Surface Observing System (ASOS): User Concerns and Opportunity for Improvement”. *Bulletin*

Simiu, E., and Heckert, N. A. (1996). “Extreme wind distribution tails: a ‘peaks over threshold’ approach.” *Journal of Structural Engineering,* 122(5), 539-547.

Simiu, E., and Scanlan, R. H. (1996). *Wind Effects on Structures: Fundamentals and Applications to Design, Third Edition*. John Wiley and Sons, New York, NY.

Simiu, E., Changery, M. J., and Filliben, J. J. (1979). “Extreme wind speeds at 129 stations in the contiguous United States”. [NBS Building Science Series 118].

Smith, R. L., and Weissman, I. (1994). “Estimating the extremal index.” *Journal of the Royal Statistical Society: Series B (Methodological),* 56(3), 515-528.

Zahumenský, I. (2004). “Guidelines on quality control procedures for data from automatic weather stations”. *World Meteorological Organization, Switzerland*.

Zickar, A. S., Carsello, M., and Lombardo, F. T. (unpublished manuscript). “On The Influence of Observation Density on Estimation of Extreme Wind Speeds.” In Preparation.

APPENDIX A: SUPPLEMENTARY MATERIALS

Table A1: ISD 3505 raw data files not downloaded and confirmed absent from ISD 3505. Each trio of USAF-WBAN-year constitutes a separate file.

USAF	WBAN	Year		USAF	WBAN	Year		USAF	WBAN	Year
690230	24255	1989		723403	13963	1990		999999	14825	1948
699604	03145	1987		723600	23051	1977		725500	14942	1974
722221	13899	1985		723723	23184	1990		725741	24027	1985
722223	13899	1990		724020	93739	1991		725744	24027	1990
722610	22010	1951		724024	93739	1979		725920	24257	1991
722710	93045	1978		999999	93730	1974		726088	14606	1990
723013	13748	1990		724586	13922	1955		726223	94725	1990
723183	13877	1990		745200	23176	1983		742300	24037	1983
723303	93862	1990		745201	23176	1985		726838	94185	1980
723320	93862	1991		725118	14751	1990		999999	24122	1948
690230	24255	1989		723403	13963	1990		999999	14825	1948
699604	03145	1987		723600	23051	1977		725500	14942	1974

Table A2: Stations deleted from further analysis due to faulty metadata and short span of wind data.

USAF	WBAN	DESCRIPTION	STATE	CALL	LAT	LON
999999	4728	NIAGARA FALLS	NY	E4C8	37.864	-103.823
999999	13710	WASHINGTON DC BOLLING FIELD A	MD		38.833	-77.017
999999	13751	ANACOSTIA NAS	MD	NDV	38.85	-77.033

Table A3: List of metadata edits to the ISD History Document. Old entries are shown with strikethrough formatting with the updated entry given below it.

USAF	WBAN	DESCRIPTION	STATE	CALL	LAT	LON
720302	99999	CLARKSVILLE RED RIVE	TX	KLBR	33.593	~~-96.064~~ **-95.064**
720528	03064	CENTRAL COLORADO REGIONAL AP	CO	KAEJ	~~38.698~~ **38.817**	~~-106.07~~ **-106.117**
720643	99999	FOREST CITY MUNI	IA	KFXY	~~43.233~~ **43.235**	~~-93.783~~ **-93.624**
722045	12843	VERO BEACH MUNI	FL	KVRB	~~27.653~~ **27.651**	~~-80.243~~ **-80.42**
722051	12841	~~ATOKA MUNI~~ **ORLANDO MUNICIPAL**	~~OK~~ **FL**	~~KAQR~~ **KORL**	28.545	-81.333
722132	63801	CONCORD REGIONAL AIRPORT	NC	KJQF	~~35.382~~ **35.383**	~~-80.491~~ **-80.7**
722351	12953	WHARTON REGIONAL AIRPORT	TX	KARM	~~29.266~~ **29.254**	~~-96.008~~ **-96.154**
722390	99999	FORT POLK (ARMY)	LA	KPOE	~~31.033~~ **31.05**	~~-93.033~~ **-93.183**
722726	93045	~~NOGALES (AMOS)~~ **TRUTH OR CONSEQUENCES**	~~AZ~~ **NM**	KTCS	33.237	-107.268
722720	93063	~~BISBEE DOUGLAS INTL~~ **SILVER CITY GRANT CO**	~~AZ~~ **NM**	KSVC	32.633	-108.167
722785	23111	LUKE AFB AIRPORT	AZ	KLUF	~~33.55~~ **33.533**	~~-112.367~~ **-112.383**
722820	99999	PEASON RIDGE FT POLK	LA	KAQV	~~31.37~~ **31.4**	~~-93.16~~ **-93.283**
722821	99999	FULLERTON LANDING ST	LA	KBKB	~~31.022~~ **31.114**	~~-92.11~~ **-92.966**
746941	13786	~~MONROE CO~~ **ELIZABETH CITY**	~~MS~~ **NC**	KECG	36.261	-76.175
723290	03849	~~CAPE GIRARDEAU RGNL~~ **LONDON-CORBIN**	~~MO~~ **KY**	KLOZ	37.087	-84.077
723300	99999	POPLAR BLUFF(AMOS)	MO	KPOF	~~36.767~~ **36.773**	~~-90.467~~ **-90.325**
723415	03962	MEMORIAL FIELD AIRPORT	AR	KHOT	~~34.29~~ **34.467**	~~-93.06~~ **-93.083**
723447	99999	FLIPPIN (AWOS)	AR	KFLP	~~36.3~~ **36.291**	~~-92.467~~ **-92.59**
723528	03981	FREDERICK MUNICIPAL AIRPT	OK	KFDR	~~34.21~~ **34.352**	~~-98.59~~ **-98.984**
724270	03804	~~OAK RIDGE~~ **PARKERSBURG WOOD CO**	~~TN~~ **WV**	KPKB	39.2	-81.27
724680	99999	FORT CARSON/BUTTS	CO	KFCS	~~38.7~~ **38.678**	~~-104.767~~ **-104.757**
725121	14761	~~BURLIGTON/COLCHE~~ **PHILIPSBURG**	~~VT~~ **PA**	KPSB	40.9	-78.083
725374	99999	ANN ARBOR MUNICIPAL	MI	KARB	42.223	~~-87.746~~ **-83.744**
726358	00384	MICHIGAN CITY MUNICIPAL AIRPORT PHILLIPS FIELD	IN	KMGC	41.703	~~-86.282~~ **-86.821**
726560	94966	~~PIERRE RGNL~~ **FERGUS FALLS**	~~SD~~ **MN**	KFFM	46.283	-96.15
727466	04918	MDSON-LAC QUI PARLE CO APT	MN	KDXX	44.986	~~-96.043~~ **-96.178**

Table A4: Oklahoma Mesonet stations eliminated for insufficient length of time history.

Number	ID	Time History Length (years)		Number	ID	Time History Length (years)
80	RETR	21.45		129	OKCW	8.18
96	TULL	5.84		130	OKCE	11.61
109	NINN	23.81		131	CARL	10.75
112	CATO	7.33		137	TULN	5.42
114	PRES	6.05		138	TALA	4.18
115	VANO	14.39		139	ELKC	3.47
118	PORT	19.07		140	VALL	3.12
119	BEEX	4.28		141	EVAX	2.53
120	INOL	17.00		142	YUKO	0.44
123	NEWP	16.16		143	SEMI	0.07
127	FITT	13.55		1028	CLA3	20.34
128	OKCN	11.18				

Table A5: Manually chosen pairings of call sign, USAF, and general location for ambiguous grouping situations used in the unified extreme value analysis procedure.

Call Sign	USAF	Location		Call Sign	USAF	Location		Call Sign	USAF	Location
KACK	725061	Nantucket		KGLS	722420	Galveston		KNZJ	722908	El Toro
KANJ	727340	Sault Ste. Marie		KGNA	727554	Grand Marais		KOAR	724916	Marina Muni
KATT	722540	Austin Municipal		KGRF	742071	Gray AAF		KOLS	722726	Nogales
KAUS	722540	Austin Bergstrom		KHLR	722570	Fort Hood		KONT	747040	Ontario
KAUW	726463	Wausau		KHMN	747320	Holloman AFB		KORL	722053	Orlando Executive
KBED	725059	Bedford		KHQM	727923	Hoquiam		KPAH	724350	Paducah
KBGR	726088	Bangor		KHRT	693254	Hurlburt Field		KPIR	726686	Pierre
KBKB	722821	Fullerton Strip		KHSE	723040	Cape Hatteras		KPNS	722223	Pensacola
KBTM	726785	Butte Silver Bow		KHUA	691164	Redstone Arsenal		KPRC	723723	Prescott
KBTR	722317	Baton Rouge		KHUF	724373	Terre Haute		KQSL	691334	Wendover
KBYS	746110	Fort Irwin		KHUL	727033	Houlton		KRDD	725920	Redding
KCAO	723600	Clayton		KILM	723013	Wilmington		KRDG	725103	Reading
KCDS	723604	Childress		KLEB	726116	Lebanon		KRIW	725765	Riverton
KCGI	723489	Cape Girardeau		KLIT	723403	Little Rock		KRKS	725744	Rock Springs
KCXY	725118	Harrisburg Capital		KLOZ	724243	London Corbin		KRWL	725745	Rawlins
KDAL	722583	Dallas Love Field		KLXV	724673	Leadville		KSNY	725610	Sidney
KDEW	727854	Deer Park		KMKC	724463	Kansas City		KSPS	723510	Wichita Falls
KDPG	740030	Dugway		KMLF	724750	Milford		KTCS	722710	Truth or Consequences
KDUG	722735	Bisbee Douglas		KMLS	742300	Miles City		KTRI	723183	Bristol Tri Cities
KDYS	690190	Dyess AFB		KMSS	726223	Massena		KTTS	747946	NASA Shuttle Facility
KECG	746943	Elizabeth City		KNDZ	722226	Whiting Field NAS		KUNO	723484	West Plains
KFLG	723750	Flagstaff		KNKX	722930	San Diego Miramar		KVBG	723930	Vandenberg AFB
KGAG	723527	Gage Shattuck		KNSE	722226	Whiting Field NAS		KVRB	722045	Vero Beach
KGCN	723783	Grand Canyon		KNUW	690230	Whidbey Island		KWAL	724020	Wallops
KGFK	727576	Grand Forks		KNXP	690150	Twentynine Palms				
KGGG	722470	Longview		KNYL	722800	Yuma				

Table A6: V50 values (all in knots) for selected cities evaluated using the Sep 12 QC and US L48 databases, all six extrapolation methods, and **COMMINGLED** storm type.

City	Gum. AM		Harris AM		GEV AM		MIS		POT GPD		POT Exp	
	Sep12 QC	US L48	Sep12 QC	US L48	Sep12 QC	US L48	Sep12 QC	US L48	Sep12 QC	US L48	Sep12 QC	US L48
Hartford	58.9	60.2	60.7	61.8	58.1	58.2	60.7	60.6	54.6	55.3	57.7	57.1
Great Falls	65.8	65.6	66.4	66.4	68.1	68.1	67.9	67.9	63.0	64.0	65.5	64.8
Baton Rouge	63.7	63.7	66.5	65.5	65.6	64.5	68.4	68.3	64.4	61.3	61.5	60.4
Decatur	67.2	68.2	68.6	70.6	64.9	63.3	67.7	68.2	63.3	63.5	64.6	64.6
Columbus	65.2	65.9	66.6	67.3	63.2	63.1	66.0	66.6	61.3	61.5	62.8	63.0
Augusta	59.1	60.0	61.4	62.0	62.4	60.9	61.8	61.8	57.1	57.0	59.5	57.0
Fargo	70.4	69.9	69.9	70.0	68.8	69.0	70.3	70.5	66.9	65.9	63.4	63.7
Colo. Springs	69.3	70.3	71.8	73.1	65.7	66.2	67.4	67.7	63.9	63.1	66.5	66.4
Sacramento	63.6	62.7	66.9	65.1	62.9	61.5	65.6	64.0	61.3	58.9	60.9	58.9
Roswell	67.2	68.8	69.5	70.8	66.7	68.1	69.3	70.6	61.6	61.5	65.6	67.2
Skowhegan	58.5	59.3	60.0	60.9	57.4	57.1	59.2	59.1	56.2	56.4	58.0	57.1
Glenns Ferry	61.7	61.0	64.4	63.5	60.6	60.1	64.6	64.2	59.3	57.9	60.2	60.0
Arcadia	66.7	68.5	70.1	71.2	69.9	70.5	68.1	67.2	68.5	68.4	61.3	59.0
Red Cloud	70.8	71.8	73.3	73.5	72.7	70.4	73.6	72.9	67.7	68.2	67.9	67.4
Keysville	60.1	60.2	63.2	62.0	58.6	60.3	60.5	61.3	55.7	55.8	56.6	57.8
Kosciusko	64.1	67.5	66.7	69.9	63.0	62.3	65.9	66.5	60.8	61.5	61.2	60.2
Ontonagon	62.6	59.8	64.7	61.7	58.5	55.8	63.8	62.5	62.1	59.2	63.5	61.7
Duchesne	64.5	68.9	67.2	70.1	61.2	60.5	63.7	64.1	59.1	59.0	63.7	62.5
South Bend	62.8	63.7	65.8	66.3	62.2	61.0	64.8	62.7	59.2	56.4	62.3	55.3
Guthrie	71.3	71.6	72.8	73.0	71.0	71.0	70.8	70.7	67.6	68.1	67.5	67.4

Table A7: V50 values (all in knots) for selected cities evaluated using the Sep 12 QC and US L48 databases, all six extrapolation methods, and **THUNDERSTORM** storm type.

City	Gum. AM		Harris AM		GEV AM		MIS		POT GPD		POT Exp	
	Sep12 QC	US L48	Sep12 QC	US L48	Sep12 QC	US L48	Sep12 QC	US L48	Sep12 QC	US L48	Sep12 QC	US L48
Hartford	53.9	54.0	56.7	56.9	56.8	58.2	57.4	57.7	30.9	29.9	66.1	64.7
Great Falls	66.4	67.4	67.5	68.5	58.1	58.2	64.8	64.7	53.3	56.4	66.8	64.3
Baton Rouge	63.4	63.6	66.4	65.3	71.3	68.1	66.7	66.4	60.8	59.9	58.8	58.8
Decatur	68.4	70.3	71.7	73.5	60.9	60.2	69.2	68.8	58.4	58.2	66.2	65.0
Columbus	62.2	63.3	65.3	65.7	68.7	67.4	65.3	63.2	56.1	56.5	62.0	61.8
Augusta	58.8	60.7	61.3	62.4	59.2	58.4	59.6	60.0	51.0	51.6	59.3	58.7
Fargo	68.4	67.8	69.7	71.3	70.1	67.2	70.0	70.2	57.0	57.7	65.5	64.5
Colo. Springs	61.7	61.9	64.8	64.3	58.1	58.3	62.8	61.4	55.3	51.0	63.8	62.0
Sacramento	52.0	52.0	55.2	55.5	131.7	113.4	56.2	57.0	25.6	23.4	59.8	59.4
Roswell	65.4	68.0	68.0	68.5	107.3	111.8	69.5	68.9	51.0	49.5	64.9	65.0
Skowhegan	49.6	49.5	52.9	52.6	55.8	56.3	50.5	53.0	21.4	21.4	64.9	65.0
Glenns Ferry	55.3	55.4	57.8	57.1	94.9	87.3	56.1	54.9	38.4	38.7	65.5	59.4
Arcadia	58.6	61.7	60.5	63.7	99.7	94.1	59.3	62.6	51.9	56.1	57.3	55.1
Red Cloud	74.8	73.7	75.1	75.6	74.3	71.5	74.4	73.5	57.5	59.9	72.0	69.8
Keysville	58.1	58.8	61.0	61.1	53.0	55.1	56.3	59.8	42.7	45.1	61.5	59.4
Kosciusko	62.9	64.9	64.3	66.8	60.2	62.5	64.2	65.3	56.4	56.5	60.1	59.7
Ontonagon	60.3	54.7	63.3	53.7	59.9	52.6	62.0	53.4	41.6	27.2	58.5	66.0
Duchesne	62.8	68.4	66.3	72.2	56.8	56.3	61.2	62.7	56.0	56.9	61.8	60.6
South Bend	57.7	55.4	63.1	61.2	81.3	76.5	56.1	51.6	21.9	21.7	65.3	64.0
Guthrie	67.6	67.4	72.8	72.3	87.7	87.5	72.7	70.5	64.8	64.6	67.6	64.3

Table A8: V50 values (all in knots) for selected cities evaluated using the Sep 12 QC and US L48 databases, all six extrapolation methods, and **NON-THUNDERSTORM** storm type.

City	Gum. AM		Harris AM		GEV AM		MIS		POT GPD		POT Exp	
	Sep12 QC	US L48	Sep12 QC	US L48	Sep12 QC	US L48	Sep12 QC	US L48	Sep12 QC	US L48	Sep12 QC	US L48
Hartford	57.4	58.4	59.2	60.3	56.2	55.6	57.8	58.4	54.2	54.1	56.1	55.5
Great Falls	63.8	63.7	64.4	64.2	66.8	66.4	66.7	66.1	62.3	62.8	63.5	62.9
Baton Rouge	62.3	56.5	63.2	57.7	59.6	60.9	61.4	64.2	56.7	56.0	55.5	52.4
Decatur	61.3	62.0	63.1	63.3	57.3	58.7	62.4	62.3	58.3	58.0	58.7	58.3
Columbus	61.3	62.0	62.8	63.7	58.1	58.9	62.1	62.5	57.5	58.1	60.6	60.5
Augusta	55.0	54.4	56.0	56.0	57.7	56.9	57.0	57.0	50.7	51.3	53.8	52.9
Fargo	62.8	63.9	63.3	64.7	60.7	61.7	64.5	64.3	61.4	60.9	61.0	61.4
Colo. Springs	68.0	68.5	71.3	72.9	65.3	65.8	67.3	67.4	63.7	63.5	66.1	64.8
Sacramento	62.1	61.2	65.8	63.3	61.7	60.3	64.9	62.7	58.6	58.1	60.6	58.4
Roswell	65.3	64.2	67.3	66.3	62.4	62.5	64.2	65.0	58.0	58.5	67.2	66.1
Skowhegan	57.4	57.5	60.1	59.1	55.7	54.8	57.8	57.4	54.4	54.3	57.0	56.5
Glenns Ferry	61.1	61.2	63.1	63.0	61.0	59.4	61.6	61.2	59.0	58.4	58.3	58.4
Arcadia	64.3	62.2	65.9	65.5	69.7	68.0	68.7	69.2	63.5	62.3	59.8	57.2
Red Cloud	64.8	64.9	66.4	66.3	65.1	64.0	66.9	65.7	60.7	60.5	64.9	64.5
Keysville	55.3	56.3	57.6	57.8	61.0	57.2	57.5	57.0	51.8	51.6	54.1	52.7
Kosciusko	59.3	57.0	62.0	60.1	58.8	58.6	58.5	57.7	54.5	52.9	53.1	53.2
Ontonagon	60.9	59.2	62.7	60.8	57.8	55.6	61.3	61.8	60.2	58.1	62.4	61.1
Duchesne	62.6	64.8	64.4	70.2	63.4	58.5	63.3	62.7	56.5	57.9	61.4	60.6
South Bend	57.5	58.5	65.9	66.2	62.2	60.0	64.4	62.6	59.2	57.0	62.1	54.5
Guthrie	63.0	64.2	65.2	65.0	60.4	60.5	65.7	60.8	61.5	61.4	64.8	64.9

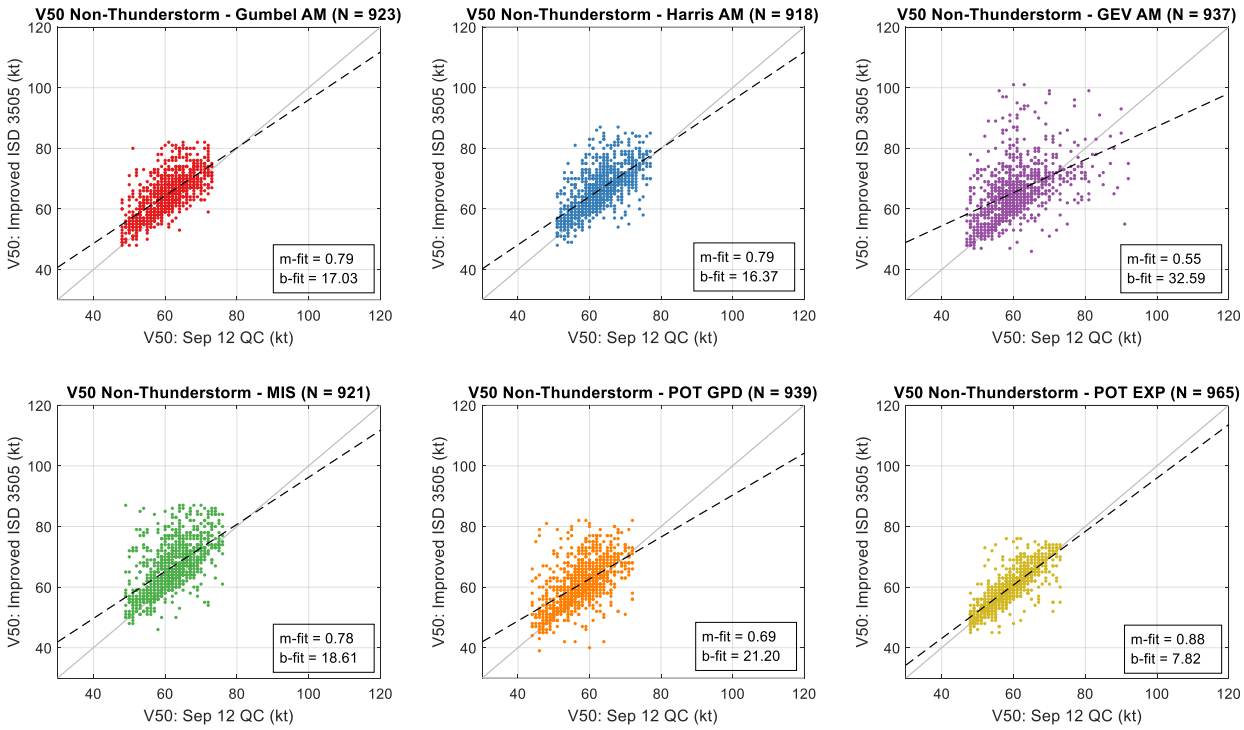

Figure A1: Scatter plots showing comparisons between V50 calculated using the Sep 12 QC database and the Improved ISD 3505 database for the **NON-THUNDERSTORM** storm type.

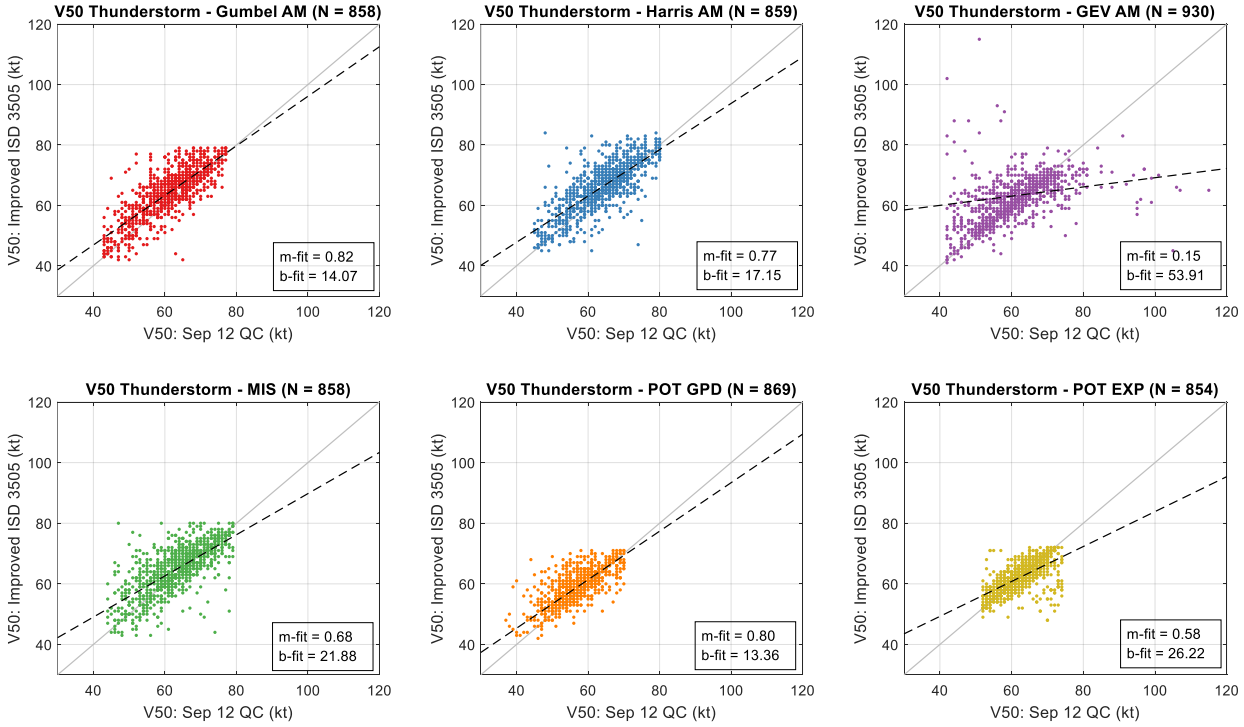

Figure A2: Scatter plots showing comparisons between V50 calculated using the Sep 12 QC database and the Improved ISD 3505 database for the **THUNDERSTORM** storm type

Table A9: V50 results for selected cities using the Improved ISD 3505 database, all EVA methods, and the **THUNDERSTORM** storm type. Percentages show comparisons to Sep 12 QC V50 estimates of the same storm type and EVA method.

City	Improved ISD 3505 V50 Estimates (in knots) for Thunderstorm Winds (in knots) By Extrapolation Method					
	Gum. AM	Harris AM	GEV AM	MIS	POT GPD	POT Exp
Hartford	57.0 (+6%)	58.4 (+3%)	58.1 (+2%)	56.2 (-2%)	32.8 (+6%)	63.5 (-4%)
Great Falls	66.0 (0%)	67.9 (+1%)	92.2 (+59%)	62.9 (-3%)	56.0 (+5%)	64.4 (-4%)
Baton Rouge	58.9 (-7%)	62.5 (-6%)	77.2 (+8%)	60.8 (-9%)	48.8 (-20%)	58.1 (-1%)
Decatur	65.7 (-4%)	67.8 (-5%)	57.5 (-5%)	63.8 (-8%)	60.0 (+3%)	59.7 (-10%)
Columbus	66.3 (+7%)	68.2 (+4%)	77.6 (+13%)	65.5 (0%)	59.5 (+6%)	61.3 (-1%)
Augusta	54.2 (-8%)	57.3 (-6%)	84.3 (+43%)	54.5 (-8%)	48.8 (-4%)	56.7 (-4%)
Fargo	65.1 (-5%)	68.0 (-2%)	80.6 (+15%)	63.3 (-10%)	56.9 (0%)	60.4 (-8%)
Colo. Springs	67.1 (+9%)	70.9 (+9%)	72.4 (+25%)	64.1 (+2%)	55.1 (0%)	61.0 (-4%)
Sacramento	49.0 (-6%)	53.8 (-2%)	64.0 (-51%)	52.9 (-6%)	21.1 (-17%)	58.8 (-2%)
Roswell	64.9 (-1%)	67.3 (-1%)	85.8 (-20%)	65.8 (-5%)	53.1 (+4%)	63.1 (-3%)
Skowhegan	47.8 (-3%)	50.4 (-5%)	54.6 (-2%)	50.2 (-1%)	23.4 (+10%)	61.7 (-5%)
Glenns Ferry	55.6 (+1%)	58.6 (+2%)	58.5 (-38%)	59.2 (+6%)	40.8 (+7%)	59.1 (-10%)
Arcadia	61.4 (+5%)	62.4 (+3%)	73.7 (-26%)	59.6 (+1%)	53.1 (+2%)	55.8 (-3%)
Red Cloud	74.2 (-1%)	77.0 (+3%)	66.1 (-11%)	71.8 (-3%)	63.4 (+10%)	66.7 (-7%)
Keysville	58.1 (0%)	59.0 (-3%)	61.6 (+16%)	58.8 (+4%)	51.0 (+20%)	58.4 (-5%)
Kosciusko	63.2 (+1%)	65.4 (+2%)	65.1 (+8%)	65.0 (+1%)	58.5 (+4%)	59.8 (0%)
Ontonagon	57.5 (-5%)	60.2 (-5%)	72.4 (+21%)	59.3 (-4%)	48.3 (+16%)	58.1 (0%)
Duchesne	65.8 (+5%)	73.3 (+11%)	103.2 (+82%)	64.5 (+5%)	55.0 (-2%)	61.1 (-1%)
South Bend	54.9 (-5%)	58.7 (-7%)	80.4 (-1%)	56.0 (0%)	27.3 (+25%)	62.3 (-5%)
Guthrie	64.5 (-5%)	68.6 (-6%)	109.8 (+25%)	68.0 (-6%)	63.4 (-2%)	62.7 (-7%)

Table A10: V50 results for selected cities using the Improved ISD 3505 database, all EVA methods, and the **NON-THUNDERSTORM** storm type. Percentages show comparisons to Sep 12 QC V50 estimates of the same storm type and EVA method.

City	Improved ISD 3505 V50 Estimates (in knots) for Non-Thunderstorm Winds By Extrapolation Method					
	Gum. AM	Harris AM	GEV AM	MIS	POT GPD	POT Exp
Hartford	63.7 (+11%)	64.9 (+10%)	63.7 (+13%)	64.8 (+12%)	58.9 (+9%)	57.7 (+3%)
Great Falls	72.1 (+13%)	75.9 (+18%)	72.8 (+9%)	76.1 (+14%)	71.2 (+14%)	67.3 (+6%)
Baton Rouge	58.1 (-7%)	60.7 (-4%)	63.3 (+6%)	62.7 (+2%)	57.0 (+1%)	51.4 (-7%)
Decatur	59.0 (-4%)	60.2 (-5%)	58.7 (+3%)	60.8 (-3%)	54.7 (-6%)	55.4 (-5%)
Columbus	61.5 (0%)	63.0 (0%)	61.3 (+6%)	62.6 (+1%)	58.6 (+2%)	59.5 (-2%)
Augusta	52.8 (-4%)	54.5 (-3%)	56.0 (-3%)	56.4 (-1%)	50.1 (-1%)	50.6 (-6%)
Fargo	60.4 (-4%)	61.8 (-2%)	59.0 (-3%)	64.2 (0%)	56.7 (-8%)	58.5 (-4%)
Colo. Springs	67.2 (-1%)	70.0 (-2%)	67.8 (+4%)	73.1 (+9%)	67.3 (+6%)	65.7 (-1%)
Sacramento	67.8 (+9%)	69.6 (+6%)	69.4 (+13%)	69.0 (+7%)	65.0 (+11%)	62.5 (+3%)
Roswell	68.8 (+5%)	72.6 (+8%)	65.4 (+5%)	67.6 (+5%)	65.0 (+12%)	63.7 (-5%)
Skowhegan	56.1 (-2%)	58.0 (-3%)	56.9 (+2%)	59.2 (+2%)	54.0 (-1%)	56.0 (-2%)
Glenns Ferry	61.3 (0%)	62.7 (0%)	61.7 (+1%)	63.3 (+3%)	59.6 (+1%)	56.6 (-3%)
Arcadia	61.8 (-4%)	65.5 (0%)	71.6 (+3%)	70.8 (+3%)	61.2 (-3%)	57.4 (-4%)
Red Cloud	65.8 (+2%)	66.8 (+1%)	64.6 (-1%)	66.9 (0%)	62.4 (+3%)	63.4 (-2%)
Keysville	53.4 (-3%)	55.1 (-4%)	55.1 (-10%)	57.6 (0%)	53.3 (+3%)	50.5 (-6%)
Kosciusko	58.6 (-1%)	58.9 (-5%)	62.6 (+7%)	61.6 (+5%)	51.7 (-5%)	52.1 (-2%)
Ontonagon	58.3 (-4%)	61.1 (-2%)	64.5 (+12%)	62.3 (+2%)	52.6 (-13%)	56.7 (-9%)
Duchesne	65.3 (+4%)	68.3 (+6%)	62.7 (-1%)	66.2 (+5%)	62.6 (+11%)	62.5 (+2%)
South Bend	67.6 (+18%)	68.0 (+3%)	65.3 (+5%)	66.7 (+4%)	61.8 (+4%)	61.9 (0%)
Guthrie	67.5 (+7%)	69.4 (+7%)	65.8 (+9%)	67.8 (+3%)	59.7 (-3%)	63.2 (-2%)

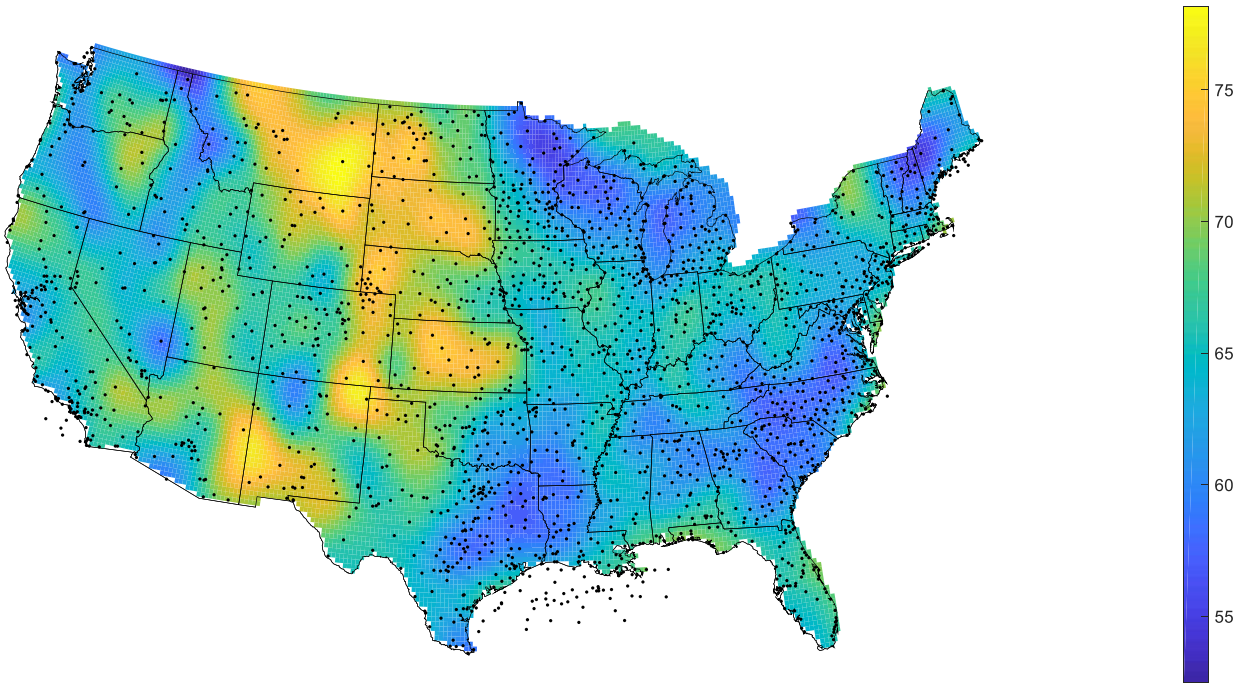

Figure A3: V50 mapped using the Improved ISD 3505 database, **Gumbel annual maxima** method and commingled storms. Number of stations plotted is 2,154. Units are knots (1 knot = 1.15 mph).

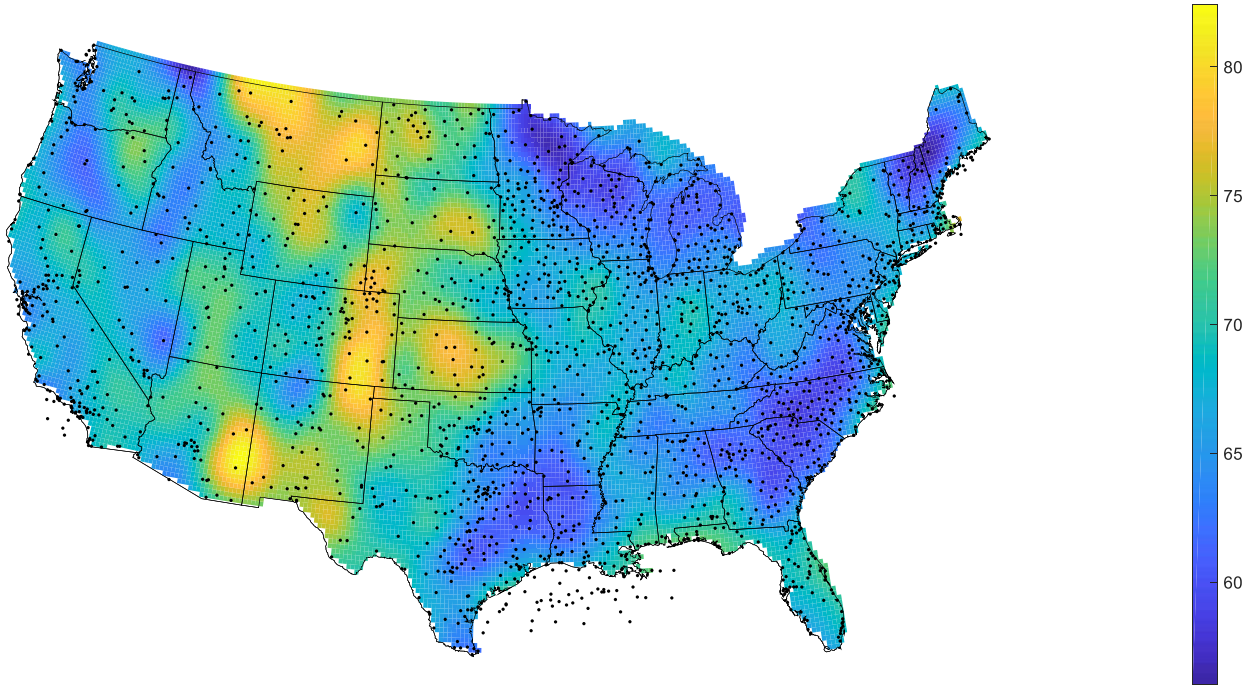

Figure A4: V50 mapped using the Improved ISD 3505 database, **Harris annual maxima** method and commingled storms. Number of stations plotted is 2,165. Units are knots (1 knot = 1.15 mph).

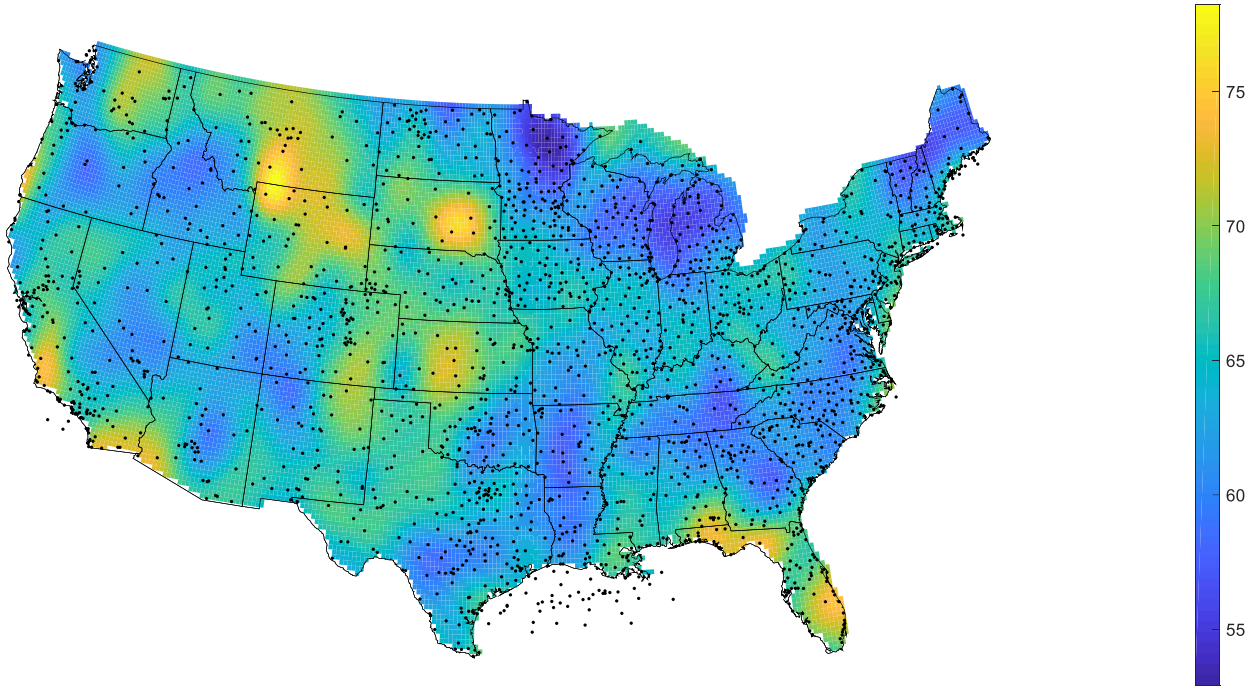

Figure A5: V50 mapped using the Improved ISD 3505 database, **GEV annual maxima** method and commingled storms. Number of stations plotted is 2,158. Units are knots (1 knot = 1.15 mph).

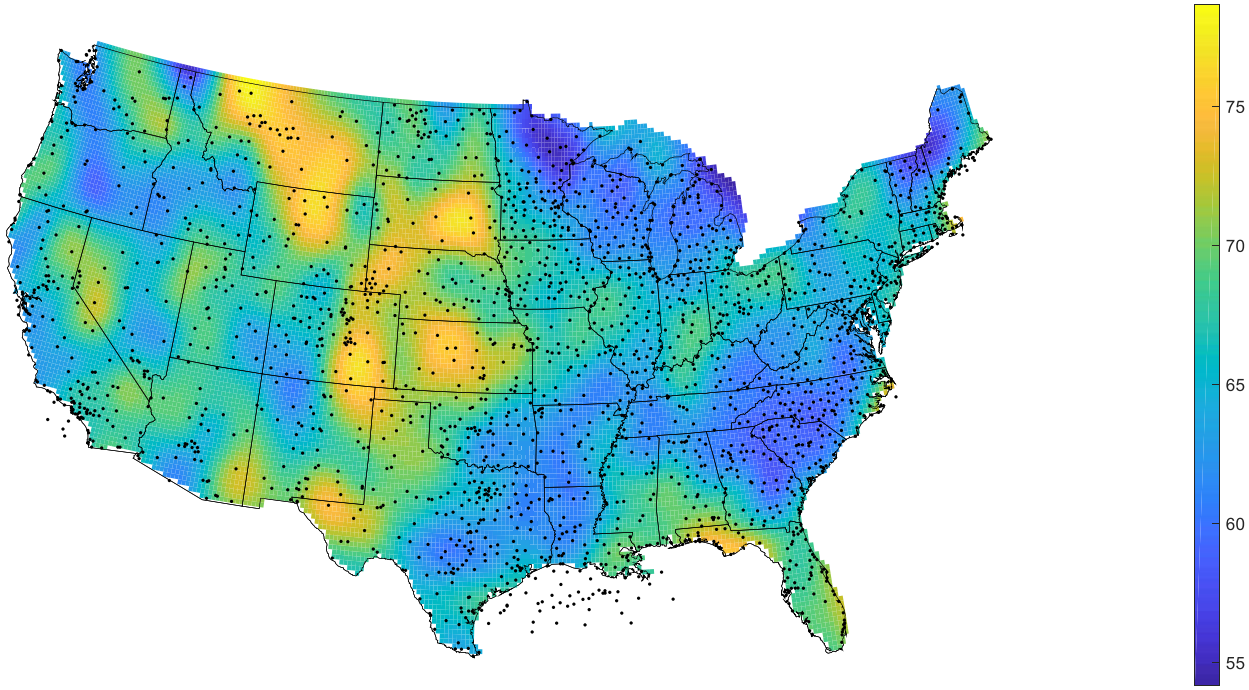

Figure A6: V50 mapped using the Improved ISD 3505 database, **method of independent storms (MIS)** and commingled storms. Number of stations plotted is 2,167. Units are knots (1 knot = 1.15 mph).

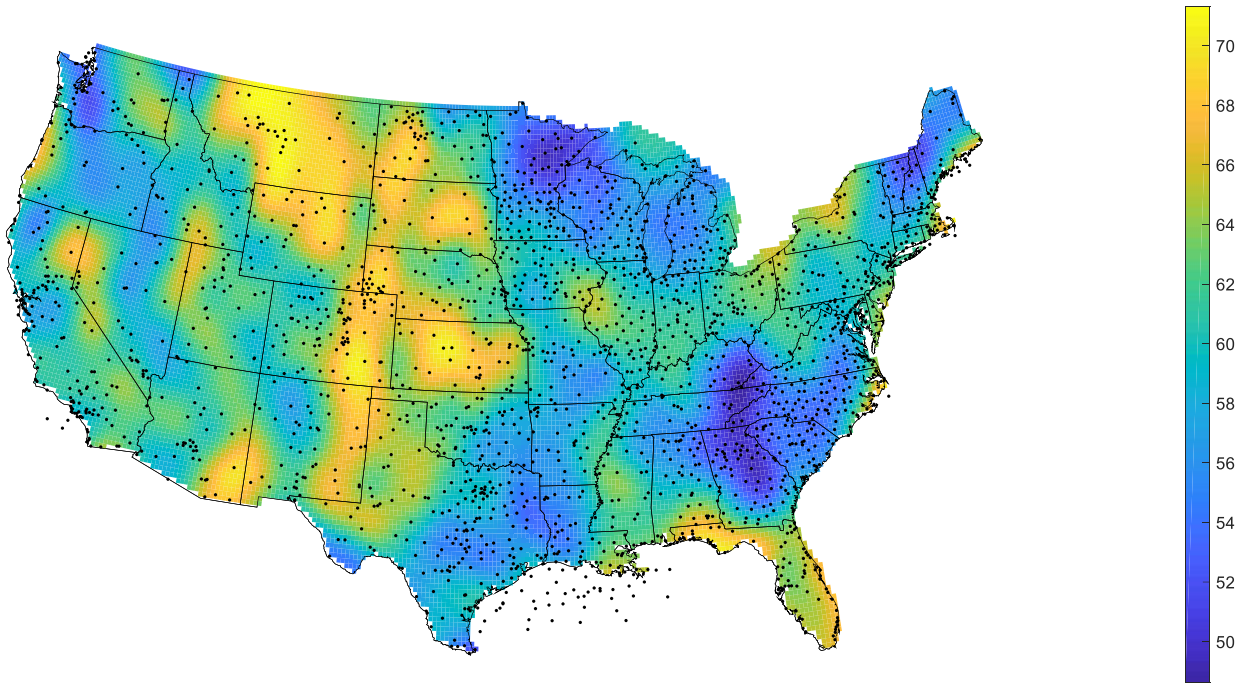

Figure A7: V50 mapped using the Improved ISD 3505 database, **GPD peaks over threshold** and commingled storms. Number of stations plotted is 2,172. Units are knots (1 knot = 1.15 mph).

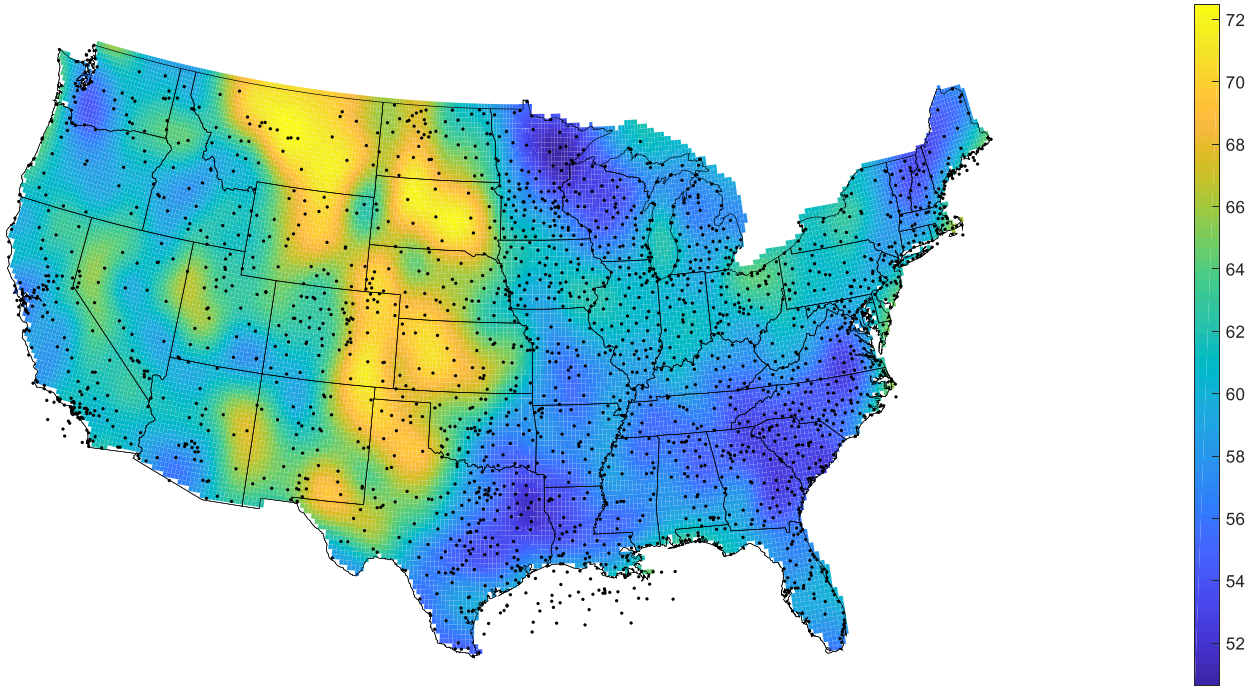

Figure A8: V50 mapped using the Improved ISD 3505 database, **exponential peaks over threshold** and commingled storms. Number of stations plotted is 2,189. Units are knots (1 knot = 1.15 mph).

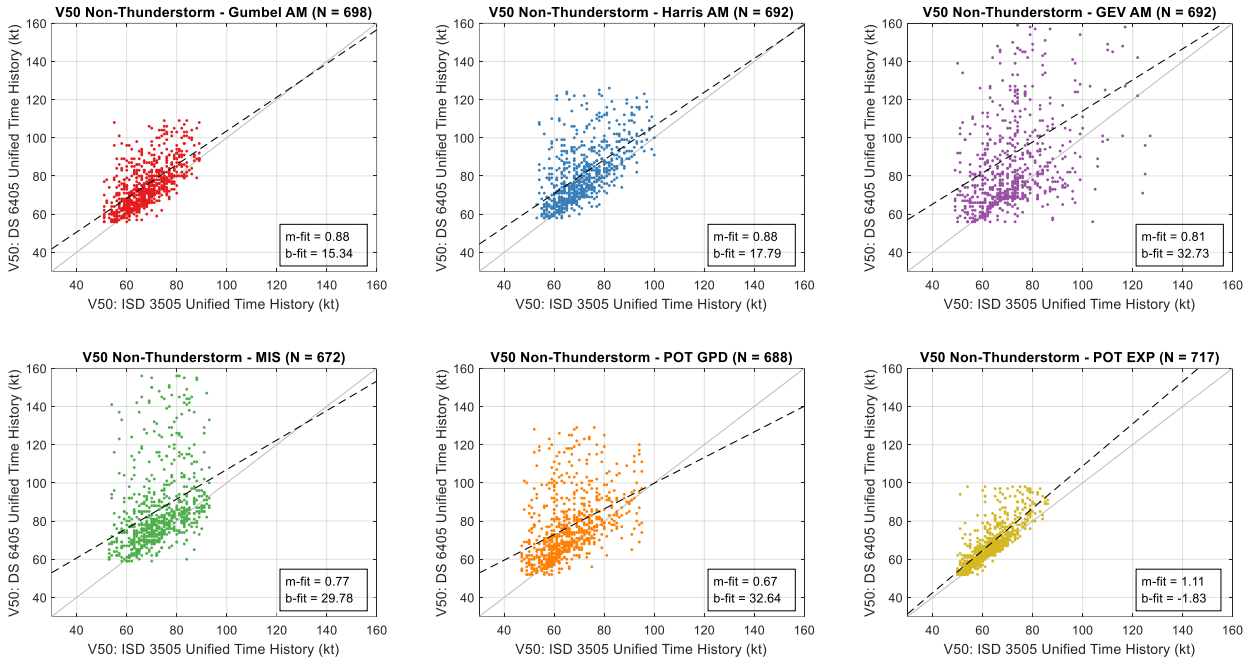

Figure A9: Scatter plots showing comparisons between V50 calculated using the DS 6405 UTH database and the ISD 3505 UTH database for the **NON-THUNDERSTORM** storm type.

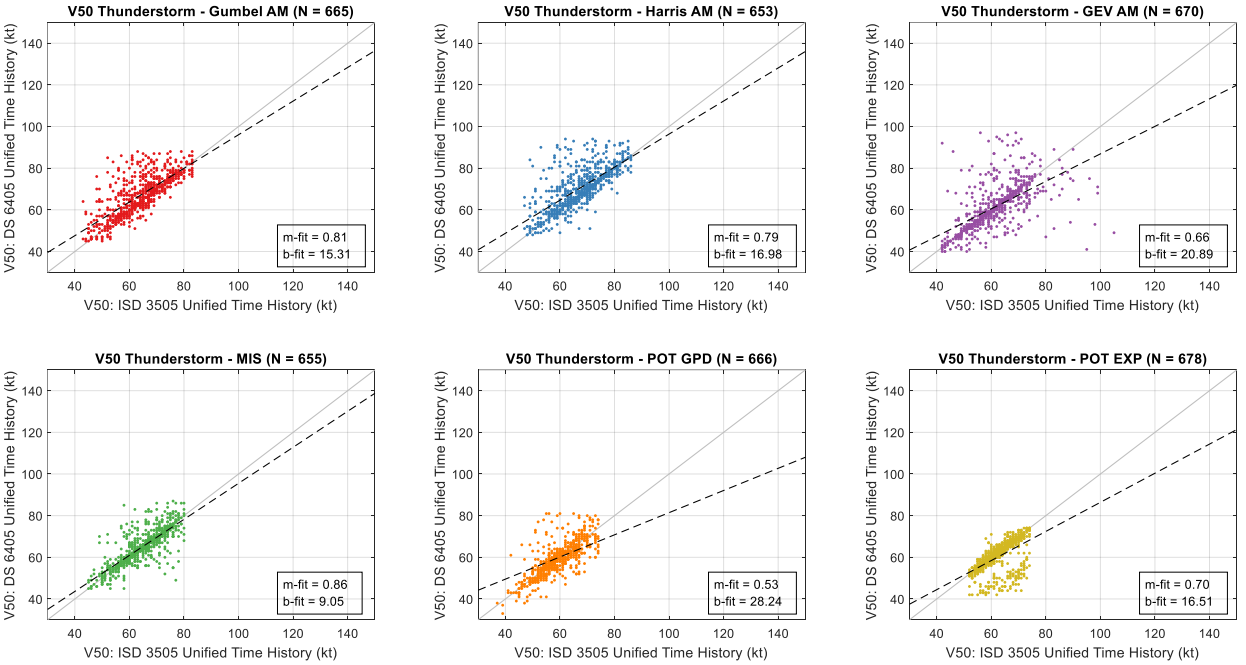

Figure A10: Scatter plots showing comparisons between V50 calculated using the DS 6405 UTH database and the ISD 3505 UTH database for the **THUNDERSTORM** storm type.

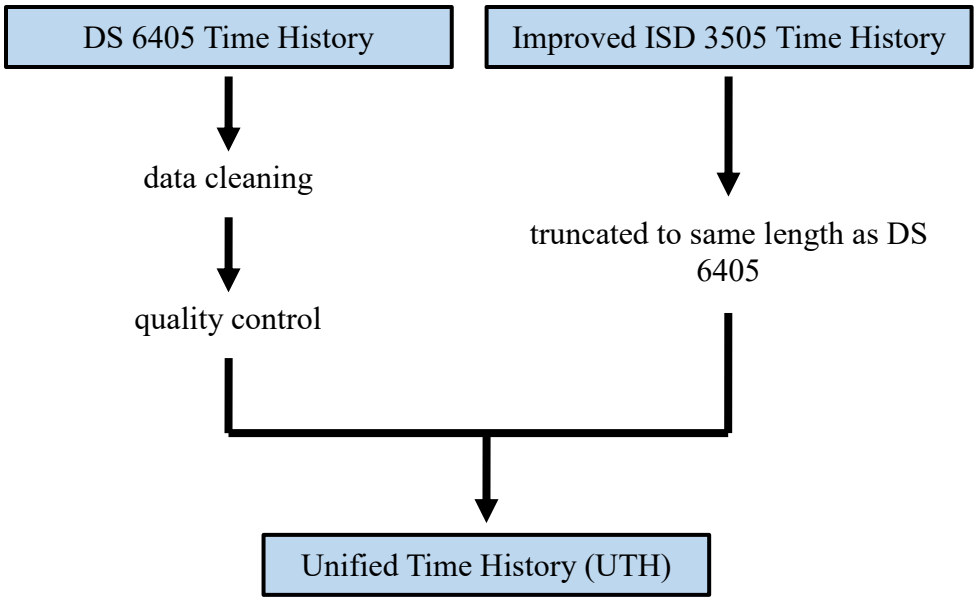

Figure A11: Flow chart depicting the creation of the Unified Time History from the separate DS 6405 and Improved ISD 3505 time histories.

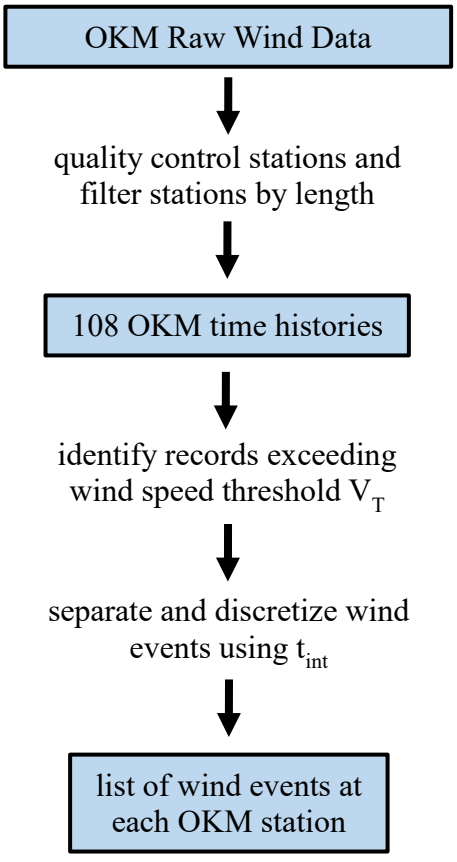

Figure A12: Flow chart depicting the process of identifying high wind events at OKM stations from the raw OKM wind data.

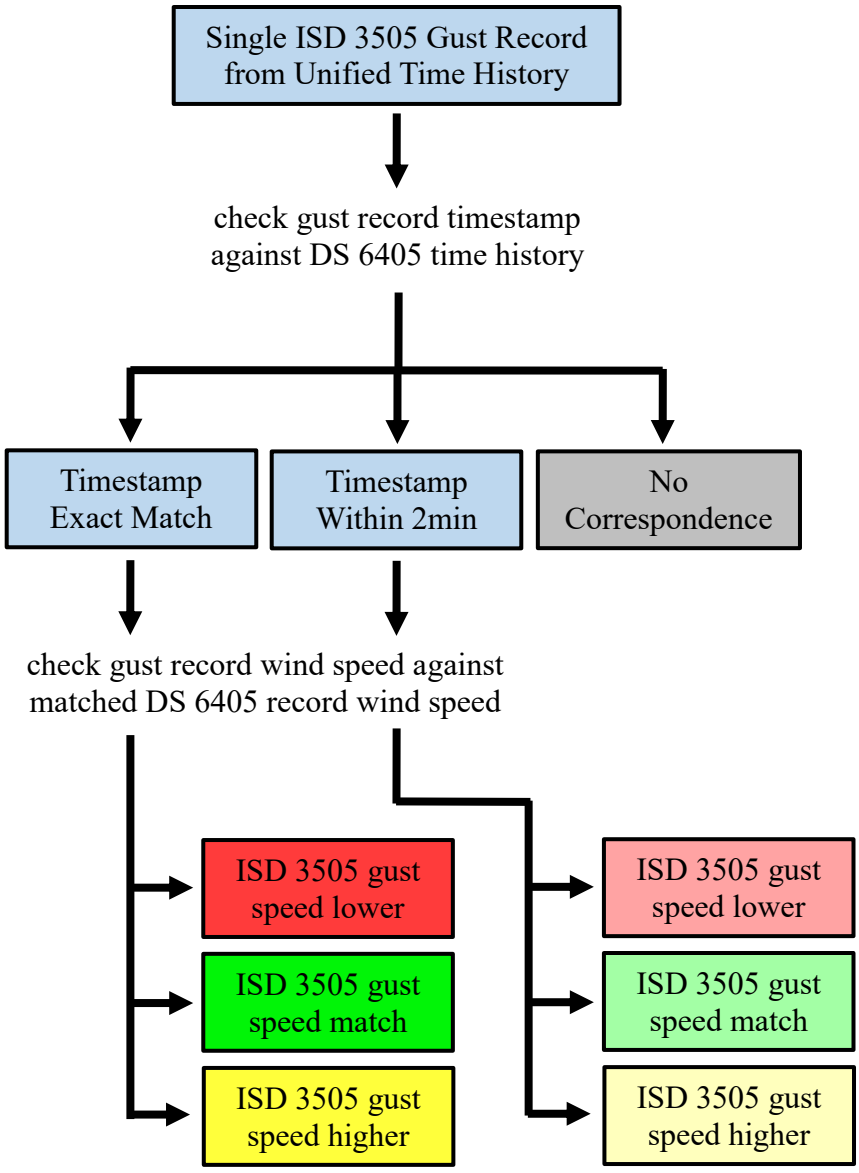

Figure A13: Flow chart depicting the gust comparison (between ISD 3505 and DS 6405) analysis process and the development of the categorization matrix

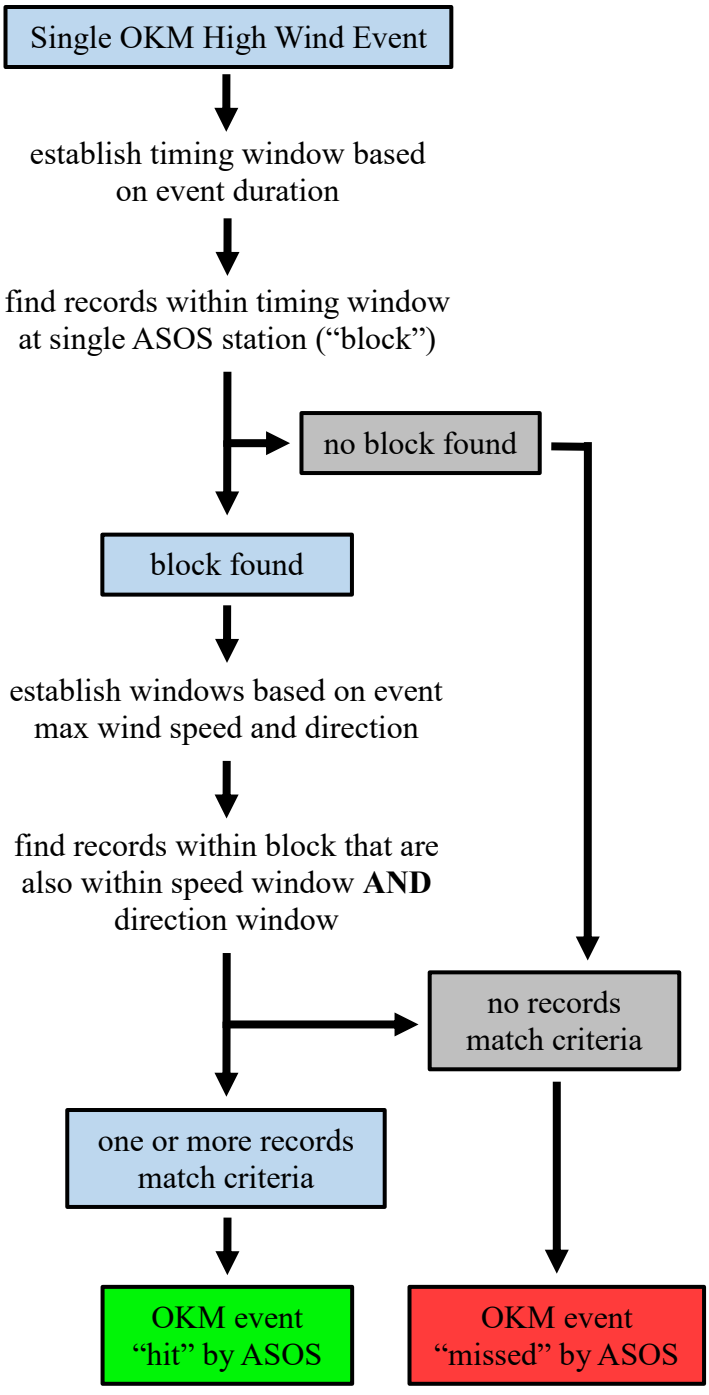

Figure A14: Flow chart depicting the “hit-or-miss” analysis for a single OKM high wind event analyzed against a single ASOS station.

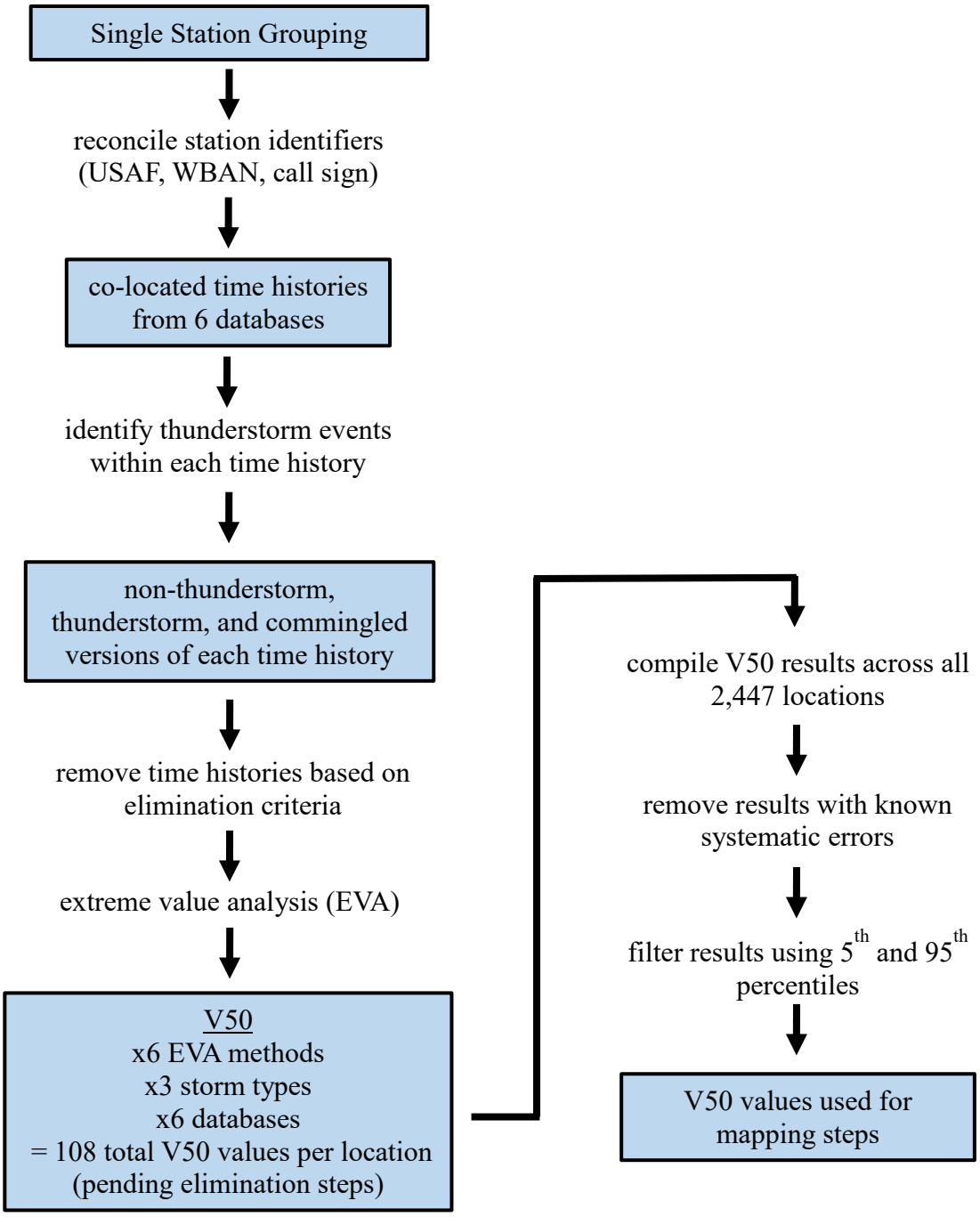

Figure A15: Flow chart depicting the steps taken in the unified extreme value analysis (EVA) procedure used to produce V50 estimates from all databases.